12-2017

A Hybrid Approach for Treatment of Naphthenic Acid Fraction Compounds in Oil Sands Process-Affected Water

Daniel Peter Gaspari
Clemson University

A HYBRID APPROACH FOR TREATMENT OF NAPHTHENIC ACID FRACTION COMPOUNDS IN OIL SANDS PROCESS-AFFECTED WATER

A Thesis
Presented to
the Graduate School of
Clemson University

In Partial Fulfillment
of the Requirements for the Degree
Master of Science
Hydrogeology

---

by
Daniel Peter Gaspari
December 2017

Accepted by:
Dr. James W. Castle, Committee Chair
Dr. John H. Rodgers, Jr.
Dr. Monique Simair

ABSTRACT

Extensive volumes of oil sands process-affected waters (OSPWs) are produced at surface mines in the Athabasca Oil Sands. OSPW contains constituents, including a complex mixture of refractory organics known as naphthenic acid fraction compounds (NAFCs), that require treatment prior to government-mandated reclamation of mining leases. Hybrid constructed wetland treatment systems (CWTSs) implementing film-based TiO_2 photocatalysis were investigated as a passive, low-energy method for treatment of constituents of concern (COCs) in OSPW.

Bench-scale settled TiO_2 batch reactors were assembled and degradation of NAFCs in a specific OSPW was measured as a function of cumulative solar ultraviolet radiation (UV insolation) and by high performance liquid chromatography (HPLC) of naphthenic acids (NA) derivatives. Settled layers of TiO_2 were photoactivated by solar UV-A radiation transmitted through OSPW, which decreased naphthenic acid (NA) mass by 86% at an exponential rate with a mean UV insolation half-life of 1.1±0.2 $MJ \cdot m^{-2}$. Evapotranspiration increased half-lives for NA concentration removal by approximately 90%, highlighting the need for further experimentation with flow-through fixed-film reactors to evaluate if this approach can increase removal rates and efficiencies of NA concentration in OSPW. Following this proof of concept experiment, solar TiO_2 fixed-film photocatalytic reactors and wetland cells were implemented into a hybrid pilot-scale CWTS. Performance of the hybrid CWTS was measured in terms of changes in toxicity and constituent concentration and composition over three sampling periods. NAFC concentrations decreased by 75.9% from inflow (43.1±5.9 mg/L) to outflow (10.4±6.0

mg/L) of the hybrid pilot-scale CWTS, and class distribution shifted from regimes dominated by acutely toxic classical NAs (i.e. O_2 NAs; O_2=40.3%, $\sum O_{3–9}$=45.0%) to sparingly toxic poly-oxygenated classes ($O_{3–9}$; O_2=13.6%, $\sum O_{3–9}$=77.0%). The influence of weather conditions on performance was demonstrated by increases in Cl^- concentrations due to evapotranspiration during the first sampling period and inhibition of NAFC aerobic degradation by near freezing temperatures in the third sampling period. In sampling periods 2 and 3, toxicity to *C. dubia* was eliminated in all samples collected from the hybrid CWTS. Reproduction of *C. dubia* was impaired in 4 of 8 samples collected during sampling period 1, likely due to increased Cl^- concentrations. Changes in toxicity and distribution of NAFC classes reported with biogeochemical conditions in the hybrid pilot-scale CWTS will inform further development of this technology.

In this study of a specific OSPW, solar photocatalysis over settled TiO_2 significantly decreased NA concentration and mass, aerobic degradation in wetland cells paired with fixed-film photocatalysis altered composition and decreased concentration of NAFCs, and in both experiments toxicity associated with NAFCs in OSPW decreased. Results from these bench- and pilot-scale experiments provide proof of concept data supporting further development of fixed-film photocatalytic reactors and testing of CWTSs in the Athabasca Oil Sands for treatment of NAFCs in OSPW.

DEDICATION

This thesis is dedicated to my parents, Michael and Marsha. Dad, following your example has taught me that hard work is always rewarded. Your devotion to your family and to help others will always inspire me. Mom, you fostered my curiosity of the natural world, which guided my path through academia. Both of your love, support, and advice made this thesis possible.

ACKNOWLEDGEMENTS

Dr. Castle's wise advice, both scientific and professional, and meticulous reviews have made me a better writer and scientist. I wish him a fulfilling and relaxing retirement. I thank Dr. Rodgers for teaching me invaluable professional skills throughout my participation in the Oil Sands Process-Affected Water Research Group. Discussions with Dr. Simair, as well as her thorough reviews, have expanded my knowledge of topics essential to completion of this thesis. I was extremely fortunate to work with a group of highly motivated and intelligent graduate students. Maas, Andrew, Ciera, Sam, Alyssa, Rebecca, Megan, and Tyler, thank you for your collaboration, assistance, and discussions. Dr. Chao provided analytical assistance, help locating laboratory supplies, and always a cheery disposition. I greatly appreciate the work of Dr. Headley, Kerry Peru, and their colleagues at the Environment and Climate Change Canada National Hydrology Research Centre, who performed extraction and ultra-high resolution mass spectrometry of NAFCs in samples from the hybrid pilot-scale CWTS. The staff of Contango Strategies are thanked for their assistance in relaying these samples. Finally, I thank my girlfriend Bailey for her unwavering love and support throughout the completion of this thesis.

TABLE OF CONTENTS

Page

LIST OF TABLES

Table Page

Chapter II

List of Tables (continued)

Table Page

Chapter III

List of Tables (continued)

Table Page

Chapter III

LIST OF FIGURES

Figure Page

Chapter II

List of Figures (continued)

Figure Page

Chapter II

List of Figures (continued)

Figure Page

Chapter III

List of Figures (continued)

Figure Page

Chapter III

CHAPTER I

INTRODUCTION

The Athabasca Oil Sands (AOS) of northern Alberta, Canada are the third largest petroleum deposit in the world (AER, 2012; Hein et al., 2013). Bitumen, a highly viscous and heavily degraded oil (Hein et al., 2013), is recovered from surface mined ore through an alkaline extraction process that produces liquid tailings called oil sands process-affected water (OSPW). Continued production of this impaired water combined with a ban on the release of liquid tailings by the Alberta Environmental Protection and Enhancement Act have caused 800-1,000 million m^3 of OSPW to accumulate in tailings ponds across the AOS (Madill et al., 2001; Mikula, 2013). Refractory naphthenic acid fraction compounds (NAFCs), which include a complex mixture of alkyl-substituted cylcoaliphatic carboxylic acids traditionally called naphthenic acids (NAs), are the predominant source of toxicity in OSPW (MacKinnon and Boerger, 1986; Verbeek, 1994; Marentette et al., 2015a,b; Morandi et al., 2015; McQueen et al., 2017a). Ultrahigh resolution mass spectrometry (UHRMS) has confirmed that NAFCs are also composed of poly-oxygenated species as well as nitrogen and sulfur heteroatom classes (Grewer et al., 2010; Headley et al., 2012). OSPW also contains metals, metalloids, residual hydrocarbons, and suspended and dissolved solids in concentrations exceeding protective water quality criteria (Allen, 2008a; Mahaffey and Dube, 2016; McQueen et al., 2017a). The government of Alberta's tailings management framework is implemented by Directive 085 (AER, 2016), which mandates that liquid tailings (OSPW) must be treated progressively and ready to reclaim within 10 years of oil sands mine closure. Oil sands

operators are seeking passive approaches for treating large volumes of OSPW to comply with this directive (COSIA, 2015).

Specifically designed constructed wetland treatment systems (CWTSs) have successfully remediated impaired waters containing complex mixtures of constituents, including refinery effluents and oil field produced waters (Gillespie et al., 2000; Huddleston et al., 2000; Murray-Gulde et al., 2003). These versatile systems support a diverse array of reactions, including biodegradation, photolysis, precipitation, oxidation, reduction, and sorption (Reddy and DeLaune, 2008; Rodgers and Castle, 2008; Vymazal, 2010), and may be constructed and operated at lower cost than conventional water treatment systems (Halverson et al., 2004; Mooney and Murray-Gulde, 2008). By promoting aerobic biodegradation, wetland sediment microcosms decreased NA concentrations (Toor et al., 2013), hydroponic treatments with macrophytes decreased toxicity of OSPW (Armstrong et al., 2009), and pilot-scale CWTSs eliminated acute toxicity of OSPW to *Ceriodaphnia dubia* (McQueen et al., 2017b). Treatment of NAFCs in CWTSs may be augmented by implementing an advanced oxidation process as a hybrid component (McQueen et al., 2017b). Photocatalysis over TiO_2 is a potent advanced oxidation process that generates reactive radical species in the presence of water and ultraviolet (UV) radiation (<400 nm; Fujishima et al., 2000). Bench-scale experiments demonstrate that solar photocatalysis over TiO_2 slurries can decrease concentration and change composition of NAFCs in OSPW (Leshuk et al., 2017). In this research, fixed-film photocatalytic reactors were implemented into a hybrid pilot-scale CWTS to enhance degradation and transformation of NAFCs in a specific OSPW.

To meet the goal of implementing hybrid CWTSs for remediation of OSPW, fundamental questions must be answered concerning the ability of film-based photocatalysis to treat NAFCs in OSPW and the performance of hybrid pilot-scale CWTSs for OSPW. The major objectives of this research were to 1) measure rates and extents of NA degradation and responses of sentinel aquatic organisms in OSPW treated by solar photocatalysis over settled-TiO_2, and 2) measure performance of a hybrid pilot-scale CWTS treating a specific OSPW.

Measure rates and extents of NA degradation and responses of sentinel aquatic organisms in OSPW treated by solar photocatalysis over settled-TiO_2

This research assessed the feasibility of using film-based solar TiO_2 photocatalysis to decrease concentrations of NAs in OSPW and subsequently decrease toxicity of this complex mixture. This goal was achieved by completing the following objectives:

1. measure absorption and attenuation of UV radiation in a specific OSPW;
2. measure rates and extents of NA degradation with respect to UV insolation in settled TiO_2 photocatalytic reactors treating the OSPW; and
3. compare survival and reproduction of *Ceriodaphnia dubia* and survival and biomass of *Pimephales promelas* exposed to the OSPW before and after treatment.

Measure performance of a hybrid pilot-scale CWTS treating a specific OSPW

The aim of this research was to measure biogeochemical conditions and treatment performance, in terms of changes in toxicity and COC concentration and composition, in

a hybrid pilot-scale CWTS treating a specific OSPW. To achieve this overall objective, specific objectives were to:

1) characterize OSPW treated by a hybrid pilot-scale CWTS for identification of COCs;
2) assemble and operate a hybrid pilot-scale constructed wetland for treatment of the OSPW;
3) analyze changes in NAFC concentration and class distribution measured by UHRMS in Dr. John Headley's laboratory at the Environment and Climate Change Canada National Hydrology Research Center; and
4) measure changes in concentration of COCs and survival and reproduction of *Ceriodaphnia dubia*.

Thesis Organization

This thesis is organized into four chapters including the introduction (Chapter I) and conclusions (Chapter IV). Chapters II and III are written as independent manuscripts; therefore, some content may be repeated in the chapters. The manuscripts are:

Chapter II: Solar Photocatalysis of an Oil Sands Process-Affected Water over Settled TiO_2;

Chapter III: A Hybrid Pilot-Scale Constructed Wetland Treatment System for Remediation of an Oil Sands Process-affected Water.

These manuscripts provide proof of concepts for film-based photocatalysis of OSPW and for implementing this technology into hybrid pilot-scale constructed wetlands treating OSPW.

References

Ajaero, C., McMartin, D.W., Peru, K.M., Bailey, J., Haakensen, M., Friesen, V., Martz, R., Hughes, S.A., Brown, C., Chen, H., McKenna, A.M., 2017. Fourier Transform Ion Cyclotron Resonance Mass Spectrometry Characterization of Athabasca Oil Sand Process-Affected Waters Incubated in the Presence of Wetland Plants. *Energy & Fuels*. 31(2), 1731-1740.

Alberta Energy Regulator (AER), 2016. Fluid Tailings Management for Oil Sands Mining Projects. Oil Sands Conservation Act Directive 085. Alberta Energy Regulator, Calgary, AB. https://www.aer.ca/documents/directives/Directive085.pdf.

Allen, E.W., 2008. Process water treatment in Canada's oil sands industry: I. Target pollutants and treatment objectives. *Journal of Environmental Engineering and Science.* 7, 123-138.

Armstrong, S.A., Headley, J.V., Peru, K.M., Germida, J.J., 2009. Differences in phytotoxicity and dissipation between ionized and nonionized oil sands naphthenic acids in wetland plants. *Environmental Toxicology and Chemistry.* 28, 2167-2174.

Canada's Oil Sands Innovation Alliance (COSIA), 2015. Passive Organics Treatment Technology. Canada's Oil Sands Innovation Alliance, Calgary, AB. http://www.cosia.ca/uploads/files/challenges/water/COSIA%20Challenge%20Water%20-%20Passive%20Organics%20Treatment%20Technology.pdf

Fujishima, A., Rao, T.N., Tryk, D.A., 2000. Titanium dioxide photocatalysis. *Journal of Photochemistry and Photobiology C: Photochemistry Reviews.* 1, 1-21.

Gillespie, W.B., Hawkins, W.B., Rodgers, J.H., Cano, M.L., Dorn, P.B., 2000. Transfers and transformations of zinc in constructed wetlands: Mitigation of a refinery effluent. *Ecological Engineering.* 14, 279-292.

Grewer, D.M., Young, R.F., Whittal, R.M., Fedorak, P.M., 2010. Naphthenic acids and other acid-extractables in water samples from Alberta: what is being measured? *Science of the Total Environment*. 408, 5997-6010.

Halverson, N.V., 2004. Review of Constructed Subsurface Flow vs. Surface Flow Wetlands. Westinghouse Savannah River Company, Aiken, SC, Prepared for US Department of Energy (DOE). DOE Contract number: WSRC-TR-2004-00509. US DOE, Washington, DC.

Headley, J.V., Peru, K.M., Fahlman, B., McMartin, D.W., Mapolelo, M.M., Rodgers, R.P., Marshall, A.G., 2012. Comparison of the levels of chloride ions to the characterization of oil sands polar organics in natural waters by use of Fourier transform ion cyclotron resonance mass spectrometry. *Energy & Fuels*, 26(5), 2585-2590.

Hein, F.J., Leckie, D., Larter, S., Suter, J.R., 2013. Heavy oil and bitumen petroleum systems in Alberta and beyond: The future is nonconventional and the future is now. In: Hein, F.J., Leckie, D., Larter, S., Suter, J.R. (Eds.). Heavy-Oil and Oil-Sand Petroleum Systems in Alberta and Beyond. *AAPG Studies in Geology*. 64: 1, 1-21. American Association of Petroleum Geologists (AAPG) Special Volumes.

Huddleston, G.M., Gillespie, W.B., Rodgers, J.H., 2000. Using constructed wetlands to treat biochemical oxygen demand and ammonia associated with a refinery effluent. *Ecotoxicology and Environmental Safety*. 45, 188-193.

Leshuk, T., Wong, T., Linley, S., Peru, K.M., Headley, J.V., Gu, F., 2016. Solar photocatalytic degradation of naphthenic acids in oil sands process-affected water. *Chemosphere*. 144, 1854-1861.

MacKinnon, M.D. and Boerger, H., 1986. Description of two treatment methods for detoxifying oil sands tailings pond water. *Water Quality Research Journal of Canada*. 21, 496-512.

Madill, R.E., Orzechowski, M.T., Chen, G., Brownlee, B.G., Bunce, N.J., 2001. Preliminary risk assessment of the wet landscape option for reclamation of oil sands mine tailings: bioassays with mature fine tailings pore water. *Environmental Toxicology*. 16, 197-208.

Mahaffey, A., and Dubé, M., 2016. Review of the composition and toxicity of oil sands process-affected water. *Environmental Reviews*. 25, 97-114.

Marentette, J.R., Frank, R.A., Bartlett, A.J., Gillis, P.L., Hewitt, L.M., Peru, K.M., Headley, J.V., Brunswick, P., Shang, D., Parrott, J.L., 2015. Toxicity of naphthenic acid fraction components extracted from fresh and aged oil sands process-affected waters, and commercial naphthenic acid mixtures, to fathead minnow (*Pimephales promelas*) embryos. *Aquatic Toxicology*. 164, 108-117.

Marentette, J.R., Frank, R.A., Hewitt, L.M., Gillis, P.L., Bartlett, A.J., Brunswick, P., Shang, D., Parrott, J.L., 2015. Sensitivity of walleye (*Sander vitreus*) and fathead minnow (*Pimephales promelas*) early-life stages to naphthenic acid fraction components extracted from fresh oil sands process-affected waters. *Environmental Pollution*. 207, 59-67.

McQueen, A.D., Kinley, C.M., Hendrikse, M., Gaspari, D.P., Calomeni, A.J., Iwinski, K.J., Castle, J.W., Haakensen, M.C., Peru, K.M., Headley, J.V., 2017a. A risk-based approach for identifying constituents of concern in oil sands process-affected water from the Athabasca Oil Sands region. *Chemosphere*. 173, 340-350.

McQueen, A.D., Hendrikse, M., Gaspari, D.P., Kinley, C.M., Rodgers, J.H., Castle, J.W., 2017b. Performance of a hybrid pilot-scale constructed wetland system for treating oil sands process-affected water from the Athabasca oil sands. *Ecological Engineering*. 102, 152-165.

Mikula, R., 2013. Trading water for oil: Tailings management and water use in surface-mined oil sands. In: Hein, F.J., Leckie, D., Larter, S., Suter, J.R. (Eds.). Heavy Oil and Oil-Sand Petroleum Systems in Alberta and Beyond. *AAPG Studies in Geology* 64: 1, 689-699. American Association of Petroleum Geologists (AAPG) Special Volumes.

Mooney, F.D., and Murray-Gulde, C., 2008. Constructed treatment wetlands for flue gas desulfurization waters: Full-scale design, construction issues, and performance. *Environmental Geosciences.* 15, 131-141.

Morandi, G.D., Wiseman, S.B., Pereira, A., Mankidy, R., Gault, I.G., Martin, J.W., Giesy, J.P., 2015. Effects-directed analysis of dissolved organic compounds in oil sands process-affected water. *Environmental Science & Technology.* 49, 12395-12404.

Murray-Gulde, C., Heatley, J.E., Karanfil, T., Rodgers, J.H., Myers, J.E., 2003. Performance of a hybrid reverse osmosis-constructed wetland treatment system for brackish oil field produced water. *Water Research.* 37, 705-713.

Reddy, K.R., and DeLaune, R.D., 2008. Biogeochemistry of wetlands: science and applications. CRC Press, Boca Raton, FL.

Rodgers Jr, J.H., Castle, J.W., 2008. Constructed wetland systems for efficient and effective treatment of contaminated waters for reuse. *Environmental Geosciences.* 15, 1-8.

Toor, N.S., Franz, E.D., Fedorak, P.M., MacKinnon, M.D., Liber, K., 2013. Degradation and aquatic toxicity of naphthenic acids in oil sands process-affected waters using simulated wetlands. *Chemosphere.* 90, 449-458.

Verbeek, A.G., 1994. A toxicity assessment of oil sands wastewater. University of Alberta, Edmonton, AB. Master's Thesis.

Vymazal, J., 2010. Constructed wetlands for wastewater treatment: five decades of experience. *Environmental Science & Technology.* 45, 61-69.

CHAPTER II

SOLAR PHOTOCATALYSIS OF AN OIL SANDS PROCESS-AFFECTED WATER OVER SETTLED TiO_2

Abstract

Extensive volumes of oil sands process-affected waters (OSPWs) containing a complex mixture of toxic and refractory organics, consisting largely of naphthenic acids (NAs), are stored in tailings ponds on mining leases in the Athabasca Oil Sands. Film-based solar photocatalysis over TiO_2 was evaluated as a passive method for degrading NAs and decreasing toxicity of OSPW. The primary objective of this study was to measure rates and extents of NA degradation and responses of sentinel aquatic organisms in a specific OSPW treated by solar photocatalysis over settled-TiO_2. Photocatalytic reactors consisted of thin films (~0.5 mm) of TiO_2 settled in OSPW. OSPW without TiO_2 was irradiated by sunlight in photolytic reactors, and dark control reactors accounted for sorption or aerobic degradation of NAs. Rates and extents of changes in NA mass and concentration were calculated with respect to cumulative solar UV radiation (UV insolation) and photoperiod. Photocatalysis over settled TiO_2 decreased NA concentration by an average of 37% after 1.78 $MJ \cdot m^{-2}$ UV insolation accumulated over a 16-h photoperiod and decreased NA mass by 86% after 3.57 $MJ \cdot m^{-2}$ UV insolation (32-h photoperiod). In photocatalytic reactors, removal of NA mass as functions of UV insolation and photoperiod was modeled using first-order rate kinetics with 50% degradation occurring at 1.1±0.2 $MJ \cdot m^{-2}$ and 10.2±0.8 h of sunlight exposure. Photolysis decreased NA mass by 39% after 32 h of sunlight exposure and 3.57 $MJ \cdot m^{-2}$, but

increased NA concentration by 59±9% after a 16-h photoperiod because evaporative volume loss outpaced mass removal. Compared to a laboratory control, OSPW adversely affected *C. dubia* survival and reproduction. Toxicity was eliminated after treatment in photocatalytic, photolytic, and dark control reactors. Removal of NA mass and concentration in the settled TiO_2 reactors provides a proof of concept for film-based solar photocatalysis. Further experimentation with flow-through fixed-film reactors is warranted to improve performance of film-based TiO_2 photocatalysis for treatment of OSPW.

1.0 Introduction

The oil sands of northern Alberta, Canada are the third largest petroleum deposit in the world (AER, 2012; Hein et al., 2013). Oil sands ore is surface mined and bitumen is recovered through an alkaline extraction process, which produces liquid tailings called oil sands process-affected water (OSPW). Continued production of this impaired water combined with prohibition on liquid tailings release by the Alberta Environmental Protection and Enhancement Act and lack of scalable treatment technologies have caused 800-1,000 million m^3 of OSPW to accumulate in tailings ponds (Madill et al., 2001; Mikula, 2013; Quinlan and Tam, 2015). OSPW is a complex effluent containing suspended sediments, dissolved salts, metals, metalloids, and an organic fraction predominantly composed of naphthenic acids and residual bitumen (Allen, 2008).

Naphthenic acids (NAs) are considered the most problematic constituent in OSPW (MacKinnon and Boerger, 1986), as they have adversely affected aquatic invertebrates (Bartlett et al., 2017), fish (Kavanagh et al., 2011), macrophytes (Armstrong

et al., 2008), and mammals (Rogers et al., 2002), and are recalcitrant to biodegradation, with estimated degradation half-lives of 13-14 years in tailings ponds (Han et al., 2009). NAs are a complex mixture of thousands of alkyl-substituted cylcoaliphatic carboxylic acids traditionally defined by the formula $C_nH_{2n+Z}O_2$, where *n* is the number of carbon atoms and *Z* is the hydrogen deficiency (Brient et al., 1995; Headley and McMartin, 2004; Clemente and Fedorak, 2005). Ultrahigh-resolution mass spectrometry of OSPW organics has identified compounds with structures that do not conform to the "classical" NA formula, including aromatic (Mohamed et al., 2008), diamondoid (Rowland et al., 2011), heteroatomic (Mohamed et al., 2008), and poly-oxygenated species (Barrow et al., 2009; Martin et al., 2009). Grewer et al. (2010) found that <50% of compounds in extracts of OSPW were classical NAs, and Headley et al. (2012) submitted the term naphthenic acid fraction compounds (NAFCs) to more accurately describe this group. NAFCs having greater cyclicity, carbon number, and alkyl branching are increasingly resistant to biodegradation (Scott et al., 2005; Han et al., 2008; Toor et al., 2013) and require more robust treatment methods to decrease concentration and alter composition.

Advanced oxidation processes, such as ozonation (Scott et al., 2008; Hwang et al., 2013) and persulfate and permanganate oxidation (Drzewicz et al., 2012; Soharbi et al., 2013), have decreased NAs concentrations and may increase the biodegradability of residual NAs (Martin et al., 2009). Solar photocatalysis over TiO_2 is a potent advanced oxidation process that generates highly reactive radical species, such as hydroxyl radicals (+2.27 V) and superoxide anions (-0.52 V), in the presence of water and ultraviolet (UV) radiation (<400 nm; Fujishima et al., 2000). Degussa® and Aeroxide® P25 are blends of

TiO_2 polymorphs (~70% anatase, ~30% rutile) that are widely used due to their low cost, low toxicity, high photoreactivity, and chemical stability (Gaya and Abudulla, 2008; Malato et al., 2009). TiO_2 photocatalysis driven by solar radiation has degraded an array of recalcitrant organic compounds, including pharmaceuticals, polycyclic aromatic hydrocarbons, and NAs (Headley et al., 2009; Malato et al., 2009; Chong et al., 2010). In a bench-scale study, Leshuk et al. (2016) utilized solar photocatalysis of OSPW over an agitated TiO_2 slurry to remove >98% of NAFCs over 14 h of sunlight exposure. Slurry photocatalysis requires vigorous mixing and post-treatment recovery of TiO_2 by microfiltration (Malato et al., 2009). These energy intensive steps impede the commercialization of this processes (Chong et al., 2010) and may preclude this technology from implementation at scales required for treating OSPW. TiO_2 fixed-films may provide a low-energy method for implementing solar photocatalysis, as they eliminate catalyst recovery and mixing (Malato et al., 2009; Zayani et al., 2009). McQueen et al. (2016) utilized fixed-film photocatalysis to decrease concentrations of a commercial NA blend (Fluka NAs) by >92% and eliminate acute toxicity to *Daphnia magna* and *Pimephales promelas*. To date, no investigations of photocatalytic degradation of NAs in OSPW have used film-based TiO_2, assessed performance using sentinel aquatic organisms, or measured rates and extents of NA degradation with respect to cumulative solar UV radiation (UV insolation; McMartin et al., 2004; Headley et al., 2009; Mishra et al., 2010; Leshuk et al., 2016a,b).

To investigate the feasibility of film-based photocatalysis as a method for degrading NAs and decreasing acute OSPW toxicity, settled layers of TiO_2 were used in

place of immobilized catalysts for treatment of a specific OSPW. Settled TiO_2 is functionally similar to fixed-films because UV radiation is attenuated before activating catalysts (Malato et al., 2009). Attenuation of UV radiation decreases efficiency of film-based photocatalytic reactors (Malato et al., 2009; Zayani et al., 2009) necessitating characterization of attenuation and absorption of UV radiation (250 to 400 nm) by constituents in OSPW. This research is a first-order demonstration of film-based photocatalysis of OSPW to determine rates and extents of NA concentration and mass removal in bench-scale batch reactors.

The overall objective of this research was to measure rates and extents of NA degradation and responses of sentinel aquatic organisms in OSPW treated by solar photocatalysis over settled-TiO_2. Specific objectives were to: 1) measure absorption and attenuation of UV radiation in the OSPW, 2) measure rates and extents of NA degradation with respect to UV insolation in settled TiO_2 photocatalytic reactors treating the OSPW, and 3) compare survival and reproduction of *Ceriodaphnia dubia* and survival and biomass of *Pimephales promelas* exposed to the OSPW before and after treatment.

2.0 Materials and Methods

2.1 OSPW Source

In November 2015, ~40,000 L of OSPW was collected from the clarified zone of an external tailings facility in northern Alberta, Canada and shipped to Clemson University. The OSPW was stored outdoors in 3,875 L polypropylene storage tanks and a

~20,000 L tanker trailer. OSPW used in photocatalysis experiments was collected from a storage tank after being mixed for 24 h by a 0.56 kW (0.75 HP) submersible pump.

2.2 Absorption and attenuation of UV radiation in OSPW

The absorption of UV radiation by OSPW was measured using a SpectraMax®M2 spectrophotometer (Molecular Devices Corp.; Sunnyvale, CA) in quartz cuvettes with a 1 cm pathlength. Absorbance (*A*) was measured from 250 to 400 nm and converted to transmittance (*T*) using Eqn. 1:

$$T = 10^{-(A-A_o)} \quad (1)$$

where A_o is the absorbance of a quartz cuvette with NANOpure® water.

UV irradiance was measured with an Apogee Instruments Inc. SU-100 broadband UV sensor (Logon, UT; spectral range 250 to 400 nm) connected to a HOBO UX120-006M data logger (Onset; Bourne, MA). The sensor was placed in a waterproof housing constructed from polyvinyl chloride (PVC) pipes and joints, a quartz disk, and silicone caulk (GE Silicone I). This device was used to measure relative differences in UV irradiance, but could not determine absolute values of irradiance because the quartz glass cover altered the sensor's spectral response. The device was secured to the side of a leveled, 20-L polyethylene bucket filled with OSPW and was used to measure UV irradiance between depths of 0 to 20 cm at 1-3 cm intervals. UV attenuation experiments were conducted in Clemson, SC on cloudless days in October 2016. Total suspended solids (TSS) were measured as explanatory parameters for UV attenuation in OSPW according to methods 2130B and 2540D, respectively (APHA, 2012).

The Beer-Lambert Law states that UV irradiance attenuates exponentially with increased depth in a medium (Eqn. 2):

$$I = I_o e^{-\mu z} \qquad (2)$$

where I is UV irradiance ($W \cdot m^{-2} \cdot s^{-1}$), I_o is incident UV irradiance ($W \cdot m^{-2} \cdot s^{-1}$), μ is the attenuation coefficient (cm^{-1}), and z is depth (cm). This relationship can be expressed in terms of transmittance and transformed to a linear function (Eqns. 3, 4):

$$T = \frac{I}{I_o} = e^{-\mu z} \qquad (3)$$

$$-ln\, T = \mu z \qquad (4)$$

Linear regression through the origin (RTO) of depth and natural logarithm transmittance produced a strong correlation (r^2 = 0.997) supporting that the device was suitable to measure UV attenuation in OSPW. After verifying this method, UV irradiance was measured at the surface and then immediately at depth in OSPW, and attenuation coefficients were calculated (Eqn. 5):

$$\mu = -ln(I/I_o)\,/z \qquad (5)$$

2.3 Rates and extents of naphthenic acid removal

2.3.1 Photoreactor assembly and experimental design

The experimental design included photocatalytic, photolytic, and dark control reactors with three independent replicates for each reactor type. Photocatalytic reactors were assembled in leveled 59x59x4.5 cm laboratory-grade fiberglass trays (MFG Tray Company; Linesville, PA) by pouring 3.48 L suspensions of 1,000 mg/L TiO_2 (Aeroxide™ P25; Fisher Scientific, Fair Lawn, NJ) in OSPW. This same method was

followed to make dark control reactors, which used opaque high-density polyethylene (HDPE) covers to block sunlight. TiO_2 in the photocatalytic and dark control reactors aggregated and settled out of suspension rapidly, forming ~0.5 mm thick layers of catalyst on the bottom surface of the trays. Transmittance of samples collected 0.5 and 2 h after TiO_2/OSPW suspensions were poured into the photocatalytic reactors was measured to assess settling. Photolytic reactors consisted of fiberglass trays containing OSPW exposed to sunlight without TiO_2. Depth of OSPW in all reactors was 1 cm. The experiment was conducted from February 27, 2016 to March 1, 2016 on a roof receiving direct sunlight (34° 40' 27.25" N, 82° 50' 7.46" W). HDPE covers were placed on all reactors between ~6:00 PM and 9:00 AM each day of the experiment.

To measure changes in NA concentration during the experiment, 10 mL samples were pipetted from the water column of each reactor and stored in 15 mL glass vessels. Conductivity, dissolved oxygen, and pH were measured *in situ* at each sampling event (Table S1). Conductivity and pH were measured using an Orion Star A221 portable meter (Thermo Fisher Scientific, Waltham, MA) equipped with a 9157BNMD Triode pH probe and a 013010MD conductivity cell. DO was measured using a HQ30d meter with a LDO101 optical dissolved oxygen probe (HACH; Loveland, CO). Water temperature and depth were measured at each sampling event. Ambient temperature data were collected from a proximal weather station (Weather Underground, 2016; N 34° 40' 48", W 82° 49' 55"). Incident UV irradiance ($W \cdot m^{-2}$) was measured throughout the experiment using a SU-100 UV sensor (without waterproof housing). Irradiance data were collected using a UX120-006M data logger and integrated to UV insolation ($MJ \cdot m^2$) using Simpson's rule.

As the experiment progressed, volumes in the photocatalytic and photolytic reactors decreased due to evaporation. To maintain a water depth of 1 cm and preserve volume for chemical analyses and bioassays, photocatalytic and photolytic reactors were reconstituted to initial volumes (3.48 L) after 16, 24, and 32 h of sunlight exposure. Reconstitution was performed by collecting and measuring volumes of TiO_2/OSPW suspensions and OSPW in the photocatalytic and photolytic reactors and replacing evaporated volumes with NANOpure® water. After reconstitution, TiO_2/OSPW suspensions were poured back into trays and settled overnight. The covered dark controls lost <18% volume to evaporation and were not reconstituted.

2.3.2 Chemical analysis

Naphthenic acids concentrations were quantified using derivatization and high performance liquid chromatography (HPLC) methods modified from Yen et al. (2004). In this method, 2-nitrophenolhydrazine is derivatized to nitrophenolhydrazide by naphthenic acids. Samples were derivatized in 2.0 mL glass HPLC vials, and concentrations were measured using a Dionex UltiMate-3000 HPLC (Sunnyvale, CA) equipped with an Agilent LiChrospher 100 RP-18 column (5 µm particle size, 125mm x 4 mm) and a guard column containing 2 µm RP-18 solid phase material. Column temperature was fixed at 40°C. Samples were mobilized with HPLC grade methanol (Fisher Scientific, Fair Lawn, NJ) at a flow rate of 60 $\mu L \cdot min^{-1}$. Absorbance of naphthenic acid derivatives was measured at 400 nm. Chromatograms were integrated using a baseline hold between retention times of 2.9 and 6 min, and integrated areas were used to calculate NA concentration. Quantification of NA concentrations was performed using a 5-point

calibration curve of nominal concentrations of a commercial NA blend (Fluka NAs; Sigma-Aldrich; St. Louis, MO). All samples and standards analyzed by derivatization and HPLC were divided into pseudo-replicates, and NA concentrations were expressed as means of pseudo-replicates (n=3). Fluka NA standards were made from serial dilution of a water accommodated fraction (WAF) containing 140 mg/L NAs. WAFs were mixed for 24±4 h in 1-L volumetric flasks using magnetic stirrers producing vortices extending to 30-50% of the solution depth (OECD, 2002).

Biochemical oxygen demand (BOD) and chemical oxygen demand (COD) were measured in OSPW before and after treatment by photocatalysis. PolySeed® (InterLab; Spring, TX) was used to inoculate samples in BOD experiments. Alkalinity, BOD, COD, hardness, total suspended solids (TSS), and total dissolved solids (TDS) were measured in all reactors according to *Standard Methods for Examination of Water and Wastewater* (APHA, 2012; Table S1). Concentrations of oil and grease (O&G) were measured in untreated OSPW according to USEPA method 1664A (USEPA, 1999). Concentrations of acid soluble Al, B, Ca, Cl, Cu, Fe, Mg, Mn, P, Na, and Zn were determined by inductively coupled plasma-atomic emission spectroscopy (ICP-AES) using EPA method 200.7 (USEPA, 2001). ICP-AES analysis was conducted at Clemson University's Agricultural Services Laboratory.

2.3.3 Calculating naphthenic acid removal rates and efficiencies

NA degradation in photocatalytic and photolytic reactors was assessed by calculating rates of change in concentration and mass as functions of UV insolation and photoperiod. First order rate kinetics was used to model decreases in NA concentration in

the photocatalytic reactors with respect to UV insolation and photoperiod. The first-order rate equation was arranged so that rate coefficients were calculated as slopes of trend lines determined by linear RTO of natural log transformed NA concentrations and UV insolation or photoperiod (Eqn. 6, 7):

$$ln(C_i/C_o) = -k_{E_c}E_i \qquad (6)$$

$$ln(C_i/C_o) = -k_{t_c}t_i \qquad (7)$$

Where C_i is naphthenic acid concentration (mg/L), C_o is initial naphthenic acid concentration (mg/L), E_i is UV insolation (MJ·m^{-2}), t_i is photoperiod (h), and k_{E_c} and k_{t_c} are rate coefficients for change in NA concentration as functions of UV insolation (m^2·MJ^{-1}) and photoperiod (h^{-1}), respectively. Rate coefficients were used to calculate NA degradation half-lives in terms of UV insolation and photoperiod (Eqn. 8, 9):

$$T_{0.5E_c} = -ln(0.5)/k_{E_c} \qquad (8)$$

$$T_{0.5\mathrm{t}_c} = -ln(0.5)/k_{t_c} \qquad (9)$$

Where $T_{0.5E_c}$ and $T_{0.5\mathrm{t}_c}$ are degradation half-lives for NA concentration as functions of UV insolation (MJ·m^{-2}) and photoperiod (h), respectively. Removal efficiencies (%) for NA concentration were calculated using Eqn. 10:

$$\text{Removal Efficiency (\%)} = (C_o - C_i)/C_o \cdot 100 \qquad (10)$$

Rate coefficients, half-lives, and removal efficiencies for NA concentration removal were calculated at the midpoint of the experiment when photocatalytic reactors were reconstituted after a photoperiod of 16 h and 1.79 MJ·m^{-2} UV insolation.

Volumes of OSPW in photocatalytic and photolytic reactors were not measured prior to reconstitution at the experiment midpoint. To estimate volume and calculate NA mass prior to reconstitution, UV insolation was correlated with evaporated volumes measured in the photocatalytic and photolytic reactors at t = 0, 16, 24, 32 h. Linear regression showed a strong correlation between UV insolation and cumulative evaporated volume (R^2 = 0.99). The slope of this regression line (β; 1.08 L·m^2·MJ^{-1}) was multiplied by UV insolation (E_i; MJ·m^2) to estimate evaporated volume (V_E; L; Eqn. 11).

$$V_E = E_i\beta \qquad (11)$$

This model predicted measured evaporated volumes within 5.1% and was substituted into Eqn. 12 to calculate reactor volume (V_i; L):

$$V_i = V_o - V_E - V_s \qquad (12)$$

where V_o is initial volume of the reactor and V_s is the volume removed by sampling. Once reactor volume was calculated, Eqn. 13 was used to determine NA mass.

$$M_i = C_i V_i \qquad (13)$$

where M_i is NA mass (mg). This equation was also used to calculate NA mass after the experiment midpoint when volumes were measured directly.

NA mass removal was modeled by first-order rate kinetics. First-order rate coefficients were calculated by linear RTO of natural log transformed NA mass and UV insolation or photoperiod (Eqn. 14, 15):

$$ln(M_i/M_o) = -k_{E_m}E_i \qquad (14)$$

$$ln(M_i/M_o) = -k_{t_m} t_i \qquad (15)$$

Where M_o is initial naphthenic acid mass and k_{E_m} and k_{t_m} are rate coefficients for change in NA mass as functions of UV insolation ($m^2 \cdot MJ^{-1}$) and photoperiod (h^{-1}), respectively. UV insolation and photoperiod half-lives for NA mass removal were calculated using rate coefficients (Eqn. 16, 17).

$$T_{0.5E_m} = -ln(0.5)/k_{E_m} \qquad (16)$$

$$T_{0.5\mathrm{t}_m} = -ln(0.5)/k_{t_m} \qquad (17)$$

Where $T_{0.5E_m}$ and $T_{0.5t_m}$ are degradation half-lives for NA mass with respect to UV insolation ($MJ \cdot m^{-2}$) and photoperiod (h), respectively. Removal efficiencies (%) for NA mass were calculated using Eqn. 18:

$$\text{Removal Efficiency (\%)} = (M_o - M_i)/M_o \cdot 100 \qquad (18)$$

2.4 Toxicity Testing

Photocatalytic, photolytic, and dark control reactors were assessed for their ability to alter exposures of OSPW to *Pimephales promelas* and *Ceriodaphnia dubia*. These organisms were selected for toxicity testing because they occur in freshwaters across the United States and Canada (Scott and Crossman, 1973; Pennak, 1978; Carpenter et al., 1985) and respond adversely to NAs in OSPW (Zubot et al., 2012; Marentette et al., 2015b; Morandi et al., 2015). *P. promelas* larvae and *C. dubia* neonates, both <24h old, were obtained from healthy cultures at the Clemson University Aquatic Animal Research Laboratory. Procedures for measuring survival and growth of *P. promelas* and survival and reproduction of *C. dubia* were adapted from Environment and Climate Change

Canada (ECCC, 2007; ECCC, 2011) biological test methods. Single concentration tests were conducted, where the presence or absence of toxicity was assessed by statistical comparison to laboratory controls, which consisted of formulated moderately-hard water (USEPA, 2002).

Reproduction of *C. dubia* and biomass of *P. promelas* were tested for normality and homogeneity using Chi-square and Barlett's tests, respectively. Differences between normally distributed, homogenous data were determined by analysis of variance (ANOVA) followed by many-to-one comparison of treatments (i.e. photocatalytic, photolytic, and dark control reactors) to laboratory controls using Dunett's test or by all-possible pairwise comparisons via Tukey's test. Quantal data, including the survival of *C. dubia* and *P. promelas*, were compared with laboratory controls using Fisher's exact test. Differences were considered significant at $p \leq 0.05$. Statistical analyses were performed in JMP (version 12.1; SAS Institute Inc.; Cary, NC, USA).

3.0 Results

3.1 Absorption and attenuation of UV radiation in OSPW

UV-C and UV-B (200-280 nm and 280-315 nm, respectively) radiation are more strongly absorbed than UV-A radiation (315-400 nm; Figure 1) in OSPW. Transmittance of UV-C and UV-B radiation in OSPW are <49% and 49 to 70%, respectively, and transmittance increased by ~0.62%·nm^{-1} from 250 to 315 nm. By comparison, transmittance of UV-A radiation in OSPW ranges from 70 to 88%, and increased by ~0.21%·nm^{-1} from 315 to 400 nm. When measured immediately following mixing, a suspension of 0.01 g/L TiO_2 in OSPW significantly decreased transmittance of UV

radiation between 8 and 20% (250 to 400 nm, $p<0.0001$). However, TiO_2 settled rapidly after 1 g/L TiO_2/OSPW slurries were poured in photocatalytic reactors. Mean transmittance of a sample collected 0.5 h after TiO_2/OSPW slurries were poured was slightly less than OSPW without TiO_2 (58±13% and 68±18%, respectively). After TiO_2 had settled for 2 h, transmittance was equal or slightly greater than in OSPW without TiO_2.

The Beer-Lambert law accurately modeled UV light attenuation in OSPW (R^2 = 0.997, 0.993; Eqn. 2). The mean attenuation coefficient (μ) for the OSPW used in this experiment was -0.13±0.02 cm^{-1} (Figure 2). The UV attenuation device (Section 2.2) determined that at a depth of 1 cm in OSPW, which is the same depth as the reactors, UV irradiance decreased by 12%, and 50% of UV light energy was attenuated at 5.4 cm. To assess the effect of TSS and O&G on attenuation of UV radiation in OSPW, an experiment was conducted on OSPW with 69±11 mg/L TSS and 30 mg/L O&G. These values of TSS and O&G approximately doubled the UV attenuation coefficient of OSPW (μ =-0.28±0.02 cm^{-1}). UV irradiance decreased by 25% at a depth of 1 cm in this turbid OSPW and decreased by 50% at 2.5 cm.

3.2 Environmental conditions

Over the 82 h duration of the experiment (τ), photoperiod (t_p) of the photocatalytic and photolytic reactors was 32 h and UV insolation (E) was 3.57 $MJ \cdot m^{-2}$. Solar UV irradiance ranged from 1.55 to 45.54 $W \cdot m^{-2}$ (Figure S1) when the photocatalytic and photolytic reactors were uncovered and exposed to direct sunlight. Over the 4 days and 3 nights that the experiment was conducted, ambient air temperature

ranged from 0.5 to 23°C. Water temperature measured in the reactors during each sampling event ranged from 8.6 and 17.7 °C (Table S2). Mean pH in the photocatalytic reactors was 8.25±0.12, which was less than pH in the photolytic reactors or dark controls (8.79±0.12 and 8.66±0.22, respectively). Mean DO in the photocatalytic reactors was 9.40±1.48 mg/L, indicating that oxygen concentrations were near saturation. Evaporation increased mean conductivity in photocatalytic and photolytic reactors (2,638±584 and 2,589±568 µS/cm, respectively) relative to covered dark control reactors (2,047±104 µS/cm).

3.3 Rates and extents of NA degradation

3.3.1 Photocatalysis

Initial mean NA concentration in the photocatalytic reactors was 89±7 mg/L. NA concentrations in these reactors decreased by 36±6% to 57±6 mg/L after 1.78 MJ/m^2 of UV insolation, which occurred over an experimental duration of 32 h and a photoperiod of 16 h (Table 1, Figure 3). Concentration data from each reactor (n=3) was plotted against UV insolation using a first-order kinetic model, resulting in a mean rate coefficient of -0.33±0.03 m^2·MJ^{-1}. Coefficients of determination (R^2) for regression of the first-order model ranged from 0.63 to 0.93. NA concentration decreased by 50% after 2.1±0.2 MJ·m^{-2} UV insolation (Eqn. 8). Decreases in NA concentration were measured with photoperiod, and followed similar trends as NA degradation with respect to UV insolation. The mean first-order rate coefficient for change in NA concentration with photoperiod was -0.036±0.003 h^{-1} (R^2 =0.67 to 0.94; Table 1), which resulted in a half-life of 19±2 h of sunlight exposure (Eqn. 9).

At the midpoint of the experiment (E=1.78 MJ/m^2, t=16 h, τ=32 h), volumes in the photocatalytic and photolytic reactors had decreased between 52 and 57% due to evaporation. To continue the experiment, evaporated volumes were replaced with Nanopure® water, and NA degradation was assessed in terms of mass removal. Initial mean NA mass in the photocatalytic reactors was 310±16 mg (n=3). After 3.57 MJ·m^{-2} UV insolation, which accumulated over an experimental duration of 82 h and a photoperiod of 32 h, NA mass decreased by 86±3% on average (n=3) to an extent of 44±11 mg (Table 1, Figure 4). Exponential regression of NA mass and UV insolation showed a strong correlation (R^2 = 0.87 to 0.98) supporting that mass removal by photocatalysis conformed to first-order rate kinetics. The mean rate coefficient (Eqn. 14) determined from regression of UV insolation and NA mass was -0.68±0.011 m^2·MJ^{-1}. The UV insolation half-life for NA mass removal (Eqn. 16) supported the first-order model, as it predicted correctly that 50% removal would occur after 1.1±0.2 MJ·m^{-2} UV insolation (n=3). Mean NA mass calculated at 1.13 MJ·m^{-2} was 160±5 mg, a 49±4% decrease from initial mass. The mean first-order rate coefficient for NA mass degradation as a function of photoperiod was -0.07±0.01 h^{-1} (Eqn. 15; R^2 =0.85 to 0.98), resulting in a mean half-life of 10.0±1.6 h (Eqn. 17). NA mass in the reactors was 160±5 mg at 8.6 h of sunlight exposure, supporting that photoperiod-based model accurately predicted NA degradation in this experiment.

3.3.2 Photolysis and dark control

Initial NA concentrations in the photolytic reactors and dark controls were 92±13 and 89±7 mg/L on average (n=3), respectively. After 1.78 MJ·m^{-2} UV insolation

accumulated over a photoperiod of 16 h, NA concentrations in the photolytic reactors increased between 50 and 66%, resulting in a mean NA concentration of 146±7 mg/L (Table 1, Figure 3). By the midpoint of the experiment (τ=32 h), NA concentrations had increased significantly in the dark control reactors (110±6 mg/L; p=<0.0001); however, conductivity was 1,981±51 µS/cm, which is not statistically different from initial conductivity (1,949±5 µS/cm; p= 0.38), and volume decreased by <8.6% (<0.3 L). Figure 3 shows that in the dark controls most of the increase in NA concentrations between experiment initiation and midpoint occurred from τ = 27 to 32 h (1.14 and 1.78 MJ·m^{-2}). These data suggest that the increase in NA concentrations measured in the dark controls at the experiment midpoint was likely an artifact of derivatization.

OSPW volume in the photolytic reactors decreased by an average of ~54% after 16 h of sunlight exposure (E=1.78 MJ·m^2) causing NA concentrations to increase significantly (p<0.001). However, NA mass decreased from 320±8 mg to 230±14 mg during this interval (Figure 4). After 3.57 MJ·m^{-2} of UV insolation, photolysis decreased NA mass by 39±8% to 195±23 mg. In the photolytic reactors, change in NA mass with respect to UV insolation was modeled by first-order rate kinetics (R^2= 0.80 to 0.95). The mean rate coefficient for change in NA mass by photolysis as a function of UV insolation was -0.14±0.04 m^2·MJ^{-1}. The mean first-order rate coefficient for change in NA mass with photoperiod was -0.015±0.004 h^{-1} (R^2 =0.80 to 0.95), which results in a mean half-life of 46±13 h. Final mean NA mass in the dark reactors was 280±27 mg, which was lower, but not significantly different, from initial mass (310±16 mg, p = 0.21).

3.4 Toxicity testing

3.4.1 Exposure Characterization

Water quality characteristics and concentrations of metals, metalloids, major ions, and NAs were measured to characterize exposures of untreated OSPW and OSPW from photocatalytic, photolytic reactors, and dark control reactors (Tables S3, S4). Evaporation decreased volume in the dark control reactors by 16.7±0.9%, accounting for increases in conductivity, TDS, and concentrations of ions (e.g, HCO_3^-, Cl^-, and Na^+) relative to OSPW and samples from the reconstituted photocatalytic and photolytic reactors. Concentrations of Cu and Zn in untreated OSPW exceeded water quality criteria (0.011 mg Cu/L [USEPA, 2007] and 0.03 mg Zn/L [CCME, 2011], respectively), but Cu was detected above the USEPA criteria only in the photolysis treatment. B and Cl^- were measured in excess of Canadian Council of Ministers of the Environment (CCME) criteria (1.5 mg B/L and 120 mg Cl^-/L [CCME, 2011]) in all treatments and in untreated OSPW. Final concentrations of NAs in photocatalysis, photolysis, and dark control treatments were 18±5, 79±9, and 97±8 mg/L, respectively. These values exceed a 96 h EC50 for *P. promelas* embryo viability (7.5 mg/L; Marentette et al., 2015a); however, toxicity of NAs in OSPW is determined by concentration and speciation (Brown and Ulrich, 2015; Maffey and Dubé, 2016; McQueen et al., 2017b).

3.4.2 Ceriodaphnia dubia

Survival and reproduction of *C. dubia* was measured to assess the ability of each treatment (i.e., photocatalysis, photolysis, and dark control) to mitigate risk associated with OSPW (Figure 5; Table S5). Untreated OSPW was toxic to *C. dubia,* as survival (55%; $p = 0.004$) and reproduction (14±7 neonate·adult^{-1}; $p < 0.001$) were significantly

less than a laboratory control (95%; 28±6 neonate·adult^{-1}). Photocatalysis increased survival and reproduction of *C. dubia* relative to untreated OSPW. No mortality and the highest reproduction of all treatments (23±6 neonates·adult^{-1}) were observed in OSPW treated by photocatalysis. Reproduction and survival in the dark and photolysis treatments also were not significantly different from a laboratory control. However, Tukey's test indicates that daphnids exposed to OSPW treated by photocatalysis had significantly greater reproduction than *C. dubia* exposed to photolysis (p = 0.025) and dark (p = 0.017) treatments.

3.4.3 Pimephales promelas

Survival and biomass of juvenile *P. promelas* exposed to untreated OSPW was 88% and 472±32 µg, respectively (Figure 6; Table S6). These endpoints were not significantly different from a laboratory control (p=0.502 and 0.321, respectively). Survival and biomass of *P. promelas* fry exposed to OSPW in the photocatalysis, photolysis, and dark control treatments were not significantly different from a laboratory control (Table S6). However, fry exposed to OSPW treated by photocatalysis had the greatest biomass (494±39 µg) followed by photolysis (432±77 µg), and biomass was least in the dark control (409±28 µg).

4.0 Discussion

4.1 Absorption and attenuation of UV radiation in OSPW

To achieve charge separation and initiate photocatalysis, TiO_2 must absorb UV radiation with wavelengths <400 nm (Fujishima et al., 2000). Comparison of terrestrial and spaceborne reference solar irradiance spectra demonstrates that 0% of UV-C, 0 to

15% of UV-B, and 15 to 65% of UV-A radiation is transmitted through the atmosphere (Figure S2; ATSM, 2012; Gueymard, 2003). Terrestrial irradiance distribution deviates from the ASTM reference spectrum with changes in location, elevation, and atmospheric conditions (ATSM, 2012). Mean transmittance of detectable terrestrial UV-B wavelengths (i.e. 305 to 315 nm; ASTM, 2012) is 67% in OSPW, and mean transmittance of UV-A radiation in OSPW is 80%. Photoexcitation conditions of TiO_2 and transmittance of UV radiation in OSPW and the atmosphere suggest that wavelengths between 305 and 400 nm are the primary source of irradiance for film-based photocatalysis of OSPW. Across this range, UV-A radiation has greater terrestrial spectral irradiance and transmittance through OSPW than UV-B radiation, supporting that UV-A radiation is the primary source of UV photons for film-based solar photocatalysis of OSPW.

These data suggest that the broadband UV sensor used to determine attenuation of solar UV irradiance in OSPW was measuring predominantly UV-A radiation. Compared to oligotrophic freshwater water lakes, in which UV radiation may penetrate meters (Wetzel, 1975), OSPW used in the photocatalysis experiment strongly attenuated solar UV radiation, as <10% of surface UV irradiance was measured at depths >20 cm. Multiple studies measuring light absorption in OSPWs and solutions of NAFCs found that UV radiation is strongly absorbed by OSPW NAs (McMartin et al., 2004; Leshuk et al., 2016a,b). TSS and O&G increased attenuation of UV light in OSPW by scattering and absorbing UV photons, as demonstrated by 2.2-times greater attenuation coefficients in turbid OSPW (69±11 mg/L TSS, 30 mg/L O&G) compared to OSPW with 6±2 mg/L

TSS and no measurable O&G. Floating bitumen and hydrocarbon sheens, which have been observed in some OSPWs (Gosselin et al., 2010; Allen, 2008; McQueen et al., 2017a), may require treatment prior to photocatalysis to decrease attenuation of UV radiation (Clark et al., 2009). Dissolved iron may complex with organic acids in OSPW and strongly absorb UV light (Leshuk et al., 2016b). Iron concentrations in OSPW treated in this study were only 0.086±0.010 mg/L, compared to 13.1 mg/L measured by Leshuk et al. (2016b) in strongly colored OSPW, and likely did not have a measureable effect on UV absorption.

Measurement of UV absorption and attenuation in OSPW will be important steps in designing pilot- and full-scale photocatalytic reactors and determining if pretreatment is necessary, as attenuation of solar UV radiation is a major factor in determining throughput of fixed-bed photoreactors (Bousselmi et al., 2004; Zayani et al., 2009). Low TSS and absence of a hydrocarbon sheen (oil and grease <4 mg/L) precluded OSPW used in this experiment from pretreatment prior to photocatalysis. For pretreatment of OSPW at tailings facilities, constructed wetlands offer a low-energy and low-maintenance approach for settling suspended solids, precipitating soluble iron, and degrading hydrocarbons (Rodgers and Castle, 2008; Pardue et al., 2014; McQueen et al., 2017b).

Absorption spectra of samples from the photocatalytic reactors and previous research on agglomeration and sedimentation of TiO_2 (Keller et al., 2010; Brunelli et al., 2013) support that bench-scale settled TiO_2 photocatalytic reactors were suitable proxies for immobilized catalyst layers. Samples collected from the water column of the photocatalytic reactors 0.5 h after OSPW/TiO_2 suspensions were poured showed only

slightly lower transmittance of UV radiation than OSPW with no TiO_2 (73% versus 88% at 400 nm), suggesting that a small amount of TiO_2 was still suspended. However, transmittance in a sample collected 2 h after experiment initiation was equal or greater than in initial OSPW, supporting that TiO_2 had settled. Keller et al. (2010) found that agglomeration and settling rates of TiO_2 increase commensurately with initial concentration, supporting that high initial TiO_2 concentrations (1,000 mg/L) in the photocatalytic reactors promoted rapid sedimentation. Brunelli et al. (2013) concluded that initial concentration, over ionic strength and dissolved organic matter concentration, was the primary factor in determining settling rates even at low TiO_2 concentrations (i.e. 0.01 to 10 mg/L).

4.2 Rates and extents of NA degradation

NA degradation proceeded at faster rates and achieved greater removal in terms of both concentration and mass in photocatalytic reactors, compared to photolytic and dark control reactors. Photocatalytic reactors decreased NA concentration by the midpoint of the experiment (t=16 h; E=1.78 MJ·m^{-2}; τ=32 h), while concentrations increased in photolytic reactors due to evaporation. Photolysis decreased NA mass by 39±8% after a 32-h photoperiod and 3.57 MJ·m^{-2} of UV insolation; however, the mean UV insolation half-life for photolysis was 4.5 times greater than the half-life for photocatalysis. Settled TiO_2 photocatalytic reactors decreased NA mass by 40% after only 7 h of sunlight exposure and 0.7 MJ·m^{-2} of UV insolation. NA mass in the dark controls decreased by ~8% while concentration increased by ~9%, but neither change was significantly different from initial values (p=0.21 and 0.24, respectively).

Settled TiO_2 photocatalytic reactors achieved approximately 86% removal of NA mass in OSPW, but degradation rates were slower than in studies utilizing TiO_2 slurries. Headley et al. (2009) observed 86% removal of NAFCs in solution with distilled water after 8 h of sunlight exposure in bench-scale TiO_2 slurry photoreactors (i.e. transparent Petri flasks with 2 g/L TiO_2). Leshuk et al. (2016a) decreased NAFC concentrations by >98% after one day of direct sunlight (~14 h photoperiod) using solar photocatalysis over a 0.5 mg/L agitated suspension of TiO_2 in OSPW. The inorganic composition of OSPW used in this research is similar to centrifuged OSPWs used by Leshuk et al. (2016 a,b), so the discrepancy in performance is attributed primarily to poor mass transfer in the settled TiO_2 reactors, where only diffusion and wind-shear contributed to mixing. When photocatalyst particles are immobilized in films or are poorly agitated, photonic efficiency is diminished due to decreased surface area available for adsorption of contaminants and absorption of UV photons (Malato et al., 2009). Efficiency of film-based reactors is increased by maximizing throughput, which improves mass transfer of reactants, oxygen, and degradation byproducts (Zayani et al., 2009). However, Bouseelmi et al. (2004) and Zayani et al. (2009) found that improving degradation rates by increasing throughput in pilot-scale thin film fixed-bed photocatalytic reactors was eventually limited by increases in laminar liquid film thickness, which attenuated solar UV radiation. Rates and extents of NA removal in settled TiO_2 batch reactors provide a conservative proof of concept for film-based photocatalysis of NAs in OSPW and may be improved by introducing flow and utilizing films of immobilized TiO_2.

The photolytic reactors used in this study represent close to ideal conditions for photolysis as they received direct sunlight, were reconstituted, and had a high surface area relative to depth (3,481 cm^2 to 1 cm). Thus, the removal of NA mass by photolysis was greater in this research compared to previous studies (McMartin et al., 2007; Headley et al., 2009; Leshuk et al., 2016a), which used UV-transparent sealed vessels that prevented evaporation. However, NA concentrations in the photolytic reactors increased by 59% at the experiment midpoint, demonstrating that photolysis is not a viable pathway without reconstitution.

The minor removal of NA mass in dark control reactors (~8% decrease) is consistent with previous photocatalysis experiments in closed systems, which report 4 to 9% decreases in NA concentration attributed to adsorption onto TiO_2 (Headley et al., 2009; Leshuk et al., 2016a). Concentrations of Na^+, Ca^{2+}, Mg^{2+}, and SO_4^{2-} measured in the dark controls may decrease solubility of NAs (Janfada et al., 2006), which combined with the high surface area of Aeroxide® TiO_2 (55±15 $m^2 \cdot g^{-1}$) may promote adsorption of weakly polar, hydrophobic polycyclic NAs onto catalyst particles (Kannel and Gan, 2012). Janfada et al. (2006) concluded that low partitioning to the water column is expected for NAs and observed rapid sorption of OSPW NAs dissolved in synthetic groundwater to soil particles under pH and temperature conditions (8.0±0.4 and 23±1°C, respectively) similar to pH and temperature in the photocatalysis experiment. Additionally, surrogate NAs, such as benzoic acid, have been shown to adsorb to TiO_2 nanoparticles (Zhang et al., 2005; Chan et al., 2002; Vione et al., 2005).

As indicated by final concentrations of NAs and COD (18±5 and 31±33 mg/L, respectively), complete mineralization of NAs was not achieved in the photocatalytic reactors. However, BOD/COD ratios, which can be used as an indicator of biodegradability (OECD, 1992), increased from 0.018 to 0.19 after photocatalysis of OSPW. Increased biological activity in inoculated samples of post-photocatalysis OSPW is attributed to transformation of NAs to more labile degradation intermediates (Leshuk et al. 2016a). Early work on photocatalysis of OSPW NAs suggested that lower molecular weight NAs were targeted (Headley et al., 2009), but ultra-high resolution Oribtrap-MS indicates that structurally complex (i.e. polycyclic and/or high double bond equivalence) and higher carbon-number NAs are preferentially degraded during photocatalysis (Leshuk et al., 2016a). Additionally, photocatalysis shifts distributions of NAFC classes from regimes dominated by classical NAs (i.e. O_2 NAFCs) to regimes enriched in poly-oxygenated NAs (Leshuk et al., 2016a). Complex, higher molecular weight NAFCs are recalcitrant to biodegradation (Scott et al., 2005; Han et al., 2008; Martin et al., 2009, Brown and Ulrich, 2015), and the ability of photocatalysis to transform these compounds into more labile degradation intermediates suggests that this pathway could be paired with aerobic degradation as a hybrid approach for treating NAs in OSPW.

4.3 Changes in Toxicity to Sentinel Species

Survival and reproduction of *C. dubia* were more sensitive endpoints for measuring toxicity of OSPW exposures and treatments (i.e. photocatalysis, photolysis, dark controls) compared to survival and biomass of *P. promelas*. A previous toxicological investigation of OSPW received in the ~40,000 L shipment measured

lowest observed effect concentrations (LOECs) for *P. promelas* growth and *C. dubia* reproduction of 50% and 25% OSPW, respectively (McQueen et al., 2017a). However, as noted in the results, survival and biomass of *P. promelas* exposed to OSPW used in the current investigation was not significantly different from laboratory controls (p=0.502 and 0.321, respectively) in this experiment. In the first toxicity identification evaluation of OSPW, Verbeek (1994) ameliorated acute OSPW toxicity by C18 absorption, thus attributing adverse effects to polar organics. Multiple studies have confirmed the conclusion of this seminal work (Marentette et al., 2015a,b; McQueen et al., 2017a), and effects directed analysis has specifically implicated classical O_2 NAs as the primary source of toxicity in OSPW (Morandi et al., 2015; Hughes et al, 2017). However, Zubot et al. (2012) concluded that impaired survival and reproduction of salinity-sensitive *C. dubia* (Cl^- EC_{50}=461 mg/L) in OSPW may be attributed to synergism between dissolved salts and the organic fraction.

Photocatalysis was the most effective treatment for altering exposures of OSPW to *C. dubia*, yielding the least mortality and greatest number of neonates per adult daphnid. However, survival and reproduction of *C. dubia* also improved in photolysis and dark control treatments, relative to untreated OSPW. NA concentrations were significantly different between treatments and OSPW (p<0.001), yet survival and reproduction of *C. dubia* exposed to all treatments was not different from control organisms. This result is another example of how changes in NA concentration are not necessarily correlated to toxicity (Brown and Ulrich, 2015; Mahaffey and Dubé, 2016; McQueen et al., 2017b). Minor differences in water quality characteristics and

concentrations of ions and metals measured in OSPW and the treatments were unlikely to significantly influence toxicity. The change in response of *C. dubia* exposed to OSPW from the photocatalytic and photolytic reactors and the dark controls is therefore attributed to compositional alteration of NAs.

After photocatalysis over suspended TiO_2, Leshuk et al. (2016a) measured a shift in the relative abundance of NA classes from "classical", O_2 NAFCs to poly-oxygenated classes, which are sparingly toxic relative to O_2 NAs (Morandi et al., 2015). Slurry photocatalysis of OSPW altered composition within NAFCs classes, increasing the relative abundance of lower weight and less complex (i.e. lower double bond equivalence) compounds (Leshuk et al., 2016a). Similar compositional alteration of NAs is assumed to have occurred in the settled TiO_2 photocatalytic reactors used in this experiment, although the extent of transformation may be lower. Klamerth et al. (2015) suggested that degradation byproducts from advanced oxidation of NAs in OSPW may potentially increase toxicity. However, no evidence of increased toxicity after photocatalysis was found in this study, which may be the first to measure toxicity of OSPW to sentinel aquatic species before and after photocatalysis.

Photolysis decreased NA mass and likely altered the composition of NAs in OSPW. Prince et al. (2003) determined that polycyclic aromatic hydrocarbons with greater degrees of alkylation are more susceptible to photolysis. Because naphthenic acids consist predominantly of alkyl-substituted cycloaliphatic carboxylic acids (Headley and McMartin, 2004) and are known to contain aromatic compounds (Mohamed et al., 2008), it is feasible that these compounds would be targeted in photolysis of OSPW.

Scarlett et al. (2013) found that an aromatic fraction of NAs extracted from OSPW was acutely toxic to larval zebra fish, and it is possible that elimination of these compounds explains increased survival and reproduction of *C. dubia* after photolysis of OSPW.

Removal of toxicity by the dark controls was unexpected, especially since the samples were not reconstituted resulting in higher concentrations of NAs and salinity. This result may be anomalous, as it seems unlikely that adsorption or aerobic degradation, which are the most likely treatment pathways in the dark controls, could have altered NA composition sufficiently to improve survival and reproduction of *C. dubia*. Phosphorus concentrations decreased in the dark control, and temperature, DO, and pH were within ranges found to promote degradation of a commercial blend of NAs (Kinley et al., 2016), but only continuous flow biofilm reactors have achieved measurable degradation of NAs in OSPW within a duration similar to that of this experiment (i.e., 64 h; Hwang et al., 2013; McKenzie et al., 2014). Removal of benzoic acid, a simple single ring aromatic carboxylic acid that has been used as a surrogate NA (Zhang et al., 2005), has been detected in dark controls in previous photocatalysis experiments and attributed to sorption (Chan et al., 2002; Vione et al., 2005). However, since removal of NA mass was not significant in the dark controls, changes in NA exposure by either aerobic degradation or sorption would have been limited to compositional changes not detectable by derivatization and HPLC.

These toxicity experiments suggest that photocatalysis may be a suitable mechanism for rapid amelioration of toxicity from OSPW. However, it must be noted that exposures from the photocatalytic and photolytic reactors were altered by periodic

reconstitution during sunlight exposure. This procedure impacted results of the bioassays, given the low salt tolerance of *C. dubia*, but allowed effects of changes in the organic fraction to be assessed.

5.0 Conclusions

Rates and extents of NA degradation and changes in response of *Ceriodaphnia dubia* and *Pimephales promelas* were measured in a specific OSPW treated by photocatalysis over settled TiO_2 as a proof-of-concept for film-based photocatalysis. Absorption of UV light in OSPW was measured, determining that UV-A radiation is the primary source of solar irradiance driving film-based photocatalysis. In OSPW with <4 mg/L O&G and 6±2 mg/L TSS, attenuation of UV radiation was attributed to absorption by NAFCs resulting in an attenuation coefficient of -0.13 cm^{-1} for UV radiation. Photocatalysis over settled TiO_2 removed ~37% of NA concentration after 1.78 $MJ \cdot m^{-2}$ of UV insolation over a 16 h photoperiod and ~86% of NA mass after 32 h of sunlight exposure and 3.57 $MJ \cdot m^{-2}$ of UV insolation. NA mass decreased exponentially with 50% degradation at approximately 1.1 $MJ \cdot m^{-2}$ and 10 h of sunlight exposure. Measurable NA mass removal occurred in photolytic reactors (~39% removal), but degradation occurred slower rates ($T_{0.5E_m}$=5.0 $MJ \cdot m^{-2}$, $T_{0.5t_m}$= 46 h). Survival and reproduction of *C. dubia* were impaired in exposures of OSPW, but there were no significant differences in survival and biomass of *P. promelas* exposed to untreated OSPW. Daphnids exposed to OSPW treated by photocatalysis showed highest reproduction, but photolysis and dark control treatments also increased survival and reproduction of *C. dubia* relative to untreated OSPW.

In the specific OSPW studied, photocatalysis over settled TiO_2 degraded NAs, providing a proof-of-concept for film-based photocatalysis of OSPW. Bench-scale experimentation with flow-through fixed-film reactors is warranted to improve the performance of film-based TiO_2 photocatalysis for treatment of OSPW. To increase rates of NA removal, pre-treatment of suspended solids and oil sheens prior to photocatalysis may be required for some OSPWs. Increased BOD:COD ratios after photocatalysis suggests that pairing photocatalysis with aerobic degradation may be a more effective method for treating NAs in OSPW than photocatalysis alone. This study is a first step in development of film-based photocatalysis for treatment of OSPW and the integration of this technology into passive systems capable of mitigating risks associated with this mixture.

6.0 References

Alberta Energy Regulator (AER), 2012. Alberta's Energy Reserves 2011 and Supply/Demand Outlook 2012–2021. ST98-2012. https://www.aer.ca/documents/sts/ST98/ST98-2012.pdf.

Allen, E.W., 2008. Process water treatment in Canada's oil sands industry: I. Target pollutants and treatment objectives. *Journal of Environmental Engineering and Science.* 7, 123-138.

American Public Health Association (APHA), American Water Works Association, Water Environment Federation, 2012. Standard methods for the examination of water and wastewater, 21st edition. American Public Health Association, Port City Press., Baltimore, MA.

Armstrong, S.A., Headley, J.V., Peru, K.M., Germida, J.J., 2007. Phytotoxicity of oil sands naphthenic acids and dissipation from systems planted with emergent aquatic macrophytes. *Journal of Environmental Science and Health, Part A.* 43, 36-42.

American Society for Testing and Materials (ASTM), 2012. Standard Tables for Reference Solar Spectral Irradiances: Direct Normal and Hemispherical on 37 Tilted Surface. G173-03. ASTM International, West Conshohocken, PA.

Barrow, M.P., Headley, J.V., Peru, K.M., Derrick, P.J., 2009. Data visualization for the characterization of naphthenic acids within petroleum samples. *Energy & Fuels.* 23, 2592-2599.

Bartlett, A.J., Frank, R.A., Gillis, P.L., Parrott, J.L., Marentette, J.R., Brown, L.R., Hooey, T., Vanderveen, R., McInnis, R., Brunswick, P., 2017. Toxicity of naphthenic acids to invertebrates: Extracts from oil sands process-affected water versus commercial mixtures. *Environmental Pollution.* 227, 271-279.

Bousselmi, L., Geissen, S., Schroeder, H., 2004. Textile wastewater treatment and reuse by solar catalysis: results from a pilot plant in Tunisia. *Water Science and Technology.* 49, 331-337.

Brient, J.A., Wessner, P.J., Doyle, M.N., 1995. Naphthenic acids. In: Kroschwitz, J.I. (Ed.). *Encyclopedia of Chemical Technology*. John Wiley & Sons, New York, 1017-1029.

Brown, L.D. and Ulrich, A.C., 2015. Oil sands naphthenic acids: a review of properties, measurement, and treatment. *Chemosphere.* 127, 276-290.

Brunelli, A., Pojana, G., Callegaro, S., Marcomini, A., 2013. Agglomeration and sedimentation of titanium dioxide nanoparticles (n-TiO_2) in synthetic and real waters. *Journal of Nanoparticle Research.* 15, 1684.

Canadian Council of Ministers of the Environment (CCME), 2011. Canadian water quality guidelines for the protection of aquatic life. Canadian environmental quality guidelines, 1999. Canadian Council of Ministers of the Environment, Winnipeg, MB.

Carpenter, S.R., Kitchell, J.F., Hodgson, J.R., 1985. Cascading trophic interactions and lake productivity. *Bioscience.* 35, 634-639.

Chan, A.H., Chan, C.K., Barford, J.P., Porter, J.F., 2003. Solar photocatalytic thin film cascade reactor for treatment of benzoic acid containing wastewater. *Water Research.* 37, 1125-1135.

Chong, M.N., Jin, B., Chow, C.W., Saint, C., 2010. Recent developments in photocatalytic water treatment technology: a review. *Water Research.* 44, 2997-3027.

Clark, R.N., Curchin, J.M., Hoefen, T.M., Swayze, G.A., 2009. Reflectance spectroscopy of organic compounds: 1. Alkanes. *Journal of Geophysical Research: Planets.* 114.

Clemente, J.S.and Fedorak, P.M., 2005. A review of the occurrence, analyses, toxicity, and biodegradation of naphthenic acids. *Chemosphere.* 60, 585-600.

Drzewicz, P., Perez-Estrada, L., Alpatova, A., Martin, J.W., Gamal El-Din, M., 2012. Impact of peroxydisulfate in the presence of zero valent iron on the oxidation of cyclohexanoic acid and naphthenic acids from oil sands process-affected water. *Environmental Science & Technology.* 46, 8984-8991.

Environment and Climate Change Canada (ECCC), 2011. Biological test method: larval growth and survival using fathead minnows. EPS 1/RM/22. 2nd edition. Environment and Climate Change Canada, Ottawa, ON.

Environment and Climate Change Canada (ECCC), 2007. Biological test method: test of reproduction and survival using the Cladoceran *Ceriodaphnia dubia*. EPS 1/RM/21 2nd edition. Environment and Climate Change Canada, Ottawa, ON.

Fujishima, A., Rao, T.N., Tryk, D.A., 2000. Titanium dioxide photocatalysis. *Journal of Photochemistry and Photobiology C: Photochemistry Reviews.* 1, 1-21.

Gaya, U.I. and Abdullah, A.H., 2008. Heterogeneous photocatalytic degradation of organic contaminants over titanium dioxide: a review of fundamentals, progress and problems. *Journal of Photochemistry and Photobiology C: Photochemistry Reviews.* 9, 1-12.

Gosselin, P., Hrudey, S.E., Naeth, M.A., Plourde, A., Therrien, R., Van Der Kraak, G., Xu, Z., 2010. Environmental and health impacts of Canada's oil sands industry. The Royal Society of Canada, Ottawa, ON.

Grewer, D.M., Young, R.F., Whittal, R.M., Fedorak, P.M., 2010. Naphthenic acids and other acid-extractables in water samples from Alberta: what is being measured? *Science of the Total Environment.* 408, 5997-6010.

Gueymard, C.A., 2003. The sun's total and spectral irradiance for solar energy applications and solar radiation models. *Solar Energy.* 76, 423-453.

Han, X., MacKinnon, M.D., Martin, J.W., 2009. Estimating the *in-situ* biodegradation of naphthenic acids in oil sands process waters by HPLC/HRMS. *Chemosphere.* 76, 63-70.

Han, X., Scott, A.C., Fedorak, P.M., Bataineh, M., Martin, J.W., 2008. Influence of molecular structure on the biodegradability of naphthenic acids. *Environmental Science & Technology.* 42, 1290-1295.

Headley, J.V., Du, J., Peru, K.M., McMartin, D.W., 2009. Electrospray ionization mass spectrometry of the photodegradation of naphthenic acids mixtures irradiated with titanium dioxide. *Journal of Environmental Science and Health Part A.* 44, 591-597.

Headley, J.V. and McMartin, D.W., 2004. A review of the occurrence and fate of naphthenic acids in aquatic environments. *Journal of Environmental Science and Health, Part A.* 39, 1989-2010.

Headley, J.V., Peru, K.M., Fahlman, B., McMartin, D.W., Mapolelo, M.M., Rodgers, R.P., Marshall, A.G., 2012. Comparison of the levels of chloride ions to the characterization of oil sands polar organics in natural waters by use of Fourier transform ion cyclotron resonance mass spectrometry. *Energy & Fuels*, 26(5), 2585-2590.

Hein, F.J., Leckie, D., Larter, S., Suter, J.R., 2013. Heavy oil and bitumen petroleum systems in Alberta and beyond: The future is nonconventional and the future is now. In: Hein, F.J., Leckie, D., Larter, S., Suter, J.R. (Eds.). Heavy-Oil and Oil-Sand Petroleum Systems in Alberta and Beyond. *AAPG Studies in Geology*. 64, 1. 1-21. American Association of Petroleum Geologists (AAPG) Special Volumes.

Hughes, S.A., Mahaffey, A., Shore, B., Baker, J., Kilgour, B., Brown, C., Peru, K.M., Headley, J.V., Bailey, H.C., 2017. Using ultrahigh-resolution mass spectrometry and toxicity identification techniques to characterize the toxicity of oil sands process-affected water: the case for classical naphthenic acids. *Environmental Toxicology and Chemistry*. Online version of record, August 7, 2017.

Hwang, G., Dong, T., Islam, M.S., Sheng, Z., Pérez-Estrada, L.A., Liu, Y., El-Din, M.G., 2013. The impacts of ozonation on oil sands process-affected water biodegradability and biofilm formation characteristics in bioreactors. *Bioresource Technology*. 130, 269-277.

Janfada, A., Headley, J.V., Peru, K.M., Barbour, S., 2006. A laboratory evaluation of the sorption of oil sands naphthenic acids on organic rich soils. *Journal of Environmental Science and Health Part A.* 41, 985-997.

Kannel, P.R. and Gan, T.Y., 2012. Naphthenic acids degradation and toxicity mitigation in tailings wastewater systems and aquatic environments: a review. *Journal of Environmental Science and Health, Part A.* 47, 1-21.

Kavanagh, R.J., Frank, R.A., Oakes, K.D., Servos, M.R., Young, R.F., Fedorak, P.M., MacKinnon, M.D., Solomon, K.R., Dixon, D.G., Van Der Kraak, G., 2011. Fathead minnow (*Pimephales promelas*) reproduction is impaired in aged oil sands process-affected waters. *Aquatic Toxicology.* 101, 214-220.

Keller, A.A., Wang, H., Zhou, D., Lenihan, H.S., Cherr, G., Cardinale, B.J., Miller, R., Ji, Z., 2010. Stability and aggregation of metal oxide nanoparticles in natural aqueous matrices. *Environmental Science & Technology.* 44, 1962-1967.

Kinley, C.M., Gaspari, D.P., McQueen, A.D., Rodgers, J.H., Castle, J.W., Friesen, V., Haakensen, M., 2016. Effects of environmental conditions on aerobic degradation of a commercial naphthenic acid. *Chemosphere.* 161, 491-500.

Klamerth, N., Moreira, J., Li, C., Singh, A., McPhedran, K.N., Chelme-Ayala, P., Belosevic, M., El-Din, M.G., 2015. Effect of ozonation on the naphthenic acids' speciation and toxicity of pH-dependent organic extracts of oil sands process-affected water. *Science of the Total Environment.* 506, 66-75.

Leshuk, T., de Oliveira Livera, D., Peru, K.M., Headley, J.V., Vijayaraghavan, S., Wong, T., Gu, F., 2016. Photocatalytic degradation kinetics of naphthenic acids in oil sands process-affected water: Multifactorial determination of significant factors. *Chemosphere.* 165, 10-17.

Leshuk, T., Wong, T., Linley, S., Peru, K.M., Headley, J.V., Gu, F., 2016. Solar photocatalytic degradation of naphthenic acids in oil sands process-affected water. *Chemosphere.* 144, 1854-1861.

Madill, R.E., Orzechowski, M.T., Chen, G., Brownlee, B.G., Bunce, N.J., 2001. Preliminary risk assessment of the wet landscape option for reclamation of oil sands mine tailings: bioassays with mature fine tailings pore water. *Environmental Toxicology.* 16, 197-208.

Mahaffey, A. and Dubé, M., 2016. Review of the composition and toxicity of oil sands process-affected water. *Environmental Reviews.* 25, 97-114.

Malato, S., Fernández-Ibáñez, P., Maldonado, M.I., Blanco, J., Gernjak, W., 2009. Decontamination and disinfection of water by solar photocatalysis: recent overview and trends. *Catalysis Today.* 147, 1-59.

Marentette, J.R., Frank, R.A., Bartlett, A.J., Gillis, P.L., Hewitt, L.M., Peru, K.M., Headley, J.V., Brunswick, P., Shang, D., Parrott, J.L., 2015a. Toxicity of naphthenic acid fraction components extracted from fresh and aged oil sands process-affected waters, and commercial naphthenic acid mixtures, to fathead minnow (*Pimephales promelas*) embryos. *Aquatic Toxicology.* 164, 108-117.

Marentette, J.R., Frank, R.A., Hewitt, L.M., Gillis, P.L., Bartlett, A.J., Brunswick, P., Shang, D., Parrott, J.L., 2015b. Sensitivity of walleye (*Sander vitreus*) and fathead minnow (*Pimephales promelas*) early-life stages to naphthenic acid fraction components extracted from fresh oil sands process-affected waters. *Environmental Pollution.* 207, 59-67.

Martin, J.W., Barri, T., Han, X., Fedorak, P.M., El-Din, M.G., Perez, L., Scott, A.C., Jiang, J.T., 2010. Ozonation of oil sands process-affected water accelerates microbial bioremediation. *Environmental Science & Technology.* 44, 8350-8356.

McKenzie, N., Yue, S., Liu, X., Ramsay, B.A., Ramsay, J.A., 2014. Biodegradation of naphthenic acids in oils sands process waters in an immobilized soil/sediment bioreactor. *Chemosphere.* 109, 164-172.

McMartin, D.W., Headley, J.V., Friesen, D.A., Peru, K.M., Gillies, J.A., 2004. Photolysis of naphthenic acids in natural surface water. *Journal of Environmental Science and Health, Part A.* 39, 1361-1383.

McQueen, A.D., Kinley, C.M., Hendrikse, M., Gaspari, D.P., Calomeni, A.J., Iwinski, K.J., Castle, J.W., Haakensen, M.C., Peru, K.M., Headley, J.V., 2017a. A risk-based approach for identifying constituents of concern in oil sands process-affected water from the Athabasca Oil Sands region. *Chemosphere.* 173, 340-350.

McQueen, A.D., Hendrikse, M., Gaspari, D.P., Kinley, C.M., Rodgers, J.H., Castle, J.W., 2017b. Performance of a hybrid pilot-scale constructed wetland system for treating oil sands process-affected water from the Athabasca Oil Sands. *Ecological Engineering.* 102, 152-165.

McQueen, A.D., Kinley, C.M., Kiekhaefer, R.L., Calomeni, A.J., Rodgers, J.H., Castle, J.W., 2016a. Photocatalysis of a commercial naphthenic acid in water using fixed-film TiO_2. *Water, Air, & Soil Pollution.* 227, 132.

Mikula, R., 2013. Trading water for oil: Tailings management and water use in surface-mined oil sands. In: Hein, F.J., Leckie, D., Larter, S., Suter, J.R. (Eds.). Heavy Oil and Oil-Sand Petroleum Systems in Alberta and Beyond. *AAPG Studies in Geology* 64: 1, 689-699. American Association of Petroleum Geologists (AAPG) Special Volumes.

Mishra, S., Meda, V., Dalai, A.K., McMartin, D.W., Headley, J.V., Peru, K.M., 2010. Photocatalysis of naphthenic acids in water. *Journal of Water Resource and Protection.* 2, 644.

Mohamed, M.H., Wilson, L.D., Headley, J.V., Peru, K.M., 2008. Screening of oil sands naphthenic acids by UV-Vis absorption and fluorescence emission spectrophotometry. *Journal of Environmental Science and Health Part A.* 43, 1700-1705.

Morandi, G.D., Wiseman, S.B., Pereira, A., Mankidy, R., Gault, I.G., Martin, J.W., Giesy, J.P., 2015. Effects-directed analysis of dissolved organic compounds in oil sands process-affected water. *Environmental Science & Technology.* 49, 12395-12404.

Organization for Economic Cooperation and Development (OECD), 2002. Guidance Document on Aquatic Toxicity Testing of Difficult Substances and Mixtures, 23rd edition. Organization for Economic Co-operation and Development, Paris, FR.

Organization for Economic Cooperation and Development (OECD), 1992. Test No. 301: Ready Biodegradability. Organization for Economic Co-operation and Development, Paris, FR.

Pardue, M.J., Castle, J.W., Rodgers, J.H., Huddleston, G.M., 2014. Treatment of oil and grease in produced water by a pilot-scale constructed wetland system using biogeochemical processes. *Chemosphere.* 103, 67-73.

Pennak, R.W., 1978. Freshwater invertebrates of the United States, 2nd edition. John Wiley & Sons. New York, NY.

Prince, R.C., Garrett, R.M., Bare, R.E., Grossman, M.J., Townsend, T., Suflita, J.M., Lee, K., Owens, E.H., Sergy, G.A., Braddock, J.F., 2003. The roles of photooxidation and biodegradation in long-term weathering of crude and heavy fuel oils. *Spill Science & Technology Bulletin.* 8, 145-156.

Quinlan, P.J. and Tam, K.C., 2015. Water treatment technologies for the remediation of naphthenic acids in oil sands process-affected water. *Chemical Engineering Journal.* 279, 696-714.

Rodgers Jr, J.H. and Castle, J.W., 2008. Constructed wetland systems for efficient and effective treatment of contaminated waters for reuse. *Environmental Geosciences.* 15, 1-8.

Rogers, V.V., Wickstrom, M., Liber, K., MacKinnon, M.D., 2002. Acute and subchronic mammalian toxicity of naphthenic acids from oil sands tailings. *Toxicological Sciences.* 66, 347-355.

Rowland, S.J., Scarlett, A.G., Jones, D., West, C.E., Frank, R.A., 2011. Diamonds in the rough: identification of individual naphthenic acids in oil sands process water. *Environmental Science & Technology.* 45, 3154-3159.

Scarlett, A., Reinardy, H., Henry, T., West, C., Frank, R., Hewitt, L., Rowland, S., 2013. Acute toxicity of aromatic and non-aromatic fractions of naphthenic acids extracted from oil sands process-affected water to larval zebrafish. *Chemosphere.* 93, 415-420.

Scott, A.C., Mackinnon, M.D., Fedorak, P.M., 2005. Naphthenic acids in Athabasca oil sands tailings waters are less biodegradable than commercial naphthenic acids. *Environmental Science & Technology.* 39, 8388-8394.

Scott, A.C., Zubot, W., MacKinnon, M.D., Smith, D.W., Fedorak, P.M., 2008. Ozonation of oil sands process water removes naphthenic acids and toxicity. *Chemosphere.* 71, 156-160.

Scott, W.B. and Crossman, E.F., 1978. Freshwater Fishes of Canada. Fisheries Research Board of Canada, Ottawa, Ontario.

Sohrabi, V., Ross, M., Martin, J., Barker, J., 2013. Potential for *in situ* chemical oxidation of acid extractable organics in oil sands process affected groundwater. *Chemosphere.* 93, 2698-2703.

Toor, N.S., Han, X., Franz, E., MacKinnon, M.D., Martin, J.W., Liber, K., 2013. Selective biodegradation of naphthenic acids and a probable link between mixture profiles and aquatic toxicity. *Environmental Toxicology and Chemistry.* 32, 2207-2216.

United States Environmental Protection Agency (USEPA), 2007. National recommended water quality criteria-correction. EPA 822-Z-99–001. Office of Water, Washington, DC.

United States Environmental Protection Agency (USEPA), 2002. Short-term methods for estimating the chronic toxicity of effluents and receiving waters to freshwater organisms. 4th edition. EPA-821-R-02-013. Environmental Monitoring Systems Lab, Cincinnati, OH.

United States Environmental Protection Agency (USEPA), 2001. Trace elements in water, solids, and biosolids by inductively coupled plasma-atomic emission spectrometry. 5th Revision. EPA Method 200.7. EPA-821-R-01-010. Office of Water, Washington, DC.

United States Environmental Protection Agency (USEPA), 1999. Revision A: n-hexane extractable material (HEM; oil and grease) and silica gel treated n-hexane extractable material (SGTHEM; non-polar material) by extraction and gravimetry. EPA Method 1664. EPA-821-R-10-001. Office of Water, Washington, DC.

Verbeek, A.G., 1994. A toxicity assessment of oil sands wastewater. University of Alberta, Edmonton, AB. Master's Thesis.

Vione, D., Minero, C., Maurino, V., Carlotti, M.E., Picatonotto, T., Pelizzetti, E., 2005. Degradation of phenol and benzoic acid in the presence of a TiO_2-based heterogeneous photocatalyst. *Applied Catalysis B: Environmental.* 58, 79-88.

Weather Underground, 2017. Station ID: KSCCLEMS1, Station Name: CU Ent Dept. 2016. https://www.wunderground.com/personal-weather-station/dashboard?ID=KSCCLEMS1#history/s20160227/e20160301/mcustom

Wetzel, R.G., 1975. Limnology: Lake and River Ecosystems, 3rd edition. Academic Press, San Diego, CA.

Yen, T., Marsh, W.P., MacKinnon, M.D., Fedorak, P.M., 2004. Measuring naphthenic acids concentrations in aqueous environmental samples by liquid chromatography. *Journal of Chromatography A.* 1033, 83-90.

Zayani, G., Bousselmi, L., Mhenni, F., Ghrabi, A., 2009. Solar photocatalytic degradation of commercial textile azo dyes: performance of pilot plant scale thin film fixed-bed reactor. *Desalination.* 246, 344-352.

Zhang, A., Ma, Q., Wang, K., Tang, Y., Goddard, W.A., 2005. Improved processes to remove naphthenic acids. Final Technical Report, Department of Energy (DOE) Contract number: DE-FC26-02NT15383. US DOE, Washington, DC.

Zubot, W., MacKinnon, M.D., Chelme-Ayala, P., Smith, D.W., El-Din, M.G., 2012. Petroleum coke adsorption as a water management option for oil sands process-affected water. *Science of the Total Environment.* 427, 364-372.

Figure 1. Transmittance of UV-A, UV-B, and UV-C radiation in OSPW, a suspension of 0.01 g/L TiO_2 in OSPW, and samples collected from photocatalytic reactors 0.5 and 2.0 h after a 1.0 g/L TiO_2/OSPW suspension was poured into the reactors. Wavelengths in the UV-A range were least absorbed in OSPW, and 0.01 g/L TiO_2 significantly decreased transmittance of UV radiation in OSPW (p<0.001). Transmittance of samples collected 0.5 and 2 h after TiO_2/OSPW suspensions were added to the reactors indicates that TiO_2 was suspended initially, but settled before 2 h.

Figure 2. Attenuation of solar UV radiation as a function of depth in two OSPWs. OSPW 1 contained 6±2 mg/L total suspended solids (TSS) and no measurable oil and grease (O&G; <4 mg/L), and OSPW 2 contained 69±11 mg/L TSS and 30 mg/L O&G. Each point represents mean UV irradiance (I) measured at depth, divided by incident UV irradiance (I_o). Data are correlated with exponential functions according to the Beer-Lambert law (Eqn. 2). Error bars represent standard deviation of five UV irradiance measurements made at 5-second intervals.

Figure 3. Naphthenic acid (NA) concentration in photocatalytic, photolytic, and dark control reactors plotted versus UV insolation. After an experimental duration of 32 h, UV insolation reached 1.78 $MJ \cdot m^{-2}$ over a photoperiod of 16 h. Each point represents mean NA concentration of three replicate reactors. Error bars represent one standard deviation (n=9).

Figure 4. Naphthenic acid (NA) mass in photocatalytic, photolytic, and dark control reactors plotted against UV insolation. After an experimental duration of 82 h, UV insolation reached 3.57 $MJ \cdot m^{-2}$ over a photoperiod of 32 h. Each point represents mean

NA mass measured in three replicate reactors. Error bars represent one standard deviation (n=9).

Figure 5. A) Percent survival of *C. dubia* exposed to untreated OSPW and photocatalysis, photolysis, and dark control treatments. B) Mean neonates produced in first 3 broods by *C. dubia* surviving after exposure to untreated OSPW and photocatalysis, photolysis, and dark control treatments. Asterisks above OSPW indicate survival and reproduction were statistically lower than laboratory control. Reproduction in all treatments was not different from the laboratory control (Table S5). Tukey's test indicates that the photocatalysis treatment had significantly greater reproduction than photolysis and dark control treatments (p = 0.0249 and 0.017, respectively).

Figure 6. A) Percent survival of *P. promelas* exposed to untreated OSPW and samples from photocatalytic, photolytic, and dark controls reactors. B) Cumulative mean biomass per surviving *P. promelas* fry. Error bars represent one standard deviation (n=3). There were no significant differences in survival and biomass between OSPW, the treatments, and laboratory controls (Table S6).

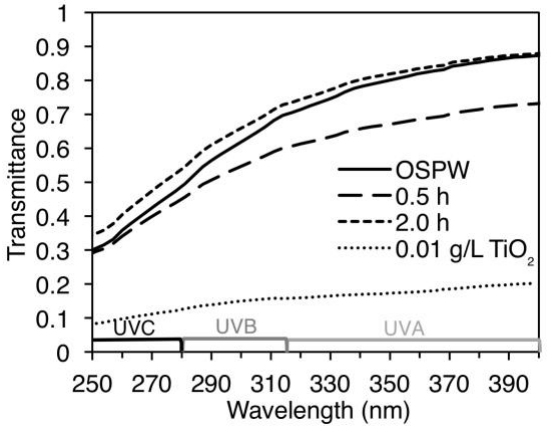

Figure 1

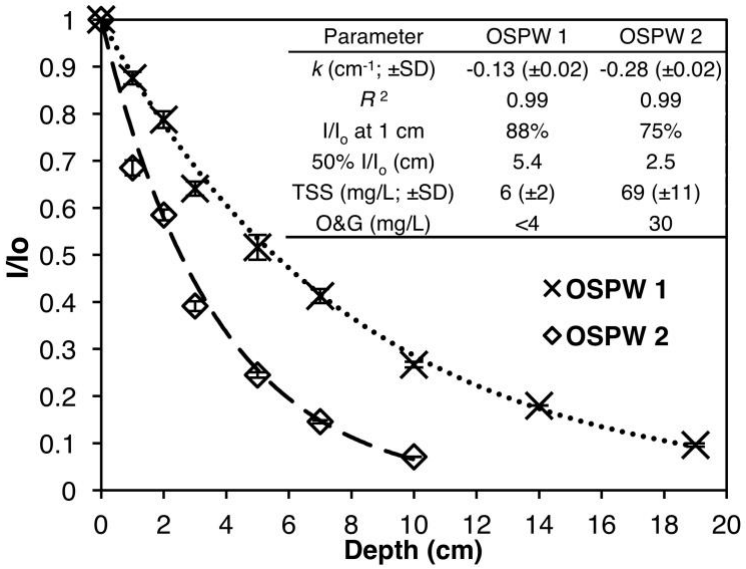

Parameter	OSPW 1	OSPW 2
k (cm^{-1}; ±SD)	-0.13 (±0.02)	-0.28 (±0.02)
R^2	0.99	0.99
I/I_o at 1 cm	88%	75%
50% I/I_o (cm)	5.4	2.5
TSS (mg/L; ±SD)	6 (±2)	69 (±11)
O&G (mg/L)	<4	30

Figure 2

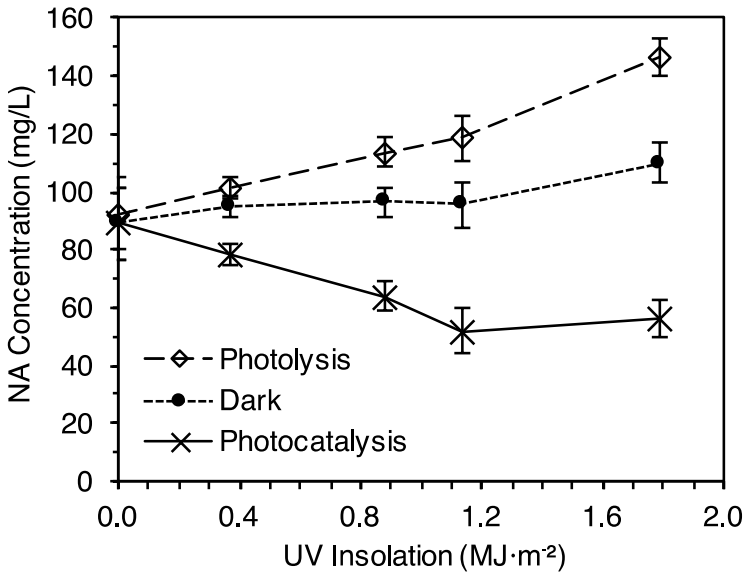

Figure 3

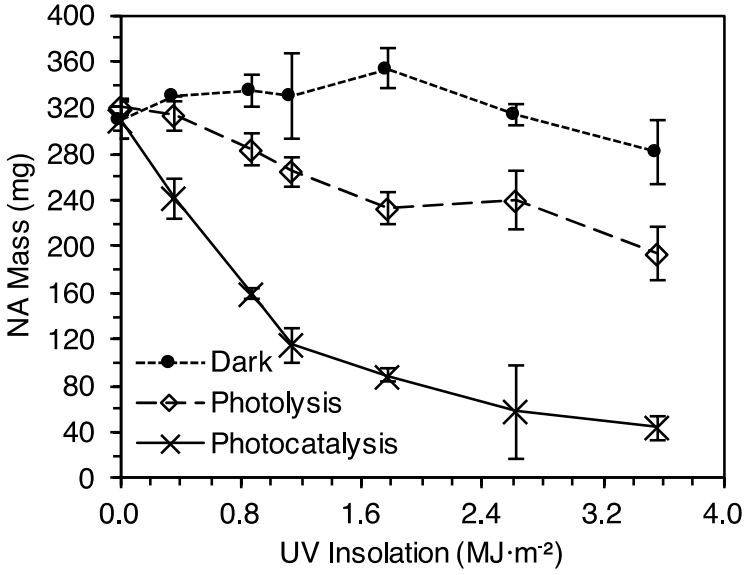

Figure 4

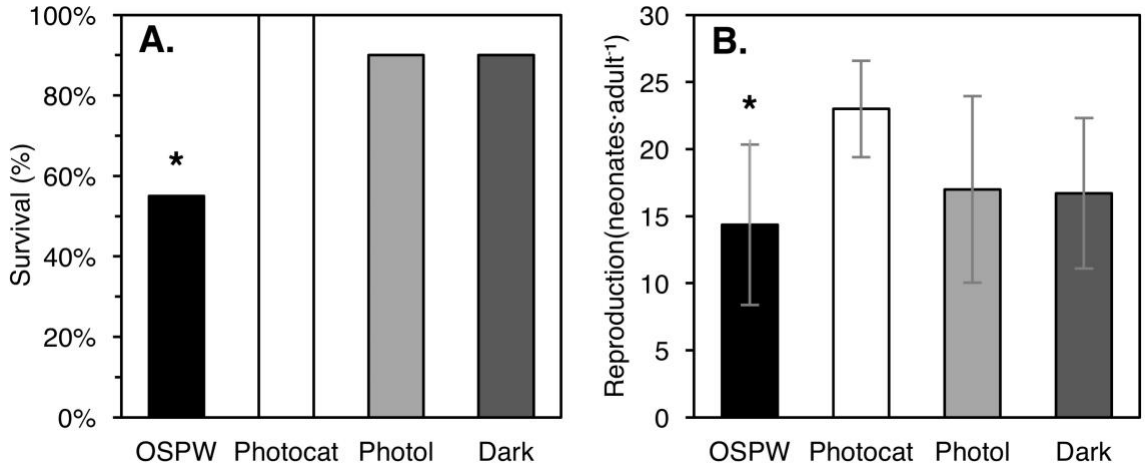

Figure 5

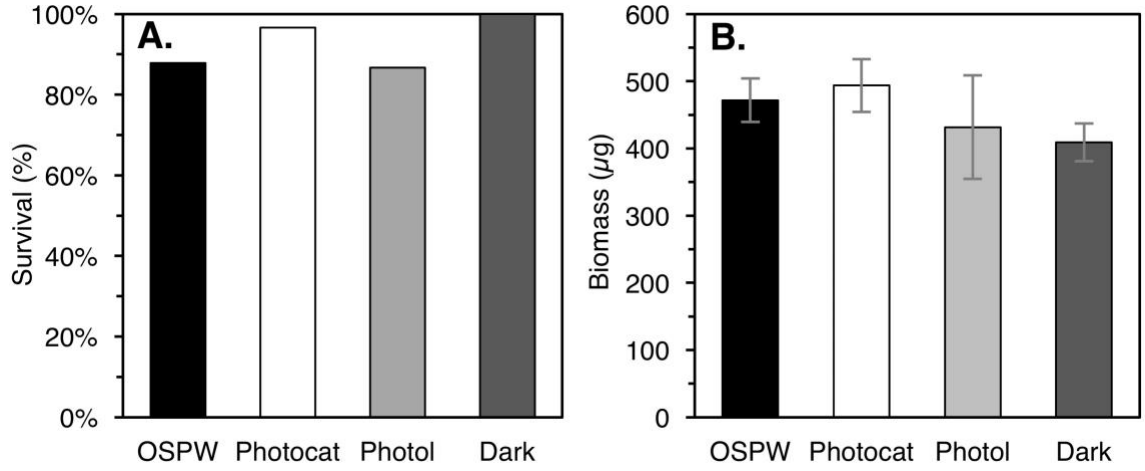

Figure 6

Table 1. Naphthenic acid (NA) mass and concentration removal extents (i.e. final mass or concentration measured), efficiencies (Eqn. 10, 18), rate coefficients (Eqn. 6-7, 14-15), and half-lives (Eqn. 8-9, 16-17) for photocatalytic, photolytic, and dark control reactors. Data are reported as means and standard deviations calculated from values measured in replicate reactors (n=3). Removal of NA concentrations were measured until the midpoint of the experiment, and NA mass removal was determined throughout the entire duration of the experiment.

Parameter	Concentration[a]			Mass[b]		
	Photocatalysis	Photolysis	Dark Control	Photocatalysis	Photolysis	Dark Control
UV Insolation ($MJ \cdot m^{-2}$)	1.78	1.78	0	3.57	3.57	0
Total Photoperiod (h)	16	16	0	32	32	0
Initial NA (±SD)	89 (±6)	92 (±13)	89 (±6)	310 (±16)	320 (±8)	310 (±16)
Removal Extent (±SD)	56 (±6)	146 (±7)	110 (±6)	44 (±11)	195 (±23)	280 (±27)
Removal Efficiency (%)	37 (±6)	-59 (±9)	-24 (±12)	86 (±3)	39 (±8)	9 (±10)
Rate Coefficient						
UV Insolation ($m^2 \cdot MJ^{-1}$)	-0.33 (±0.03)	[c]	[c]	-0.61 (±0.10)	-0.14 (±0.04)	[c]
Photoperiod (h^{-1})	-0.036 (±0.003)	[c]	[c]	-0.068 (±0.011)	-0.015 (±0.004)	[c]
R^2 [d]						
UV Insolation ($MJ \cdot m^{-2}$)	0.63 to 0.93	[c]	[c]	0.87 to 0.98	0.80 to 0.95	[c]
Photoperiod (h)	0.67 to 0.94	[c]	[c]	0.85 to 0.98	0.80 to 0.95	[c]
Half-life						
UV Insolation ($MJ \cdot m^{-2}$)	2.1 (±0.2)[e]	[c]	[c]	1.1 (±0.2)	5.0 (±1.4)[e]	[c]
Photoperiod (h)	19 (±2)[e]	[c]	[c]	10 (±2)	46 (±13)[e]	[c]

[a] Initial NA and removal extent reported in mg/L

[b] Initial NA and removal extent reported in mg

[c] Removal rates, half-lives, and R^2 were not calculated because NA concentration or mass was not significantly different from initial mass

[d] R^2 reported as minimum and maximum value

[e] Half-lives extrapolated from available data, no half-lives reached

CHAPTER III

A HYBRID PILOT-SCALE CONSTRUCTED WETLAND TREATMENT SYSTEM FOR REMEDIATION OF AN OIL SANDS PROCESS-AFFECTED WATER

Abstract

Surface mines in the Athabasca Oil Sands store massive volumes of oil sands process-affected waters (OSPWs) that contain potentially hazardous constituents, most notably the carboxylic acid class (O_2 class) of naphthenic acid fraction compounds (NAFCs). The objective of this research was to assemble a hybrid pilot-scale constructed wetland treatment system (CWTS) and assess its performance for a specific OSPW by measuring changes in concentration and composition of targeted constituents and toxicity to *Ceriodaphnia dubia*. Characterization of the OSPW indicated that As, B, Cl^-, Cu, Pb, Zn, total suspended solids (TSS), oil and grease (O&G), and NAFCs were constituents of concern (COCs). The hybrid pilot-scale CWTS was assembled outdoors in Clemson, SC, consisted of wetland cells and solar TiO_2 fixed-film photocatalytic reactors, and was measured during three sampling periods to assess performance. Orbitrap mass spectrometry (Orbitrap MS) conducted at the National Hydrology Research Centre in Saskatoon, SK showed that after treatment in wetland cells and photocatalytic reactors, NAFC class distributions shifted from regimes dominated by acutely toxic O_2 NAFCs (O_2=40.3%, $\sum O_{3-9}$=45.0%) in untreated OSPW to sparingly toxic oxidized NAFCs (i.e. O_{3-9}; O_2=13.6%, $\sum O_{3-9}$=77.0%). Concentrations of NAFCs decreased by 75.9% from inflow (43.1±5.9 mg/L) to outflow (10.4±6.0 mg/L) of the hybrid pilot-scale CWTS. TSS and O&G achieved compliance with narrative water quality criteria, mean arsenic

concentrations decreased from 0.026 to between 0.011–0.013 mg/L (48 to 57%), and mean Zn concentrations decreased from 0.129 mg/L to between 0.052 and 0.040 mg/L (49 to 54%). Between 30 and 39% of water was lost to evapotranspiration during the first two sampling events causing concentrations of NAFCs, B, Cl^-, Cu, and Pb to increase or remain constant in the wetland cells. "Polishing" photocatalytic reactors treating outflow from the final wetland cells decreased NAFC concentrations from 29.3±3.0 to 10.4±6.0 mg/L. In sampling periods 2 and 3, toxicity to *C. dubia* was eliminated at all positions within the CWTS. Reproduction of *C. dubia* was impaired in 4 of 8 samples collected during sampling period 1, likely due to increased Cl^- concentrations. This study demonstrates that pairing aerobic degradation in wetland cells with fixed-film photocatalysis can alter composition and decrease concentrations of NAFCs in OSPW. Performance data, biogeochemical conditions, and design criteria presented in this hybrid pilot-scale CWTS experiment will inform further development of this technology.

1.0 Introduction

Extraction of bitumen from surficial deposits in the Athabasca oil sands (AOS) has produced between 800 and 1,000 million m^3 of oil sands process-affected waters (OSPWs; Mikula, 2013). The accumulation of these impaired waters in tailings ponds across the AOS results from the combination of approximately 50 years of oil sands extraction without implementation of scalable treatment technologies and the Alberta Environmental Protection and Enhancement Act, which prohibits release of untreated OSPW into surface and ground-waters (Madill et al., 2001; Mikula, 2013; Quinlan and Tam, 2015). OSPW contains suspended sediments, dissolved salts, metals, metalloids,

and an organic fraction predominantly composed of organic acids and residual bitumen (Allen, 2008; McQueen et al., 2017a). Provincial laws mandating that liquid tailings (i.e. OSPW) must be reclaimed within 10 years of oil sands mine closure have hastened development of OSPW treatment technologies (AER, 2016). Oil sands operators are seeking passive approaches for treating large volumes of OSPW to comply with this directive (COSIA, 2015). Constructed wetlands are passive, low-energy treatment systems that have demonstrated potential to mitigate risks associated with constituents in OSPW.

Naphthenic acids (NAs) are the primary source of toxicity in OSPW (MacKinnon and Boerger, 1986; Verbeek, 1994; Morandi et al., 2015a; Hughes et al., 2017), and have elicited adverse effects across a diverse array of taxonomic groups including bacteria (Frank et al., 2008), fish (Kavanagh et al., 2011), invertebrates (Bartlett et al., 2017), mammals (Rogers et al., 2002), and vascular plants (Armstrong et al., 2008). NAs are a complex group of thousands of carboxylic acids produced from biodegradation of mature petroleum (Tissot and Welte, 1978; Quagraine et al., 2005), and solubilized into OSPW during the alkaline bitumen extraction process (Schramm, 2000). This complex mixture comprises cycloaliphatic carboxylic acids classically defined by the formula, $C_nH_{2n+Z}O_2$, where *n* is the number of carbon atoms and *Z* represents hydrogen deficiency (Brient et al., 1995; Headley and McMartin, 2004; Clemente and Fedorak, 2005). Ultrahigh-resolution mass spectrometry (UHRMS) of OSPW acidic extracts has found that <50% of identified compounds conform to the classical NA formula (i.e. the O_2 class; Grewer et al., 2010), with the remainder of this fraction consisting of poly-oxygenated classes ($O_{3–}$

$_9$), and sulfur and nitrogen heteroatoms (Headley et al., 2012). Thus, "naphthenic acid fraction compounds" (NAFCs) was proposed as a more appropriate term for describing this complex mixture of organic acids (Headley et al., 2012). Molecular composition varies within each heteroatom class, and resistance to biodegradation increases with greater cyclicity, carbon number, and alkyl branching (Scott et al., 2005; Han et al., 2008; Toor et al., 2013b). Robust treatment methods are required to decrease concentration and alter composition of NAFCs in OSPW.

Specifically designed constructed wetland treatment systems (CWTSs) have successfully remediated impaired waters containing complex mixtures of contaminants, including refinery effluents and oil field produced waters (Gillespie et al., 2000; Huddleston et al., 2000; Murray-Gulde et al., 2003). The versatility of these systems stems from the diverse array of reactions supported in natural wetlands, including bioconcentration, biodegradation, photolysis, precipitation, oxidation, reduction, and sorption (Rodgers and Castle, 2008; Vymazal, 2010; Reddy and DeLaune, 2008). By promoting aerobic biodegradation, wetland sediment microcosms have decreased NA concentrations (Toor et al., 2013b), hydroponic treatments with macrophytes have decreased toxicity of OSPW (Armstrong et al., 2009), and pilot-scale CWTSs have eliminated acute toxicity of OSPW to *Ceriodaphnia dubia* (McQueen et al., 2017b). Hybrid components, including oil water separators, reverse osmosis membranes, and photocatalytic reactors may be implemented into CWTSs to provide additional or enhance existing treatment processes (Murray-Gulde et al., 2003; Kanagy et al., 2008a; Pardue et al., 2014; McQueen et al., 2017b). Photocatalysis over TiO_2 is a potent

advanced oxidation process that generates reactive radical species in the presence of water and solar UV radiation (<400 nm; Fujishima et al., 2000). This pathway may augment treatment of NAFCs in OSPW when implemented as a hybrid component in CWTSs (McQueen et al., 2017b). When implemented as a "polishing step", fixed-film TiO_2 solar photocatalytic reactors decreased concentrations of residual NAs by up to 93% in the outflow of a pilot-scale CWTS designed for OSPW. In this research, fixed-film photocatalytic reactors were implemented into a hybrid pilot-scale CWTS to enhance degradation and transformation of NAFCs in a specific OSPW.

Differences in ore composition (Schramm, 2000; Romanova et al., 2004), bitumen separation methods, tailings management practices, and freshwater intake (Allen, 2008; Zubot et al., 2012) cause concentrations of elements, suspended solids, residual hydrocarbons, and NAFCs to range considerably in OSPWs produced at different mines (Allen, 2008; Marentette et al., 2015a; Leshuk et al., 2017b). A thorough characterization of OSPW to be treated in constructed wetlands is required to bound expected ranges of constituent concentrations. Constituents of concern (COCs) are elements, organics, or parameters that impede beneficial reuse of OSPW by exceeding water quality criteria (WQC) or toxicity endpoints. CWTSs are designed to promote specific treatment pathways capable of decreasing solubility, bioavailability, and reactivity of COCs (Rodgers and Castle, 2008). These transfers and transformations are promoted by careful integration of vegetation, hydrosoil, and hydroperiod (Hawkins et al., 1997; Gillespie et al., 2000; Rodgers and Castle, 2008). Once assembled, CWTS operation is largely passive and highly cost-effective, as these systems contain few mechanical parts and can

have lifetimes of over 30 years (Lehman et al., 2001; Murray-Gulde et al., 2005a; Nelson and Gladden, 2008). Operation of CWTSs involves measurement of biogeochemical parameters, flow management, and performance monitoring. Biogeochemical conditions, including pH, hydrosoil oxidation-reduction potential (ORP), dissolved oxygen concentration (DO), and shoot density, are measured to assess if conditions are suitable for promotion of targeted transfers and transformations (Lehman et al., 2001; Rodgers and Castle, 2008). Flow management consists of measuring volumetric inflow and outflow rates, calculating water balance, and using these data to assess removal of COC mass (Bishay, 1998; Lehman et al., 2001). Performance of CWTSs is monitored by measuring changes in concentration and composition of COCs and responses of sentinel aquatic species with respect to hydraulic retention time (HRT). These organisms may be vulnerable to additive and synergistic effects from mixtures of constituents in OSPW that cannot be analytically determined (Norberg-King, 1992), and thus provide a composite measure of performance. Pairing bioassays with UHRMS allows responses of test organisms to be compared with changes in distributions of NAFC classes in OSPW (Morandi et al., 2015; Hughes et al., 2017).

The overall objective of this research was to measure performance of a hybrid pilot-scale CWTS treating OSPW. Specific objectives were to: 1) Characterize a specific OSPW treated by a hybrid pilot-scale CWTS for identification of COCs, 2) assemble and operate a hybrid pilot-scale constructed wetland for treatment of the OSPW, 3) analyze changes in NAFC concentration and class distribution measured by UHRMS in Dr. John Headley's laboratory at the Environment and Climate Change Canada National

Hydrology Research Centre, and 4) measure changes in concentration of COCs and survival and reproduction of *Ceriodaphnia dubia*.

2.0 Materials and Methods

2.1 Characterizing OSPW for identification of COCs

For this study, COCs were water quality characteristics, elements, and groups of organic compounds in concentrations exceeding water quality criteria (WQC) for fresh surface waters. COCs were identified using the most protective WQC available from regulatory agencies including the Ministry of Alberta Environment and Parks (AEP), Canadian Council of Ministers of the Environment (CCME), and United States Environmental Protection Agency (USEPA). In November 2015, ~40,000 L of OSPW were collected by Shell Canada from the clarified zone (1-3 m depth below surface) of an external tailings facility at the Muskeg River Mine in northern Alberta, Canada. In addition to outfall from bitumen extraction processes, major inputs to this tailings facility include precipitation, runoff, and groundwater from mine dewatering and capture of dyke seepage (Allen, 2008; Roy et al., 2016; Shell Canada Ltd., 2016). OSPW was transported in two stainless steel tanker trailers to Clemson, SC, USA and conveyed to 3,785 L high density polyethylene (HDPE) tanks for storage. Following 24 h of mixing in the storage tanks using a 0.56 kW (0.75 HP) submersible pump, grab samples of OSPW were collected for chemical characterization and COC identification. Water quality characteristics, including pH, conductivity, alkalinity, hardness, total suspended solids (TSS), total dissolved solids (TDS), total ammonia, and total phosphorus were measured according to *Standard Methods for Examination of Water and Wastewater* (APHA,

2012). Total recoverable concentrations of elements (i.e., Al, As, Ba, B, Cd, Ca, Cr, Cl, Co, Cu, Fe, Pb, Mg, Mn, Ni, K, Se, Na, Zn) were determined by acidifying unfiltered samples with 2% (v/v) trace metal grade HNO_3 (15.9 N; Sigma-Aldrich, St. Louis, MO, USA) prior to inductively coupled plasma atomic emission spectroscopy (ICP-AES; Spectro Flame Modula, Mahwah, NJ, USA) according to EPA method 200.7 (USEPA, 2001). Concentrations of oil and grease (O&G) were measured in untreated OSPW according to USEPA method 1664A (USEPA, 1999).

After collection of samples for OSPW characterization, 500 mL aliquots were stored in 1-L HDPE bottles, frozen, and shipped to Dr. John V. Headley's laboratory at the Environment and Climate Change Canada (ECCC) National Hydrology Research Centre in Saskatoon, SK for analysis of concentration, composition, and speciation of NAFCs by electrospray ionization ultrahigh resolution mass spectrometry (ESI-UHRMS). NAFCs were recovered from thawed OSPW samples using weak anion exchange solid phase extraction (WAX) as described by Ajaero et al. (2017). This extraction method is preferred for diagnostic analysis of NAFCs in complex environmental matrices (Ajaero et al., 2017). ESI-UHRMS analysis of extracted organic acids was conducted using a LTQ Orbitrap Elite Mass Spectrometer (Oribtrap; Thermo Fisher Scientific, San Jose, CA). Total concentrations of NAFCs were determined using a 5-point calibration curve of nominal concentrations of Shell OSPW-derived acid extractable organics (Headley et al., 2011; Hughes et al., 2017). Diagnostic characterization of NAFCs was conducted with the Orbitrap in full scan, negative-ion mode, with mass resolution set to 240,000, and m/z scan range of 100-600 (Hughes et al.,

2017). Mass accuracy error was <2 ppm for all assignments, and root mean square error was 0.12-0.45 ppm for assignments associated with the entire mass spectra (Hughes et al., 2017). Detected NAFCs were grouped according to the following classes: O_x (x =1-10), O_xS (x =1-8), N_x (x=1-3), S_x (x=1-2), N_xO_y (x=1-3, y=1-5) N_xO_yS (x=1-3, y=1-3). NAFC class distribution and concentration data were sent electronically by Kerry Peru to researchers at Clemson University where the data were analyzed to identify COCs and determine changes in NAFC concentration and composition within the hybrid pilot-scale CWTS.

Derivatization and high performance liquid chromatography (HPLC) were used as a rapid, low-resolution method to quantify the carboxylic acid fraction of OSPW organics (Yen et al., 2004). Total concentrations measured by derivatization and HPLC are referred to as naphthenic acids (NAs) in this paper to differentiate between total NAFC concentrations determined by WAX and Orbitrap MS. Samples were derivatized in 2.0 mL glass vials then analyzed using a Dionex UltiMate-3000 HPLC (Sunnyvale, CA) equipped with an Agilent LiChrospher 100 RP-18 column (5 µm particle size, 125mm x 4 mm) and a guard column containing 2 µm RP-18 solid phase material. Absorbance of NA derivatives was measured at 400 nm. Chromatograms were integrated via baseline hold between retention times of 2.9 and 6 min. Concentration was calculated from integrated areas using a 5-point standard curve derived from a dilution series of a 120 mg/L stock solution of a commercial NA blend (Fluka NAs; Sigma-Aldrich; St. Louis, MO). All samples and standards were divided into pseudo-replicates prior to

derivatization, and total NA concentrations were expressed as means of pseudo-replicates (n=3).

2.2 CWTS assembly and operation

Given the composition and concentrations of NAFCs in this OSPW (Section 3.1) and the body of literature attesting to their toxicity (McKinnon and Boerger, 1986; Verbeek, 1994; Marentette et al., 2015a,b; McQueen et al., 2017a; Hughes et al., 2017), the hybrid pilot-scale CWTS was assembled using components capable of transforming OSPW organics as discussed in section 3.2.1. The hybrid pilot-scale CWTS consisted of two major parts: a hybrid constructed wetland (HCW) and a polishing photocatalytic reactor (PC2; Figure 1). The HCW was composed of duplicate series (Series A and B) with each series containing five free-water surface wetland cells (WC1-5) and an initial photocatalytic reactor (PC1) located between the first and second wetlands cells. FMI® piston pumps (Fluid Metering, Inc., Syosset, NY) conveyed OSPW from a 3,785 L HDPE storage tank to the first wetland cell in each series (A1, B1) at an inflow rate of 14.9 L/d. This flow rate was selected to achieve a nominal hydraulic retention time (HRT) of 16 d in each HCW series and was calculated using Eqn. 1.

$$Q_{in} = V/HRT \qquad (1)$$

where Q_{in} is the inflow rate (L/d), V is the aqueous volume of a series (L), and HRT is the nominal hydraulic retention time (d). HCW series were constructed on an approximately 15° slope to promote gravity driven flow. Polyvinyl chloride (PVC) fittings were used to connect photocatalytic reactors and wetland cells. Outflows from final wetland cells (WC5) in HCW series were stored in HDPE tanks and transferred by FMI pumps to the

polishing photocatalytic reactor (PC2). PC2 was composed of two duplicate series (APC2 and BPC2). Each series consisted of a photocatalytic reactor, a FMI pump, and inflow (A/BPC2 In) and outflow storage tanks (A/BPC2 Out). Outflows from HCW series were circulated through PC2 series until exposed to >1.5 MJ/m^2 UV insolation. This threshold is based on NA degradation in a solar TiO_2 fixed-film photocatalytic reactor treating OSPW collected from pilot-scale CWTS outflows (McQueen et al., 2017b). UV irradiance ($J \cdot s^{-1} \cdot m^{-2}$) was measured and recorded with an Apogee Instruments SU-100 UV sensor (spectral range 250 to 400 nm; Logan, UT) connected to a HOBO UX120-006M Analog Data Logger (Bourne, MA). Irradiance data were integrated over time to calculate UV insolation (MJ/m^2).

2.2.1 Wetland cells

Wetland cells were contained in 115 L polypropylene barrels (76 cm height, 51 cm upper diameter, 44 cm lower diameter). Hydrosoil was collected from Eighteen Mile Creek (Pendleton, SC) and consisted of alluvial sediment containing approximately 84% medium to coarse grained sand, 15% gravel, <1% clay/silt, and <1% organic matter (Kanagy et al., 2008b). Wetland cells were filled with hydrosoil to a depth of approximately 20 cm and amended with 5 g/L Osmocote® time-released fertilizer. In July 2016 mature broadleaf cattail (*Typha latifolia*) were collected from local ponds and planted at an initial density of 30 shoots/m^2 (6-8 plants per cell). Water depth was fixed at 20 cm and mean total volume of water, including saturated pore space, in the wetland cell was 44±2 L (n=10). The nominal HRT of each wetland cell was 3 d.

2.2.2 Photocatalytic reactors

TiO_2 fixed films were assembled by applying ~0.1 cm thick layers of epoxy (West System® 105 epoxy resin and 206 hardener; Bay City, MI) to 0.32 cm thick stainless steel sheets and coating the epoxy with TiO_2 (Aeroxide^{TM} P25; Fisher Scientific; Fairlawn, NJ). TiO_2 films were placed in 15x72x31 cm HDPE containers with PVC fittings installed approximately 1.5 cm above film surfaces. Each photocatalytic reactor (APC1, BPC1, APC2, BPC2) consisted of 4 fixed-film containers (reactor units). The total volume of each initial photocatalytic reactor (APC1, BPC1) was approximately 15 L, which achieved a nominal HRT of 24 h given the inflow rate of 14.9 L/d (Eqn. 1). This design ensured that under continual loading of OSPW, all throughput of the initial photocatalytic reactors was exposed to daylight.

Outfall from HCW series was collected in storage tanks for transfer into in polishing photocatalytic reactor Series A and B (APC2 In, BPC2 In). When predicted sky cover was <50% (NWS, 2017), FMI pumps were activated and OSPW was conveyed to each PC2 series. Reactor units in the PC2 series were covered when this threshold was not met or inclement weather was predicted. Inflow rates were calibrated to achieve between 6 and 8 h HRT to match daily duration of direct sunlight. Outflow from each PC2 series was collected and recirculated until volumes of OSPW had been exposed to >1.5 MJ/m^2 UV insolation (McQueen et al., 2017b).

2.2.3 Sampling of hybrid pilot-scale CWTS

Samples were collected for analysis of water quality characteristics, shifts in NAFC class distribution, and changes in COC concentration and survival and reproduction of *Ceriodaphnia dubia*. The HCW series were sampled according to a

nominal HRT (t=16 d) so that a single volume (i.e. plug) of OSPW could be analyzed. Plug flow was initiated when inflow pumps were activated. Samples were collected from outflows of initial wetland cells (WC1) and photocatalytic reactors (PC1) at HRT=3 and 4 d, respectively. Outflow samples were collected from the second (WC2), third (WC3), fourth (WC4), and fifth (WC5) wetland cells at HRT=7, 10, 13, and 16 d, respectively. Performance data for the pilot-scale CWTS were compiled over three successive sampling periods. Sampling periods started on 10/14/16, 11/9/16, and 12/2/16. On these starting dates, grab samples were collected from the OSPW storage tank for characterization of inflow. OSPW was mixed for 24 h prior to sample collection and continuously throughout each sampling period using a 0.56 kW (3/4 HP) submersible pump. Each sampling period started when inflow pumps were activated, continued as samples were collected according to plug flow, and ended when cumulative inflow volumes were equivalent to HCW series volumes.

Performance monitoring of the polishing photocatalytic reactors (PC2) was also divided into three successive sampling periods which started on 12/1/2016, 12/21/2016, and 1/12/2017. Durations of PC2 sampling periods were determined by photoperiods required to achieve UV insolation >1.5 MJ/m^2, and ranged from 28.0 to 45.8 h, depending on weather conditions. Samples were collected from PC2 series inflow tanks (APC2 In, BPC2 In) on start dates and from outflow tanks (APC2 Out, BPC2 Out) after UV insolation thresholds were achieved (Figure 1).

Water balances for each HRT were calculated for HCW and PC2 series according to Eqn. 2:

$$\Delta V = Q_{in}t - V_{out} \qquad (2)$$

where ΔV (L) is the change in volume, Q_{in} (L/d) is the volumetric inflow rate, t (d) is inflow duration, and V_{out} (L) is the sum of recovered volume and sample volume. Volumetric inflow rate was measured daily using a graduated cylinder and stopwatch, and outflow volumes were measured directly.

2.2.4 Explanatory parameters

Green shoot density and hydrosoil oxidation-reduction potential (ORP, mV) were measured biweekly starting in August 2016. Hydrosoil ORP was measured 15 cm below the sediment-water interface in the center of each wetland cell using *in situ* platinum-tipped electrodes and an Accumet® calomel (Hg_2Cl_2) reference electrode connected to a GardnerBender® GDT-311 voltmeter (Faulkner et al., 1989). Water temperature in wetland cells was monitored using a HOBO Pendant® Temperature/Light 64K Data Logger (Bourne, MA) located at the sediment water interface in wetland cell B3. Conductivity and pH were measured *in situ* using an Orion Star A221 portable meter (Thermo Fisher Scientific, Waltham, MA) equipped with a 9157BNMD Triode pH probe and a 013010MD conductivity cell. DO was measured using a HQ30d meter with a LDO101 optical dissolved oxygen probe (HACH; Loveland, CO). Conductivity, pH, and DO were measured during each sampling period at a depth of 10 cm below the wetland cell water surface and near outflows of the initial photocatalytic reactors (PC1). AVS was measured using the diffusion method (Leonard et al., 1996), in which sulfide ions were trapped in sulfide anti-oxidant buffer (SAOB) and measured using an ion-selective electrode (ISE; Fisher Accumet 950 pH/ion meter) to determine the molar concentration

of AVS. Ambient temperature and precipitation data were collected from a weather station located 1.1 km from the hybrid CWTS (Weather Underground, 2017).

2.3 Changes in NAFC concentration and class distribution

Changes in NAFC composition and concentration were determined by conducting ESI-Orbitrap MS on composite samples of OSPW from strategic locations within the hybrid pilot-scale CWTS. Composite samples consisted of 50:50 mixtures of aliquots from samples collected simultaneously at parallel positions in Series A and B. Samples collected from the following positions in Series A and B were composited: inflows to PC2 and outflows of WC1, PC1, WC5, and PC2. Distributions of NAFC class (e.g., O_2, O_4, O_2S) relative abundance, which is the abundance of a class relative to the sum of all classes, were determined for each composite sample. NAFC classes with a mean relative abundance of <1% at one or more positions in the hybrid CWTS were excluded from figures and tables.

2.4 Changes in COC concentration

COC concentrations in samples collected from wetland cells and photocatalytic reactors in HCW and PC2 Series A and B were measured according to methods described in section 2.1. Evaporation, transpiration, and precipitation influenced COC concentrations in the hybrid CWTS. Eqn. 3. was used to calculate volume-adjusted COC concentrations in outflows of the HCW and PC2 series:

$$C_{adj} = C_{out}V_{out}/V_{in} \qquad (3)$$

where C_{adj} (mg/L) is the adjusted COC concentration, C_{in} (mg/L) is inflow concentration, C_{out} (mg/L) is the outflow concentration, and V_{in} (L) is cumulative inflow volume calculated from the water balance (Eqn. 2). Extents of removal, which are COC concentrations measured in HCW or PC2 outflows, and removal efficiencies (Eqn. 4) are reported for measured and adjusted-concentrations.

$$\text{Removal Efficiency} = ((C_{in} - C_{out})/C_{in}) \cdot 100 \qquad (4)$$

2.5 Ceriodaphnia dubia bioassays and statistics

Ceriodaphnia dubia is an ecologically significant species ubiquitous in North American lentic freshwaters (Pennak, 1978; Carpenter et al., 1985). This daphnid is sensitive to constituents found in OSPW including NAFCs, major ions, and divalent metals (Goodfellow et al., 2000; Zubot et al., 2012; McQueen et al., 2017a). *C. dubia*, obtained from healthy cultures maintained at the Clemson University Aquatic Animal Research Laboratory, were used to assess toxicity of samples collected from untreated OSPW (inflow), initial photocatalytic reactor (PC1) outflows, hybrid constructed wetland (HCW) outflows, and polishing photocatalytic reactor inflows and outflows (PC2 In, PC2 Out). Survival and reproduction of *C. dubia* neonates were measured in these samples using a static/renewal bioassay conducted according to ECCC protocols (ECCC, 2007). Responses of exposures and laboratory controls, which consisted of formulated moderately hard water (USEPA, 2002), were compared following ECCC methods for single concentration tests. Exposures eliciting adverse responses had significantly different survival and reproduction compared to laboratory controls. Differences between normally distributed, homogeneous reproduction data were determined by analysis of

variance (ANOVA) followed by comparison of exposures to laboratory controls using Dunnett's test. Reproduction data were tested for normality and homogeneity using Chi-square and Barlett's tests, respectively. Survival data were compared to laboratory controls using Fisher's exact test. Students t-test for comparison of means was used to determine the statistical significance of differences between various parameters in the hybrid CWTS (e.g., COC concentrations, water quality characteristics). Statistical analyses were performed using JMP Pro V12.1 (α= 0.05; SAS Institute Inc.; Cary, NC, USA).

3.0 Results and Discussion

3.1 OSPW characterization and COC identification

Ranges of TDS (1026-1546 mg/L), hardness (116-132 mg/L as $CaCO_3$), and pH (8.62-8.91) indicate that the OSPW was slightly saline (McNeely et al., 1979), moderately soft to hard, and slightly alkaline (Table 1). In descending order of concentration, major ions in this OSPW were HCO_3^-, Na^+, Cl^-, SO_4^{2-}, K^+, Mg^{2+}, Ca^{2+}, and CO_3^{2-}. Ranges of water quality characteristics and concentrations of major ions are consistent with values reported in previous characterizations of OSPWs (Allen et al., 2008; Toor et al., 2013a; Mahaffey and Dubé, 2016; Leshuk et al., 2016b; McQueen et al., 2017a). Bicarbonate concentrations in the OSPW ranged from 326 to 415 mg/L, contributing to alkalinity and stable pH of this water. Cl^- concentrations ranged from 248 to 260 mg/L, exceeding CCME's chronic WQC and concentrations measured in freshwater bodies within the Athabasca oil sands (<1 to 73 mg/L; Golder Associates, 2001), and therefore Cl^- is considered a COC. Total suspended solids ranged from 6 to

113 mg/L, and have the potential to exceed water quality criteria if discharges increase TSS in a receiving water body by more than 25 mg/L within a 24 h period (CCME, 2011). Ammonia has historically been a source of toxicity in OSPW (Allen, 2008; Bishay et al., 1998); however, ammonia concentrations did not exceed WQC in the OSPW used in this research (CCME, 2011). Phosphorus concentrations in this OSPW exceeded CCME trigger ranges for discharge into mesotrophic receiving waters (CCME, 2011). However, for the purposes of this research, phosphorus was not identified as a COC because this nutrient is associated with lower removal extents and higher biodegradation rates for OSPW organics (Herman et al., 1994; Lai et al., 1996; Toor et al., 2013a). Acid soluble concentrations of As, B, Cu, Pb, and Zn exceeded the most conservative WQC available and were identified as COCs (Table 2). When compared to laboratory derived toxicity endpoints for *C. dubia*, maximum Zn concentrations (0.208 mg/L) exceeded a 7-d LOEC for *C. dubia* reproduction (0.128 mg Zn/L; Zuiderveen and Birge, 1997), but concentration of As, B, Cu, and Pb were less than toxicity thresholds for *C. dubia* (Belanger and Cherry, 1990; Hickey, 1989; Hu et al., 2012; Zuiderveen and Birge, 1997).

The organic acid fraction of OSPW has been identified repeatedly as a primary source of toxicity in these complex mixtures (Verbeek, 1994; Marentette et al., 2015a,b; McQueen et al., 2017a); however, WQC have not been developed for this fraction. USEPA guidance (USEPA, 1991) states that narrative criteria of "no toxics in toxic amounts" should be applied if numeric WQC are not available. Based on this guidance and literature supporting the toxicity of these compounds, NAFCs, including compounds measured as NAs by derivatization and HPLC, were identified as COCs in this OSPW.

Concentrations of NAs and NAFCs were 61 to 89 mg/L and 39.4 to 57.8 mg/L, respectively. These values exceed a 96 h EC50 for *P. promelas* embryo viability (7.5 mg/L; Marentette et al., 2015a); however, toxicity of NAFCs in OSPW is influenced by concentration and speciation (Brown and Ulrich, 2015; Mahaffey and Dubé, 2016; McQueen et al., 2017b). Untreated OSPW was composed primarily of O_2, O_3, and O_4 classes, with relative abundance of 40.8, 19.6, and 20.7%, respectively (Figure 2). Sulfur containing species of these oxygenated classes were also present in untreated OSPW, with relative abundance between 3.1 and 5.3%. Highly oxidized (O_6-O_{10}), hydroxyl, and nitrogen-containing classes were all detected at <1% relative abundance. Effect directed analysis of fractionated NAFCs have identified the O_2 class as the most acutely toxic fraction, while O_3 and O_4 classes are not considered significant sources of toxicity (Morandi et al., 2015; Yue et al., 2015a; Hughes et al., 2017). The O_2 class is composed of species which fit to classical definition of NAs (i.e., $C_nH_{2n+z}O_2$). High relative abundance of classical NAs supports that NAFCs are a significant driver of toxicity in this OSPW and the identification of this group of compounds as a COC.

Concentrations of oil and grease (O&G) were determined as an aggregate measure of residual hydrocarbon compounds in OSPW. O&G concentrations ranged from 5 to 30 mg/L, producing a sheen on untreated OSPW. The WQC for O&G is narrative mandating that sheens, films, or discolorations cannot be visible, thus, O&G was identified as a COC (Health Canada, 2012).

3.2 Assembly and operation of hybrid CWTS

3.2.1 Hybrid CWTS assembly

Wetland cells were constructed using combinations of vegetation, hydrosoil, and water depth utilized in previous pilot-scale CWTS experiments (Alley et al., 2013; Pardue et al., 2014) that maintained biogeochemical conditions suitable for heterotrophic aerobic microorganisms and decreased concentrations of hydrocarbons via aerobic degradation. Aerobic degradation promoted in biofilm reactors (Hwang et al., 2013; McKenzie et al., 2014), wetland sediment microcosms (Toor et al., 2013a), and macrophyte-planted hydroponic treatments (Armstrong et al., 2009) has altered composition and decreased concentration and toxicity of NAFCs in OSPW. In the hybrid pilot-scale CWTS, aerobic degradation was promoted in wetland cells by the following features: 1) *T. latifolia*, a macrophyte known to release oxygen from its extensive horizontal rhizome system (Inoue and Tsuchiya, 2008; Vymazal, 2013); 2) coarse-sand hydrosoil amended with Osmocote® time-released fertilizer, which provided nutrients for plants and microbial assemblages, and had sufficient hydraulic conductivity ($K=10^{-3}$–10^{0} cm/s) to promote diffusion of oxygen from rhizomes and transpiration-driven circulation (Beebe et al., 2013; Haakensen et al., 2015); 3) water depth of <23 cm, which promoted diffusion of atmospheric oxygen in the water column (Alley et al., 2014); and 4) a residence time of 3 d per wetland cell (15 d total), allowing sufficient time for measurable changes in NAFC composition and concentration via aerobic degradation to occur (unpublished data; Brown et al., 2013; McKenzie et al, 2014). In a pilot-scale CWTS treating OSPW, McQueen et al. (2017b) utilized similar combination of features to achieve conditions suitable for aerobic degradation in wetland cells, including DO >2.0 mg/L and hydrosoil ORP >-50 mV (Rodgers and Castle, 2008). Conditions supporting

dissimilatory sulfate reduction, an anaerobic form of respiration utilized by sulfate reducing bacteria (SRB), have been measured in detritus-rich sediments within the upper 20 cm of similarly designed wetland cells (Jurinko, 2013). Dissimilatory sulfate reduction generates sulfide in the presence of sulfate, hydrosoil ORP from -75 to -250 mV, and organic matter (Murray-Gulde et al., 2005b). This process is the targeted pathway for decreasing bioavailability of Cu, Pb, and Zn in the wetland cells, as sulfides form insoluble complexes with these divalent metals and become sequestered in hydrosoil (Murray-Gulde et al., 2005b; Haynes, 2016). Concentrations of As are decreased by co-precipitation with Fe (III) oxyhydroxides in the water column of wetland cells and by sulfide complexation in detritus-rich hydrosoil (Lizama et al., 2011; Schwindaman et al., 2014).

To increase rates of NAFC degradation (Headley et al., 2009; Leshuk et al., 2016a; McQueen et al., 2017b), fixed-film solar photocatalytic reactors were paired with wetland cells in hybrid constructed wetland (HCW) series. Solar photocatalysis of OSPW over agitated TiO_2 slurries has removed >98% of NAFCs and may increase susceptibility of OSPW organics to biodegradation (Leshuk et al., 2016a). TiO_2 fixed-film reactors were incorporated into the hybrid CWTS, as they do not require recovery or mixing of catalyst particles (Malato et al., 2009; Zayani et al., 2009). In HCW series, initial wetland cells (WC1) were placed before photocatalytic reactors to adsorb and degrade O&G and settle suspended solids. These constituents attenuate solar UV radiation in OSPW (Chapter 2, section 4.1), and may impede photocatalytic degradation of NAFCs. Polishing photocatalytic reactors (PC2) received outflow from the HCW series and

provided treatment of residual NAFCs. HCW outflow was circulated in the PC2 series until exposed to a UV insolation threshold of 1.5 MJ/m^2. This threshold is based on photocatalytic degradation of NAs in a solar fixed-film reactor treating OSPW collected from pilot-scale CWTS outflows (McQueen et al., 2017b). This polishing photocatalytic reactor decreased NA concentrations by an average of 77±10% (*n*=3) when exposed to mean UV insolation of 1.45±0.17 MJ/m^2 (McQueen et al., 2017b).

Hybrid CWTSs have successfully treated impaired waters with TDS exceeding 6,500 mg/L (Murray-Gulde et al., 2003) and chloride concentrations greater than 4,000 mg/L (Kanagy et al., 2008a). Murray-Gulde et al. (2003) decreased TDS by 94% in brackish oil field produced water by implementing reverse osmosis prior to treatment of residual organics (O&G) and metals in wetland cells. Concentrations of Cl^- and B in OSPW must be decreased to achieve compliance with WQC; however, reverse osmosis may not be practical for treating these constituents as this technology is subject to fouling, produces concentrated brine byproducts, and has high capital and operating costs (Igunnu and Chen, 2012). Augmentation of surface waters in the Athabasca Oil Sands with treated outflows from CWTSs is a potential method for beneficial reuse of this slightly saline water. Procedures for comanagement of wetland-treated OSPW in receiving water bodies, including development of mixing zones and scheduling of releases during high flow, may be developed in coordination with regulators (USEPA, 1991). To provide conservative estimates of performance, comanagement practices were not implemented in this hybrid pilot-scale CWTS experiment.

3.2.2 Conditions during operation of hybrid CWTS

From the start of sampling period 1 (10/14/2016) to the end of sampling period 3 (12/20/2016), hydrosoil ORP was stable with mean values in Series A and B ranging from 59 to 73 and -18 to 0 mV (*n*=7), respectively, during this period (Figure S1, Table S1). During operation of HCW series, mean DO concentrations measured in the water column of wetland cells were 3.41±2.14 and 3.26±2.19 mg/L in Series A and B, respectively (*n*=15; Table S1). Mean values of hydrosoil ORP and DO were within thresholds supportive of aerobic biodegradation (>-50 mV and >2.0 mg/L; Castle and Rodgers, 2008; McQueen et al., 2017b). However, mean hydrosoil ORP was -77 and -75 mV in wetland cells B2 and B5, respectively, and AVS was detected in detritus-rich sediments at concentrations between 1 and 10 µmol/g, with a mean concentration of 4 µmol/g. These data demonstrate that dissimilatory sulfate reduction occurred in wetland cells and sulfide was available for complexation with divalent metals (e.g., Cu, Pb, and Zn).

Following seasonal decreases in ambient air temperature (Table 3), mean water temperature in the wetland cells decreased from 16.7±3.4 °C to 6.9±2.8 °C from the first to last sampling period, respectively, and vegetation underwent senescence (Figure S2). At the beginning of sampling period 1, mean green shoot density was 75 and 87 shoots/m^2 in Series A and Series B, respectively. Green shoot density declined during sampling period 2 (from 62 to 11 shoots/m^2 in Series A and 37 to 16 shoots/m^2 in Series B) and all plants were dormant during sampling period 3. Senescence did not impair the ability of wetland cells to decrease concentrations of O&G and TSS prior to the initial

photocatalytic reactors (PC1). Mean inflow concentrations of O&G were 15±13 mg/L (*n*=3) and decreased to the detection limit (<4 mg/L) by the outflow of the initial wetland cells (WC1) during all sampling periods (Table 4). Over three sampling periods, TSS decreased from an average of 56±40 mg/L in untreated OSPW to 6±3 and 6±2 mg/L in outflows of HCW Series A and B, respectively. UV radiation attenuation coefficients measured in outflows of WC1 suggest that treatment of O&G and TSS in WC1 improved UV light penetration in OSPW, which likely improved the performance of PC1 for treatment of NAFCs. Mean UV attenuation coefficient measured in untreated OSPW collected at the initiation of sampling period 2 was -0.28±0.02 cm^{-1}, and improved to -0.14±0.07 cm^{-1} after treatment in the initial wetland cells.

Increased frequency of overcast and inclement weather and seasonal decrease in photoperiod caused mean daily UV insolation to decrease 51% during operation of the HCW series from sampling period 1 (0.690 $MJ \cdot m^{-2} \cdot d^{-1}$) to sampling period 3 (0.341 $MJ \cdot m^{-2} \cdot d^{-1}$; Table 3). During operation of the polishing photocatalytic reactor (PC2) series (12/1/2016 to 1/28/17), mean daily UV insolation increased from 0.999 $MJ \cdot m^{-2} \cdot d^{-1}$ during sampling period 1 to 1.390 $MJ \cdot m^{-2} \cdot d^{-1}$ during sampling period 3. Mean daily UV insolation is the total UV insolation accumulated while pumps were conveying OSPW through photoreactors divided by the duration of pumping in days. Despite overlapping periods of operation, mean daily UV insolation during PC2 was greater than values measured in the HCW series because PC2 reactor units were covered and pumps were not activated during cloudy or inclement weather. Outflow from HCW series was cycled through PC2 series until the UV insolation target of 1.5 MJ/m^2 was reached. Volumes of

HCW outflow were cycled through PC2 series over 28.0 to 48.8 h of direct sun exposure and accumulated between 1.476 and 2.712 MJ/m^2 of UV insolation. McQueen et al. (2017b) measured between 0.85 to 1.65 MJ/m^2 UV insolation during 12-h photoperiods at the same location from May to June 2016.

Total precipitation accumulated during operation of the HCW series was 4.28 cm (Table 3), which is less than the 17.16 cm predicted by climate normals for Clemson, SC (NOAA, 2011). These weather conditions yielded negative water balances during sampling periods 1 and 2, when between 31 and 39% of water was lost to evapotranspiration in the HCW. A neutral water balance was observed during sampling period 3. During operation of PC2, 10±4% (*n*=6) of volume was lost to evaporation.

3.3 Changes in NAFC class distribution and concentration

3.3.1 NAFC class distribution

ESI-Orbitrap MS determined that NAFC class distributions were altered by photocatalysis and biodegradation in the hybrid CWTS (Figure 3). Untreated OSPW was composed primarily of O_2, O_3, and O_4 classes, with relative abundances of 40.3±1.8, 19.5±1.0, and 20.9±0.5%, respectively. Distributions of NAFC classes shifted towards poly-oxygenated classes (i.e. O_5-O_9) after treatment in the hybrid pilot-scale CWTS. During three sampling events, relative abundance of the O_2 class decreased to 13.6±1.4%, the O_3 class increased initially and then decreased to initial values, and O_4, O_5, and O_6 classes increased by factors of 1.2, 4.8, and 10.7, respectively. The progressive increase in relative abundance of poly-oxygenated classes observed within the hybrid CWTS is consistent with previous work on photocatalysis of OSPW and has been observed during

biodegradation of NAs (Tomczyk et al., 2001; Martin et al., 2010; Marentette et al., 2015a, Leshuk et al., 2016a). The shift of NAFCs towards higher oxygen content is pertinent because poly-oxygenated NAs are less toxic than classical NAs in the O_2 class (Morandi et al., 2015; Yue et al., 2015a).

Mean relative abundance of the O_2 class declined from 40.3±1.8% in untreated OSPW to 28±6.1% in HCW series outflow (*n*=3 sampling periods). During sampling periods 1 and 2, 58.4 and 52.5% of O_2 class degradation occurring in the HCW series took place in wetland cells (i.e. WC1, WC2-5). Decreases in relative abundance of the O_2 class in the wetland cells were commensurate with increases in the O_3 and O_4 classes, suggesting that biotransformation of compounds in the O_3 and O_4 classes was outpaced by production of degradation intermediates. These speciation data support the occurrence of aerobic degradation of NAFCs in wetland cells and indicate that decreases in evapotranspiration-adjusted concentrations of NAFCs were caused predominantly by transformation of compounds in the O_2 class (Section 3.3.2). This observation is consistent with studies by Han et al. (2008) and Martin et al. (2010), who observed greater removal efficiencies for aerobic degradation of the O_2 class compared to the O_3 class, and with previous work identifying more abundant oxidized NAs in older OSPWs subjected to greater extents of *in situ* biodegradation (Han et al., 2009; Marentette et al., 2015a). However, the increase in relative abundance of poly-oxygenated classes and decrease in the O_2 class is contrary to Yue et al. (2015b), who observed declines in relative abundance of O_3 and O_4 classes and increases in the O_2 class in a continuous flow fixed-bed biofilm reactor.

Environmental conditions (i.e. nutrient concentrations, temperature, DO, and pH) influence metabolic pathways, microbiome composition, and microbial abundance (Paris et al., 1981), which in turn affect rates and extents of aerobic NA degradation (Paslawski et al., 2009; Kinley et al., 2015). During sampling period 3, NAFCs concentrations and relative abundance of the O_2 class did not decrease in wetland cells (Figure 4 and Table S2). Mean daily water temperature during sampling period 3 (6.91±2.62°C) was significantly lower than during sampling periods 1 (16.72±3.43; p=<0.0001) and 2 (9.04±2.65; p=<0.0001). Kinley et al. (2015) found that when pH, DO, and nutrients concentrations were non-limiting, a similar range of temperatures (5±1°C) decreased microbial diversity and prolonged aerobic degradation of a commercial NA blend (Fluka). Ratios of carbon to nitrogen and phosphorus (C:N=330:1; C:P=1200:1), DO (2.84 to 8.25 mg/L), and pH (7.39 to 7.95) were supportive of aerobic degradation during sampling period 3, suggesting that aerobic degradation of NAFCs was impaired by temperature.

Fixed-film solar photocatalysis achieved greater decreases in NAFC class relative abundance in less time than achieved by aerobic degradation in the wetland cells. Over three sampling events, mean removal efficiency of the O_2 class in PC1 was 18.7% over a 1-d HRT, compared to 14.8% over a 16-d HRT in the wetland cells (WC1, WC2-5). Over a mean photoperiod of 38.3±8.1 h, PC2 decreased relative abundance of the O_2 class 56.6% from inflow (31.3±2.7%) to outflow (13.5±1.4%), and increased relative abundance of degradation intermediates in the O_5, O_6, and O_7, classes by factors of 2.7, 5.5, and 13.7, respectively. Using photocatalysis over agitated TiO_2 slurries, Leshuk et al.

(2016a) observed similar shifts in class distribution and extensive degradation of NAFCs within 14 h of sunlight exposure.

Changes in class distribution demonstrate that aerobic degradation and solar fixed-film photocatalysis implemented sequentially in a hybrid pilot-scale CWTS can alter composition of the organic fraction of OSPW. These processes were effective in decreasing the relative abundance of the O_2 class, which has been identified as the primary source of toxicity within the organic fraction of NAs (Morandi et al., 2015; Yue et al., 2015a; Hughes et al., 2017). Operation of the hybrid CWTS at mean daily temperatures between 0 and 11°C suggests that biodegradation of NAFCs in the wetland cells was impaired within this range. Polishing photocatalysis in fixed film photocatalytic reactors targeting >1.5 MJ/m^2 UV insolation altered class distributions of NAFCs remaining after treatment in HCW series. The hybrid CWTS shifted NAFC classes from regimes dominated by classical NAs (i.e., O_2 class) to sparingly toxic poly-oxygenated classes (i.e. $O_{3\text{-}7}$) within 2-3 weeks, compared to natural attenuation processes (i.e. biodegradation and photolysis) that may require months to years to achieve similar alterations (Han et al., 2009; Toor et al., 2013a; Wan et al., 2014).

3.3.2 NAFC concentrations

Mean NA concentration, determined by derivatization and HPLC, in untreated OSPW was 67±4 mg/L (*n*=9). During three sampling periods, the hybrid pilot-scale CWTS decreased NA concentrations by 67±9% and 72±2% in Series A and B, respectively. Mean NAFCs concentration decreased by 77.6±11.3% (*n*=3) from inflow (43.1±5.9 mg/L) to outflow (10.4±6.0 mg/L) of the hybrid pilot-scale CWTS. Decreases

in NA and NAFC concentrations occurred primarily in PC1 and PC2 (Figures 4, 5). For example, mean NAFCs concentrations decreased from 43.4±9.6 to 34.5±4.9 mg/L (19.5±6.8%) in PC1 and from 29.3±3.0 to 10.4±6.0 mg/L (69.3±15.7%) in PC2. UV insolation during PC2 ranged from 1.48 to 2.71 MJ/m^2, which was significantly greater (p=0.0003) than insolation measured during PC1 (0.311 and 0.698 MJ/m^2), accounting for the greater removal efficiencies during polishing photocatalysis (PC2). Over three sampling events, PC2 Series A and B achieved NA removal efficiencies (67±9 and 72±2% in Series A and B, respectively) similar to McQueen et al. (2017b), but required greater UV insolation (2.07±0.59 and 2.02±0.64 MJ/m^2 in Series A and B, respectively) despite similarities in design. Rates of photocatalytic degradation of NAFCs in OSPW decrease commensurately with temperature (Leshuk et al., 2016a,b). Mean daily minimum and maximum temperatures reported in McQueen et al. (2017b) were greater than values measured during operation of PC2 (17 to 36°C and 4 to 19°C, respectively), and may account for differences in UV insolation required to achieved similar removal efficiencies.

Between 31 and 39% of OSPW was lost to evapotranspiration in the HCW series during sampling periods 1 and 2, increasing concentrations of conservative constituents (e.g., Cl^-, B) and masking treatment of recalcitrant OSPW organics. As a result, there were not significant differences between mean NAFC concentrations in untreated OSPW and outflow from WC5 (n=3 sampling periods; p=0.739; Figure 5). However, when values are adjusted for evapotranspiration (Section 2.4; Eqn. 3) mean NAFC concentration was significantly lower in WC5 outflow (p=0.0217) and decreased 29%

relative to untreated OSPW (Figure 5). NA and NAFC concentration decreased within PC1, but concentrations increased or did not change in the following wetland cells. However, between PC1 and WC5, percent increases in Cl^- concentration and conductivity were greater than increases in NAFC and NA concentration (Tables S1, S3) suggesting that OSPW organics were degraded partially in wetland cells (WC2-5) after PC1. For example, Cl^- increased 34% (Series A) and 39% (Series B) during sampling period 2, while NAFC concentration increased 12.3% and NA concentrations increased 6% and 3% in Series A and Series B, respectively. Ranges of hydrosoil ORP, and DO concentrations, and carbon to nitrogen and phosphorous ratios in wetland cells were within ranges supportive of aerobic microbial degradation of NAs (Kinley et al., 2015; McQueen et al., 2017b). In previous studies, continuous flow biofilm reactors achieved NA removal efficiencies up to 38% at rates between 2.82 and 12.6 $mg \cdot L^{-1} \cdot d^{-1}$ (Hwang et al., 2013; McKenzie et al., 2014), supporting removal of NAs by biodegradation in engineered systems. Toor et al. (2013a) observed decrease in NAFC concentrations in OSPW by 40% after 40 days in incubated wetland sediment microcosms when aeration and nutrients were provided. Similar to Toor et al. (2013a), passive treatment experiments utilizing macrophyte planted microcosms (Armstrong et al., 2009) and wetland cells to mediate aerobic degradation measured increases or no changes in NAFC concentration; (McQueen et al., 2017b). Armstrong et al., (2009), Toor et al., (2013a), and McQueen et al., (2017b) measured decreases in toxicity irrespective of changes in NA concentration, supporting the ability of microbial processes associated with wetland

sediments and macrophytes to change exposures of OSPW via compositional alteration of NAFCs.

3.4 Change in concentration of metals and metalloids

Mean As concentration in untreated OSPW was 0.026±0.004 mg/L (*n*=3 sampling events), and decreased to 0.011±0.002 and 0.013±0.005 mg/L in outflows of HCW Series A and B, respectively (Table 5). Arsenic concentrations decreased rapidly in the initial wetland cells (WC1) and photocatalytic reactors (PC1; Figure S3), but mean concentrations fluctuated between 0.008 and 0.013 mg/L in the remaining wetland cells (WC2-5). Zn decreased from mean initial concentrations of 0.129±0.071 mg/L by 49±8 and 54 ±16% in outflows of HCW Series A and B, respectively (*n*=3 sampling events). Zn concentrations decreased sharply in WC1 (Figure S3), but concentrations increased slightly by the outflow of final wetland cells (WC5). Over three sampling events, concentrations of Cu and Pb were not significantly different between untreated OSPW and outflows from HCW series (Series A: p=0.25 for Cu, p=0.35 for Pb; Series B: p=0.21 for Cu, p=0.64 for Pb). Boron concentrations increased slightly from 2.33±0.09 mg/L to 2.89±0.52 and 2.82±0.48 mg/L in HCW Series A and B, respectively. There were no significant differences in mean concentrations of B, Cu, Pb, and Zn between outflows of HCW and PC2 (Table S4).

Although concentrations of As and Zn were below WQC in samples collected within HCW series (Figure S3), concentrations of all metals and metalloids in outflows of HCW series exceeded conservative WQC (Table 2). However, when compared to laboratory derived toxicity endpoints for *C. dubia*, concentrations of As, B, Cu, Pb, and

Zn in all samples collected from HCW Series A and B outflow were less than toxicity thresholds for *C. dubia* including: a 2-d LC50 of 2.4 mg As/L (Hu et al., 2012), a 14-d LOEC of 18 mg B/L for reproduction (Hickey, 1989), a 7-d LOEC of 0.099 mg Cu/L (Belanger and Cherry, 1990), 0.080 mg Pb/L (Zuiderveen and Birge, 1997), and 0.128 mg Zn/L for reproduction (Zuiderveen and Birge, 1997). Additionally, McQueen et al. (2017a) and Verbeek (1994) concluded that metals are not a significant source of toxicity in OSPW after observing no decrease in acute toxicity of OSPW to *C. dubia* and *Vibrio fischeri*, respectively, after chelation of metals with ethylenediaminetetraacidic acid (EDTA).

When concentrations of metals and metalloids measured in outflows of HCW series were adjusted for evaporative and precipitative fluxes (Eqn. 3; Table 5), removal efficiencies improved in sampling periods 1 and 2, and changed only slightly during sampling period 3, which had a near neutral water balance. Arsenic removal efficiencies during sampling periods 1 and 2 ranged from 30 to 59% prior to adjustment for evaporation, and improved to between 53 and 74% after adjustment. Concentrations of Zn decreased by 57±9.5% in HCW series during sampling periods 1 and 2 (n=4), and mean removal efficiency improved to 72±7.7% after adjustment for evapotranspiration. Prior to adjustment, B concentrations increased up to 46.5% from inflow to outflow of HCW series. After adjustment, concentrations of B in outflows of Series A and B decreased by 7.58±4.65 and 11.2±4.52% (n=3), respectively. After adjustment for evapotranspiration, Cu and Pb concentrations decreased, but were not significantly

different from initial concentrations in Series A (p=0.19; p=0.16) or Series B (p=0.55; p=0.20).

Arsenic can be sequestered in wetland cells through co-precipitation with Fe/Mn oxy-hydroxides, which form when bulk oxidizing conditions are achieved (i.e. DO>2.0 mg/L; ORP>-50mV; Lizama et al., 2011; Schwindaman et al., 2014). Over the duration of three sampling periods, mean DO concentration was 3.64±2.15 and 8.96±1.69 mg/L in WC1 and PC1, respectively, coinciding with precipitous decreases in As concentration (Figure S3). Reddy and DeLaune (2008) and Jurinko (2012) found that co-precipitation of Zn with oxyhydroxides is the dominant pathway for decreasing aqueous Zn concentrations in wetlands at pH=6.5 to 8.0 and ORP = -50 to 250 mV. These ranges of pH, DO, and ORP are consistent with values measured in A1 and B1 (Table S1), in which mean Zn concentrations decreased from initial concentrations of 0.129±0.071 to 0.052±0.028 mg/L and 0.040±0.001 mg/L (n=3), respectively. Decreases in B concentration, which were observed only after concentrations were adjusted for evapotranspiration, are attributed to plant uptake for use in structural maintenance of cell walls (Golbach and Wimmer, 2007). When all plants senesced during sampling period 3, removal efficiencies of adjusted B concentrations decreased accordingly.

Pilot and full-scale CWTSs have decreased concentrations of Cu and Pb in impaired waters, eliminating toxicity and meeting National Pollutant Discharge Elimination System (NPDES) limits (Hawkins et al., 1997; Murray-Gulde et al., 2005b; Huddleston et al., 2008; Johnson et al., 2008; Kanagy et al., 2008a). In a study by Kanagy et al. (2008a), Cu concentrations decreased by 89% (from 0.89 to 0.099 mg/L) and Pb

concentrations decreased by 93% (from 2.56 to 0.176 mg/L) over a 4-d HRT in a pilot-scale CWTS assembled with *T. latifolia* and *Schoenoplectus californicus*. A full-scale CWTS designed specifically to sequester Cu decreased mean acid-soluble Cu concentration from 0.027±0.009 to 0.004±0.002 mg/L (85%; Murray-Gulde et al., 2005b). These CWTSs contained wetland cells designed to promote bulk reducing conditions (i.e. DO<2 mg/L; ORP =-250 to -50 mV) and production of AVS. In the hybrid pilot-scale CWTS studied in the current investigation, AVS was produced in micro-environments within the hydrosoil and detritus of wetland cells, but not in sufficient quantities to decrease concentrations of Cu and Pb to below the most protective WQC. To achieve compliance with WQC for Cu and Pb, future CWTSs for OSPW should include "reducing cells" containing hydrosoil near saturation with AVS.

3.5 Change in survival and reproduction of Ceriodaphnia dubia

Survival of *C. dubia* in untreated OSPW was significantly less than laboratory controls (i.e. moderately-hard water; USEPA, 2002) in sampling periods 1 and 2 (p=0.045 and p<0.0001, respectively; Table 6). Reproduction was impaired relative to controls in inflow samples collected during sampling periods 1 and 3 (p<0.001 and p<0.001, respectively). In sampling period 2, reproduction was not adversely affected in surviving daphnids; however, only 2 out of 20 daphnids produced three broods. Survival exceeded 95% in outflows of PC1 during all sampling periods (n=6). During sampling periods 2 and 3, reproduction improved in PC1 outflows relative to untreated OSPW; however, reproduction was significantly lower than controls in outflows from APC1 and BPC1 during sampling period 1 (p<0.001 and p=0.042, respectively). Toxicity was

eliminated in all HCW series outflow samples, except for HCW Series B during sampling period 1, in which survival was significantly lower than the control (p=0.024). Reproduction of daphnids exposed to outflow of PC2 Series B during sampling period 1 was also adversely affected. Toxicity was eliminated in all other samples collected from PC2 series.

Adverse effects to survival and reproduction of *C. dubia* were eliminated at all positions within the hybrid CWTS during sampling periods 2 and 3. During sampling period 1, reproduction was impaired in outflows of APC1, BPC1, BPC2 In, and BPC2 Out, and mortality was statistically lower than the control in B5 outflow. Approximately 40% of OSPW loaded into HCW series was lost to evapotranspiration during the first sampling period, increasing concentrations of recalcitrant constituents, most notably Cl^- and NAFCs. Process based manipulations have identified polar organics as the primary source of acute toxicity in OSPW (McQueen et., 2017a; Verbeek, 1994); however, Zubot et al. (2012) suggested that synergism between dissolved salts and NAFCs may impair survival and reproduction of salinity-sensitive *C. dubia* (e.g., EC_{50} for *C. dubia* reproduction = 461 mg Cl^- /L; Zubot et al., 2012). Additionally, Nero et al. (2006) found that the toxicity of NAFCs to juvenile yellow perch increased with salinity, resulting in greater mortality and levels of gill proliferative relative to exposures of NAFCs alone. As Cl^- concentrations increased during sampling period 1, the relative abundance of acutely toxic O_2 NAFCs decreased. Changes in relative abundance of the O_2 class were similar during sampling period 1 and 2 (Table S2), but Cl^- concentrations were up to 16% higher in sampling period 1. As the primary driver of toxicity in OSPW, similar changes in

relative abundance of O_2 NAs should yield similar responses to *C. dubia*. The higher frequency of impaired reproduction and survival in sampling period 1 may therefore be attributed to synergism between increased concentrations of Cl^- and NAFCs.

While rainbow trout and fathead minnows have been used extensively to measure toxicity of NAFCs (Verbeek, 1994; Morandi et al., 2015, Marentette et al., 2015a,b), sensitivity of *C. dubia* to OSPW organics and salts makes this species well suited for measuring performance of passive treatment systems for OSPW, where extended HRTs required for aerobic degradation of organics may increase concentrations of conservative constituents due to evapotranspiration. *C. dubia* bioassays provide endpoints representative of toxicity of the OSPW matrix as a whole, as opposed to the organic fraction alone.

4.0 Conclusions

The hybrid pilot-scale CWTS decreased concentrations and changed compositions of NAFCs in a specific OSPW by sequential implementation of fixed-film TiO_2 photocatalytic reactors and aerobic degradation in wetland cells. Orbitrap MS showed that this approach decreased NAFC concentrations by 75.9%, and shifted class distributions from regimes dominated by acutely toxic O_2 NAFCs (O_2=40.3%, $\sum O_{3-9}$=45.0%) in untreated OSPW to sparingly toxic poly-oxygenated classes (O_{3-9}; O_2=13.6%, $\sum O_{3-9}$=77.0%). The initial wetland cells (WC1) removed TSS and O&G and decreased attenuation of solar UV radiation in OSPW prior to treatment in the initial photocatalytic reactors (PC1). Concentrations of As, B, Cu, Pb, and Zn in outflows from hybrid constructed wetland (HCW) and polishing photocatalytic reactor series (PC2;

Figure 1) exceeded protective WQC, but were below LOECs for *C. dubia* survival and reproduction. Performance of the hybrid CWTS was influenced by weather conditions in this outdoor pilot-scale experiment. During sampling periods 1 and 2, evapotranspiration increased Cl^- concentrations and masked removal of NAFC concentrations by aerobic degradation in wetland cells. Changes in NAFC concentration and composition were limited outside of the photocatalytic reactors in sampling period 3, suggesting that near-freezing temperatures inhibited aerobic degradation in the wetland cells. Toxicity to *C. dubia* was eliminated in all samples recovered from the hybrid CWTS during sampling periods 2 and 3, but reproduction was impaired in 4 of 8 samples during the first sampling event and was potentially caused by synergism between Cl^- and residual NAFCs.

Hybrid CWTSs offer a comprehensive approach for treating the wide range of COCs in OSPW, as opposed to technologies which target NAFCs alone. Further development of fixed-film photocatalytic reactors and determination NAFC biodegradation kinetics in OSPW treated by photocatalysis will refine designs of future hybrid CWTS experiments. Currently, there is a dearth of literature concerning the use of constructed wetlands for treatment of OSPW and a scarcity of studies reporting performance data for COCs in OSPW alongside biogeochemical conditions in experimental wetlands. This study, which reports changes in distribution of NAFC classes measured contemporaneously with biogeochemical conditions in a hybrid pilot-scale CWTS, is a pertinent contribution to the growing body of literature supporting the application of constructed wetlands for remediation of OSPW.

5.0 References

Ajaero, C., McMartin, D.W., Peru, K.M., Bailey, J., Haakensen, M., Friesen, V., Martz, R., Hughes, S.A., Brown, C., Chen, H., 2017. Fourier Transform Ion Cyclotron Resonance Mass Spectrometry Characterization of Athabasca Oil Sand Process-Affected Waters Incubated in the Presence of Wetland Plants. Energy & Fuels. 31, 1731-1740.

Alberta Energy Regulator (AER), 2016. Fluid Tailings Management for Oil Sands Mining Projects. Oil Sands Conservation Act Directive 085. Alberta Energy Regulator, Calgary, AB. https://www.aer.ca/documents/directives/Directive085.pdf.

Alberta Environment and Parks (AEP), 2014. Environmental Quality Guidelines for Alberta Surface Waters. Water Policy Branch, Policy Division, Edmonton, AB. http://aep.alberta.ca/water/education-guidelines/documents/EnvironmentalQualitySurfaceWaters-2014.pdf.

Allen, E.W., 2008. Process water treatment in Canada's oil sands industry: I. Target pollutants and treatment objectives. Journal of Environmental Engineering and Science. 7, 123-138.

Alley, B.L., Willis, B., Rodgers, J., Castle, J.W., 2013. Water depths and treatment performance of pilot-scale free water surface constructed wetland treatment systems for simulated fresh oilfield produced water. Ecological Engineering. 61, 190-199.

American Public Health Association (APHA), American Water Works Association, Water Environment Federation, 2012. Standard methods for the examination of water and wastewater, 21st edition. American Public Health Association, Port City Press., Baltimore, MA.

Armstrong, S.A., Headley, J.V., Peru, K.M., Germida, J.J., 2009. Differences in phytotoxicity and dissipation between ionized and nonionized oil sands naphthenic acids in wetland plants. Environmental Toxicology and Chemistry. 28, 2167-2174.

Armstrong, S.A., Headley, J.V., Peru, K.M., Germida, J.J., 2008. Phytotoxicity of oil sands naphthenic acids and dissipation from systems planted with emergent aquatic macrophytes. Journal of Environmental Science and Health, Part A. 43, 36-42.

Beebe, D.A., Castle, J.W., Molz, F., Rodgers, J.H., 2014. Effects of evapotranspiration on treatment performance in constructed wetlands: Experimental studies and modeling. Ecological Engineering. 71, 394-400.

Belanger, S.E., and Cherry, D.S., 1990. Interacting effects of pH acclimation, pH, and heavy metals on acute and chronic toxicity to *Ceriodaphnia dubia* (Cladocera). Journal of Crustacean Biology. 10, 225-235.

Bishay, F.S., 1998. The use of constructed wetlands to treat oil sands wastewater. Fort McMurray, Alberta, Canada. University of Alberta. Masters Thesis.

Brient, J.A., Wessner, P.J., Doyle, M.N., 1995. Naphthenic acids. In: Encyclopedia of Chemical Technology. Kroschwitz, J.I. (Ed.). John Wiley & Sons, New York. 1017-1029.

Brown, L.D., Pérez-Estrada, L., Wang, N., El-Din, M.G., Martin, J.W., Fedorak, P.M., Ulrich, A.C., 2013. Indigenous microbes survive *in situ* ozonation improving biodegradation of dissolved organic matter in aged oil sands process-affected waters. Chemosphere. 93, 2748-2755.

Brown, L.D., and Ulrich, A.C., 2015. Oil sands naphthenic acids: a review of properties, measurement, and treatment. Chemosphere. 127, 276-290.

Canada's Oil Sands Innovation Alliance (COSIA), 2015. Passive Organics Treatment Technology. Canada's Oil Sands Innovation Alliance, Calgary, AB. http://www.cosia.ca/uploads/files/challenges/water/COSIA%20Challenge%20Water%20-%20Passive%20Organics%20Treatment %20Technology.pdf

Canadian Council of Ministers of the Environment (CCME), 2011. Canadian Water Quality Guidelines for the Protection of Aquatic Life. Canadian environmental quality guidelines, 1999. Canadian Council of Ministers of the Environment, Winnipeg, MB. http://st-ts.ccme.ca/en/index.html.

Carpenter, S.R., Kitchell, J.F., Hodgson, J.R., 1985. Cascading trophic interactions and lake productivity. Bioscience. 35, 634-639.

Clemente, J.S., and Fedorak, P.M., 2005. A review of the occurrence, analyses, toxicity, and biodegradation of naphthenic acids. Chemosphere. 60, 585-600.

Cumulative Environmental Management Association (CEMA), 2014. Guidelines for wetlands establishments on reclaimed oil sands leases. 3rd edition. Alberta Environment, Fort McMurray, AB.

Environment and Climate Change Canada (ECCC), 2007. Biological test method: test of reproduction and survival using the Cladoceran *Ceriodaphnia dubia*. EPS 1/RM/21 2nd edition. Environment and Climate Change Canada, Ottawa, ON.

Faulkner, S., Patrick, W., Gambrell, R., 1989. Field techniques for measuring wetland soil parameters. Soil Science Society of America Journal. 53, 883-890.

Frank, R.A., Kavanagh, R., Burnison, B.K., Arsenault, G., Headley, J.V., Peru, K.M., Van Der Kraak, G., Solomon, K.R., 2008. Toxicity assessment of collected fractions from an extracted naphthenic acid mixture. Chemosphere. 72, 1309-1314.

Fujishima, A., Rao, T.N., Tryk, D.A., 2000. Titanium dioxide photocatalysis. Journal of Photochemistry and Photobiology C: Photochemistry Reviews. 1, 1-21.

Gillespie, W.B., Hawkins, W.B., Rodgers, J.H., Cano, M.L., Dorn, P.B., 2000. Transfers and transformations of zinc in constructed wetlands: Mitigation of a refinery effluent. Ecological Engineering. 14, 279-292.

Goldbach, H.E., and Wimmer, M.A., 2007. Boron in plants and animals: Is there a role beyond cell-wall structure? Journal of Plant Nutrition and Soil Science. 170, 39-48.

Golder Associates, 2001. Oil Sands Regional Aquatics Monitoring Program (RAMP) 2000. Volume 1: Chemical and Biological Monitoring. Golder Associates Ltd., Calagary, AB.

Goodfellow, W.L., Ausley, L.W., Burton, D.T., Denton, D.L., Dorn, P.B., Grothe, D.R., Heber, M.A., Norberg-King, T.J., Rodgers, J.H., 2000. Major ion toxicity in effluents: a review with permitting recommendations. Environmental Toxicology and Chemistry. 19, 175-182.

Grewer, D.M., Young, R.F., Whittal, R.M., Fedorak, P.M., 2010. Naphthenic acids and other acid-extractables in water samples from Alberta: what is being measured? Science of the Total Environment. 408, 5997-6010.

Haakensen, M., Pittet, V., Spacil, M.M., Castle, J.W., Rodgers Jr, J.H., 2015. Key aspects for successful design and implementation of passive water treatment systems. Journal of Environmental Solutions for Oil, Gas, and Mining. 1, 59-81.

Han, X., MacKinnon, M.D., Martin, J.W., 2009. Estimating the *in situ* biodegradation of naphthenic acids in oil sands process waters by HPLC/HRMS. *Chemosphere.* 76, 63-70.

Han, X., Scott, A.C., Fedorak, P.M., Bataineh, M., Martin, J.W., 2008. Influence of molecular structure on the biodegradability of naphthenic acids. Environmental Science & Technology. 42, 1290-1295.

Hawkins, W.B., Rodgers, J.H., Gillespie, W., Dunn, A., Dorn, P., Cano, M., 1997. Design and construction of wetlands for aqueous transfers and transformations of selected metals. Ecotoxicology and Environmental Safety. 36, 238-248.

Haynes, W.M., 2014. CRC handbook of chemistry and physics. CRC Press. Boca Raton, FL.

Headley, J.V., Du, J., Peru, K.M., McMartin, D.W., 2009. Electrospray ionization mass spectrometry of the photodegradation of naphthenic acids mixtures irradiated with titanium dioxide. Journal of Environmental Science and Health Part A. 44, 591-597.

Headley, J.V., and McMartin, D.W., 2004. A review of the occurrence and fate of naphthenic acids in aquatic environments. Journal of Environmental Science and Health, Part A. 39, 1989-2010.

Headley, J.V., Peru, K.M., Janfada, A., Fahlman, B., Gu, C., Hassan, S., 2011. Characterization of oil sands acids in plant tissue using Orbitrap ultra-high resolution mass spectrometry with electrospray ionization. Rapid Communications in Mass Spectrometry. 25, 459-462.

Headley, J.V., Peru, K.M., Fahlman, B., McMartin, D.W., Mapolelo, M.M., Rodgers, R.P., Marshall, A.G., 2012. Comparison of the levels of chloride ions to the characterization of oil sands polar organics in natural waters by use of Fourier transform ion cyclotron resonance mass spectrometry. Energy & Fuels. 26(5), 2585-2590.

Health Canada, 2012. Guidelines for Canadian Recreational Water Quality, 3rd Edition. Water, Air and Climate Change Bureau, Healthy Environments and Consumer Safety Branch, Ottawa, ON. H129-15/2012E.

Herman, D.C., Fedorak, P.M., MacKinnon, M.D., Costerton, J., 1994. Biodegradation of naphthenic acids by microbial populations indigenous to oil sands tailings. Canadian Journal of Microbiology. 40, 467-477.

Hickey, C.W., 1989. Sensitivity of four New Zealand cladoceran species and *Daphnia magna* to aquatic toxicants. New Zealand Journal of Marine and Freshwater Research. 23, 131-137.

Hu, J., Wang, D., Forthaus, B.E., Wang, J., 2012. Quantifying the effect of nanoparticles on As (V) ecotoxicity exemplified by nano-Fe_2O_3 (magnetic) and nano-$_{Al2O3}$. Environmental Toxicology and Chemistry. 31, 2870-2876.

Huddleston III, G.M., and Rodgers Jr, J.H., 2008. Design of a constructed wetland system for treatment of copper-contaminated wastewater. Environmental Geosciences. 15, 9-19.

Huddleston, G.M., Gillespie, W.B., Rodgers, J.H., 2000. Using constructed wetlands to treat biochemical oxygen demand and ammonia associated with a refinery effluent. Ecotoxicology and Environmental Safety. 45, 188-193.

Hughes, S.A., Mahaffey, A., Shore, B., Baker, J., Kilgour, B., Brown, C., Peru, K.M., Headley, J.V., Bailey, H.C., 2017. Using ultrahigh-resolution mass spectrometry and toxicity identification techniques to characterize the toxicity of oil sands process-affected water: the case for classical naphthenic acids. Environmental Toxicology and Chemistry. Online version of record, August 7, 2017.

Hwang, G., Dong, T., Islam, M.S., Sheng, Z., Pérez-Estrada, L.A., Liu, Y., El-Din, M.G., 2013. The impacts of ozonation on oil sands process-affected water biodegradability and biofilm formation characteristics in bioreactors. Bioresource Technology. 130, 269-277.

Igunnu, E.T., and Chen, G.Z., 2012. Produced water treatment technologies. International Journal of Low-Carbon Technologies. 9, 157-177.

Inoue, T.M., and Tsuchiya, T., 2008. Interspecific differences in radial oxygen loss from the roots of three Typha species. Limnology. 9, 207-211.

Johnson, B.M., Kanagy, L.E., Rodgers Jr, J.H., Castle, J.W., 2008. Feasibility of a pilot-scale hybrid constructed wetland treatment system for simulated natural gas storage produced waters. Environmental Geosciences. 15, 91-104.

Jurinko, K.N., 2012. Biogeochemical processes in hydrosoil of a pilot-scale constructed wetland treatment system designed for treatment of metals. Clemson University, Clemson, SC. Master's Thesis.

Kanagy, L.E., Johnson, B.M., Castle, J.W., Rodgers, J.H., 2008a. Design and performance of a pilot-scale constructed wetland treatment system for natural gas storage produced water. Bioresource Technology. 99, 1877-1885.

Kanagy, L.E., Johnson, B.M., Castle, J.W., Rodgers Jr, J.H., 2008b. Hydrosoil conditions in a pilot-scale constructed wetland treatment system for natural gas storage produced waters. Environmental Geosciences. 15, 105-113.

Kinley, C.M., Gaspari, D.P., McQueen, A.D., Rodgers, J.H., Castle, J.W., Friesen, V., Haakensen, M., 2016. Effects of environmental conditions on aerobic degradation of a commercial naphthenic acid. Chemosphere. 161, 491-500.

Lai, J.W., Pinto, L.J., Bendell-Young, L.I., Moore, M.M., Kiehlmann, E., 1996. Factors that affect the degradation of naphthenic acids in oil sands wastewater by indigenous microbial communities. Environmental Toxicology and Chemistry. 15, 1482-1491.

Lehman, R.W., Gladden, J.B., Bell, J.F., Rodgers Jr., J.H., Murray-Gulde, C., Mooney, F.D., 2002. Wetlands for industrial wastewater treatment at the Savannah River Site. Westinghouse Savannah River Company (WSRC) Report Number: WSRC-MS-2002-00161. WSRC, Aiken, SC.

Leonard, E.N., Ankley, G.T., Hoke, R.A., 1996. Evaluation of metals in marine and freshwater surficial sediments from the Environmental Monitoring and Assessment Program relative to proposed sediment quality criteria for metals. Environmental Toxicology and Chemistry. 15, 2221-2232.

Leshuk, T., Wong, T., Linley, S., Peru, K.M., Headley, J.V., Gu, F., 2016a. Solar photocatalytic degradation of naphthenic acids in oil sands process-affected water. Chemosphere. 144, 1854-1861.

Leshuk, T., de Oliveira Livera, D., Peru, K.M., Headley, J.V., Vijayaraghavan, S., Wong, T., Gu, F., 2016b. Photocatalytic degradation kinetics of naphthenic acids in oil sands process-affected water: Multifactorial determination of significant factors. Chemosphere. 165, 10-17.

Lizama, K., Fletcher, T.D., Sun, G., 2011. Removal processes for arsenic in constructed wetlands. Chemosphere. 84, 1032-1043.

MacKinnon, M.D., and Boerger, H., 1986. Description of two treatment methods for detoxifying oil sands tailings pond water. Water Quality Research Journal of Canada. 21, 496-512.

Madill, R.E., Orzechowski, M.T., Chen, G., Brownlee, B.G., Bunce, N.J., 2001. Preliminary risk assessment of the wet landscape option for reclamation of oil sands mine tailings: bioassays with mature fine tailings pore water. Environmental Toxicology. 16, 197-208.

Mahaffey, A., and Dubé, M., 2016. Review of the composition and toxicity of oil sands process-affected water. Environmental Reviews. 25, 97-114.

Malato, S., Fernández-Ibáñez, P., Maldonado, M.I., Blanco, J., Gernjak, W., 2009. Decontamination and disinfection of water by solar photocatalysis: recent overview and trends. Catalysis Today. 147, 1-59.

Marentette, J.R., Frank, R.A., Bartlett, A.J., Gillis, P.L., Hewitt, L.M., Peru, K.M., Headley, J.V., Brunswick, P., Shang, D., Parrott, J.L., 2015. Toxicity of naphthenic acid fraction components extracted from fresh and aged oil sands process-affected waters, and commercial naphthenic acid mixtures, to fathead minnow (*Pimephales promelas*) embryos. Aquatic Toxicology. 164, 108-117.

Marentette, J.R., Frank, R.A., Hewitt, L.M., Gillis, P.L., Bartlett, A.J., Brunswick, P., Shang, D., Parrott, J.L., 2015. Sensitivity of walleye (*Sander vitreus*) and fathead minnow (*Pimephales promelas*) early-life stages to naphthenic acid fraction components extracted from fresh oil sands process-affected waters. Environmental Pollution. 207, 59-67.

Martin, J.W., Barri, T., Han, X., Fedorak, P.M., El-Din, M.G., Perez, L., Scott, A.C., Jiang, J.T., 2010. Ozonation of oil sands process-affected water accelerates microbial bioremediation. Environmental Science & Technology. 44, 8350-8356.

McKenzie, N., Yue, S., Liu, X., Ramsay, B.A., Ramsay, J.A., 2014. Biodegradation of naphthenic acids in oils sands process waters in an immobilized soil/sediment bioreactor. Chemosphere. 109, 164-172.

McNeely, R.N., Neimanis, V.P., Dwyer, L., 1979. Water quality sourcebook: a guide to water quality parameters. In: Water Quality Sourcebook: A Guide to Water Quality Parameters. Environment Canada, Gatineau, QC.

McQueen, A.D., Kinley, C.M., Hendrikse, M., Gaspari, D.P., Calomeni, A.J., Iwinski, K.J., Castle, J.W., Haakensen, M.C., Peru, K.M., Headley, J.V., 2017a. A risk-based approach for identifying constituents of concern in oil sands process-affected water from the Athabasca Oil Sands region. Chemosphere. 173, 340-350.

McQueen, A.D., Hendrikse, M., Gaspari, D.P., Kinley, C.M., Rodgers, J.H., Castle, J.W., 2017b. Performance of a hybrid pilot-scale constructed wetland system for treating oil sands process-affected water from the Athabasca oil sands. Ecological Engineering. 102, 152-165.

Mikula, R., 2013. Trading water for oil: Tailings management and water use in surface-mined oil sands. In: Hein, F.J., Leckie, D., Larter, S., Suter, J.R. (Eds.). Heavy Oil and Oil-Sand Petroleum Systems in Alberta and Beyond. AAPG Studies in Geology 64: 1, 689-699. American Association of Petroleum Geologists (AAPG) Special Volumes.

Morandi, G.D., Wiseman, S.B., Pereira, A., Mankidy, R., Gault, I.G., Martin, J.W., Giesy, J.P., 2015. Effects-directed analysis of dissolved organic compounds in oil sands process-affected water. Environmental Science & Technology. 49, 12395-12404.

Murray-Gulde, C.L., Bearr, J., Rodgers, J.H., 2005a. Evaluation of a constructed wetland treatment system specifically designed to decrease bioavailable copper in a wastestream. Ecotoxicology and Environmental Safety. 61, 60-73.

Murray-Gulde, C.L, Heatley, J.E., Karanfil, T., Rodgers, J.H., Myers, J.E., 2003. Performance of a hybrid reverse osmosis-constructed wetland treatment system for brackish oil field produced water. Water Research. 37, 705-713.

Murray-Gulde, C.L., Huddleston, G.M., Garber, K.V., Rodgers, J.H., 2005b. Contributions of Schoenoplectus californicus in a constructed wetland system receiving copper contaminated wastewater. Water, Air, & Soil Pollution. 163, 355-378.

National Oceanic and Atmospheric Administration (NOAA), 2011. 1981-2010 Climate Normals: Clemson University. National Centers for Environmental Information, Asheville, NC. South Carolina State Climatology Office Climate Data. http://www.dnr.sc.gov/climate/sco/ClimateData/8110Normals.php.

National Weather Service (NWS), 2017. Hourly Weather Forecast. Greenville-Spartanburg National Weather Service Forecast Office, Clemson, SC. http://forecast.weather.gov/MapClick.php?map.x=115&map.y=187&marine=0&site=GSP&zmx=1&zmy=1&FcstType=graphical&lat=&lon=.

Nelson, E.A., and Gladden, J.B., 2008. Full-scale treatment wetlands for metal removal from industrial wastewater. Environmental Geosciences. 15, 39-48.

Nero, V., Farwell, A., Lee, L., Van Meer, T., MacKinnon, M., Dixon, D., 2006. The effects of salinity on naphthenic acid toxicity to yellow perch: gill and liver histopathology. Ecotoxicology and Environmental Safety. 65, 252-264.

Norberg-King, T., 1992. Toxicity identification evaluation: Characterization of chronically toxic effluents: Phase I. EPA/600/6-91/005F. US Environmental Protection Agency, Office of Research and Development, Environmental Research Laboratory. Duluth, MN.

Pardue, M.J., Castle, J.W., Rodgers, J.H., Huddleston, G.M., 2014. Treatment of oil and grease in produced water by a pilot-scale constructed wetland system using biogeochemical processes. Chemosphere. 103, 67-73.

Paris, D.F., Steen, W.C., Baughman, G.L., Barnett, J.T., 1981. Second-order model to predict microbial degradation of organic compounds in natural waters. Applied and Environmental Microbiology. 41, 603-609.

Paslawski, J.C., Headley, J.V., Hill, G.A., Nemati, M., 2009. Biodegradation kinetics of trans-4-methyl-1-cyclohexane carboxylic acid. Biodegradation. 20, 125-133.

Pennak, R.W., 1978. Freshwater invertebrates of the United States, 2nd ed. John Wiley & Sons.

Quagraine, E., Headley, J., Peterson, H., 2005. Is biodegradation of bitumen a source of recalcitrant naphthenic acid mixtures in oil sands tailing pond waters? Journal of Environmental Science and Health. 40, 671-684.

Quinlan, P.J., and Tam, K.C., 2015. Water treatment technologies for the remediation of naphthenic acids in oil sands process-affected water. Chemical Engineering Journal. 279, 696-714.

Reddy, K.R., and DeLaune, R.D., 2008. Biogeochemistry of wetlands: science and applications. CRC Press, Boca Raton, FL.

Rodgers Jr, J.H., and Castle, J.W., 2008. Constructed wetland systems for efficient and effective treatment of contaminated waters for reuse. Environmental Geosciences. 15, 1-8.

Romanova, U.G., Yarranton, H.W., Schramm, L.L., Shelfantook, W.E., 2004. Investigation of oil sands froth treatment. The Canadian Journal of Chemical Engineering. 82, 710-721.

Roy, J., Bickerton, G., Frank, R., Grapentine, L., Hewitt, L., 2016. Assessing risks of shallow riparian groundwater quality near an oil sands tailings pond. Groundwater. 54, 545-558.

Schramm, L.L., 2000. Surfactants: fundamentals and applications in the petroleum industry. Cambridge University Press. Cambridge, UK.

Schwindaman, J.P., Castle, J.W., Rodgers, J.H., 2014. Biogeochemical Process-Based Design and Performance of a Pilot-Scale Constructed Wetland for Arsenic Removal from Simulated Bangladesh Groundwater. Water, Air, & Soil Pollution. 225, 2009-2020.

Scott, A.C., Mackinnon, M.D., Fedorak, P.M., 2005. Naphthenic acids in Athabasca oil sands tailings waters are less biodegradable than commercial naphthenic acids. Environmental Science & Technology. 39, 8388-8394.

Shell Canada, 2016. Oil Sands Performance Report 2015. Shell Canada Limited, http://s01.static-shell.com/content/dam/royaldutchshell/documents/corporate/she-2055-oil-sands-performance-report-2015-final1.pdf.

Tissot, B.P., and Welte, D.H., 1978. Petroleum Formation and Occurrence, 2nd Edition. Springer Science, New York, NY.

Tomczyk, N., Winans, R., Shinn, J., Robinson, R., 2001. On the nature and origin of acidic species in petroleum. 1. Detailed acid type distribution in a California crude oil. Energy & Fuels. 15, 1498-1504.

Toor, N.S., Franz, E.D., Fedorak, P.M., MacKinnon, M.D., Liber, K., 2013a. Degradation and aquatic toxicity of naphthenic acids in oil sands process-affected waters using simulated wetlands. Chemosphere. 90, 449-458.

Toor, N.S., Han, X., Franz, E., MacKinnon, M.D., Martin, J.W., Liber, K., 2013b. Selective biodegradation of naphthenic acids and a probable link between mixture profiles and aquatic toxicity. Environmental Toxicology and Chemistry. 32, 2207-2216.

United States Environmental Protection Agency (USEPA), 2007. National recommended water quality criteria-correction. EPA 822-Z-99–001. Office of Water, Washington, DC.

United States Environmental Protection Agency (USEPA), 2002. Short-term methods for estimating the chronic toxicity of effluents and receiving waters to freshwater organisms. 4th Edition. EPA-821-R-02-013. Environmental Monitoring Systems Lab, Cincinnati, OH.

United States Environmental Protection Agency (USEPA), 2001. Trace elements in water, solids, and biosolids by inductively coupled plasma-atomic emission spectrometry. 5th Revision. EPA Method 200.7. EPA-821-R-01-010. Office of Water, Washington, DC.

United States Environmental Protection Agency (USEPA), 1999. Revision A: n-hexane extractable material (HEM; oil and grease) and silica gel treated n-hexane extractable material (SGTHEM; non-polar material) by extraction and gravimetry. EPA Method 1664. EPA-821-R-10-001. Office of Water, Washington, DC.

United States Environmental Protection Agency (USEPA), 1991. Technical support document for water quality based toxics control. EPA/505/2-90-001. Office of Water, Washington, DC.

Verbeek, A.G., 1994. A toxicity assessment of oil sands wastewater. University of Alberta, Edmonton, AB. Master's Thesis.

Vymazal, J., 2013. Emergent plants used in free water surface constructed wetlands: a review. Ecological Engineering. 61, 582-592.

Vymazal, J., 2010. Constructed wetlands for wastewater treatment: five decades of experience. Environmental Science & Technology. 45, 61-69.

Wan, Y., Wang, B., Khim, J.S., Hong, S., Shim, W.J., Hu, J., 2014. Naphthenic acids in coastal sediments after the Hebei spirit oil spill: a potential indicator for oil contamination. Environmental Science & Technology. 48, 4153-4162.

Weather Underground, 2017. Station ID: KCEU Station Name: Oconee County Regional. February 3, 2017. https://www.wunderground.com/history/airport/KCEU/DailyHistory.html.

Yen, T., Marsh, W.P., MacKinnon, M.D., Fedorak, P.M., 2004. Measuring naphthenic acids concentrations in aqueous environmental samples by liquid chromatography. Journal of Chromatography A. 1033, 83-90.

Yue, S., Ramsay, B.A., Wang, J., Ramsay, J., 2015. Toxicity and composition profiles of solid phase extracts of oil sands process-affected water. Science of the Total Environment. 538, 573-582.

Zayani, G., Bousselmi, L., Mhenni, F., Ghrabi, A., 2009. Solar photocatalytic degradation of commercial textile azo dyes: performance of pilot plant scale thin film fixed-bed reactor. Desalination. 246, 344-352.

Zubot, W., MacKinnon, M.D., Chelme-Ayala, P., Smith, D.W., El-Din, M.G., 2012. Petroleum coke adsorption as a water management option for oil sands process-affected water. Science of the Total Environment. 427, 364-372.

Zuiderveen, J.A., Birge, W.J., 1997. The relationship between chronic values in toxicity tests with *Ceriodaphnia dubia*. In: Environmental Toxicology and Risk Assessment: Modeling and Risk Assessment Sixth Volume. ASTM International, West Conshohocken, PA.

Figure 1. Diagram of hybrid pilot-scale CWTS (not to scale). The CWTS is composed of a hybrid constructed wetland (HCW) and a polishing photocatalytic reactor (PC2). The HCW consists of duplicate series (Series A and B), each containing wetland cells (WC1-5) and an initial photocatalytic reactor (PC1), composed of 4 individual reactor units. FMI piston pumps, calibrated to achieve a nominal hydraulic retention time (HRT) of 16 d, conveyed OSPW from a storage tank to HCW series. Outflows from HCW series were collected, transferred to PC2 inflow tanks, and circulated through PC2 series (APC2, BPC2) until exposed to >1.5 MJ/m^2 UV insolation.

Figure 2. Mean relative abundance of naphthenic acid fraction component (NAFC) classes in OSPW measured by electrospray ionization Orbitrap mass spectrometry following weak anion exchange (WAX) extraction according to Ajaero et al. (2017). Error bars represent one standard deviation (n=4).

Figure 3. Mean relative abundance of NAFC classes in hybrid pilot-scale CWTS measured over three sampling periods by electrospray ionization Orbitrap mass spectrometry, which was conducted by Dr. John Headley's laboratory at the National Hydrology Research Centre in Saskatoon, SK. Samples were collected from untreated OSPW influent (inflow), outflows from initial wetland cells (WC1), initial photocatalytic reactors (PC1), and final wetland cells (WC5), and polishing photocatalytic reactor (PC2) inflow and outflow (Section 2.3). Orbitrap-MS was conducted on composite samples from replicate Series A and B (Figure 1). Error bars indicate ± one standard deviation. NAFC classes with relative abundance <1% at all positions in the hybrid pilot-scale CWTS were not included in this graph.

Figure 4. A) Change in concentration of NAs relative to nominal hydraulic retention time (HRT) during three sampling periods in hybrid constructed wetland (HCW) Series A. B) Change in NA concentration in HCW Series B. C) Change in concentration of NAFCs in composite samples from HCW Series A and B (Section 2.3). NAFC concentrations were measured by Orbitrap mass spectrometry in Dr. John Headley's laboratory at the National Hydrology Research Centre in Saskatoon, SK, and NA concentrations were measured by derivatization and HPLC.

Figure 5. A) NAFC and NA concentrations averaged over three sampling periods in hybrid constructed wetland (HCW) and polishing photocatalytic reactor (PC2) Series A and B. B) Mean NAFC and NA concentrations adjusted for volumes lost to evapotranspiration in HCW and PC2 Series A and B (Section 2.4; Eqn. 3). NAFC concentrations were determined by Orbitrap mass spectrometry of composite samples from Series A and B (Section 2.3), and NA concentrations were measured by derivatization and HPLC in samples from each series. Concentrations were measured in HCW and PC2 inflows (Inflow and PC2 In, respectively) and outflows (WC5 and PC2 Out, respectively). Error bars are one standard deviation (n=3).

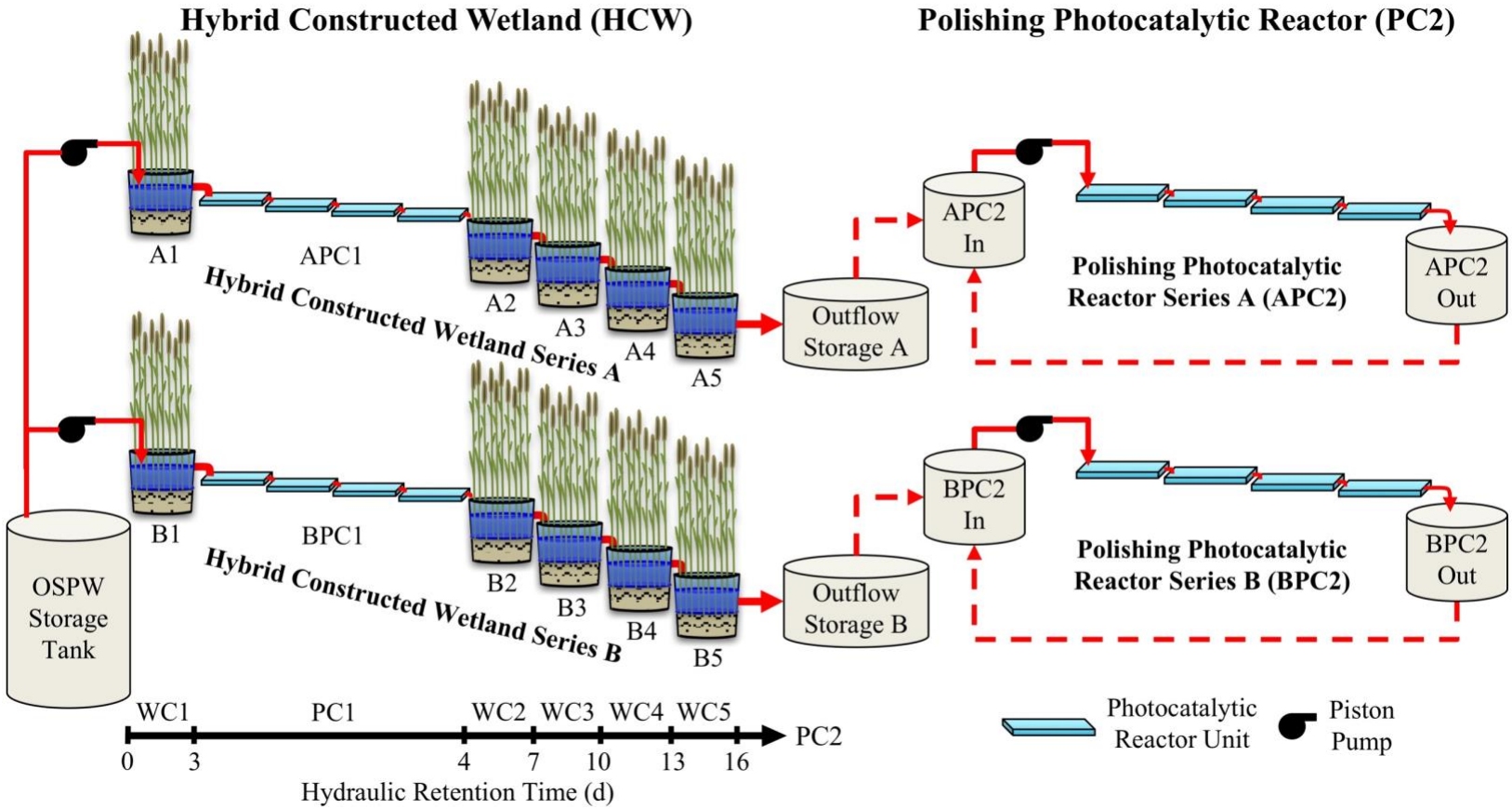
Hybrid Constructed Wetland (HCW)
Polishing Photocatalytic Reactor (PC2)
A1
APC1
A2
A3
A4
A5
Hybrid Constructed Wetland Series A
Outflow Storage A
APC2 In
Polishing Photocatalytic Reactor Series A (APC2)
APC2 Out
B1
BPC1
B2
B3
B4
B5
Hybrid Constructed Wetland Series B
OSPW Storage Tank
Outflow Storage B
BPC2 In
Polishing Photocatalytic Reactor Series B (BPC2)
BPC2 Out
WC1
PC1
WC2
WC3
WC4
WC5
PC2
0
3
4
7
10
13
16
Hydraulic Retention Time (d)
Photocatalytic Reactor Unit
Piston Pump

Figure 1.

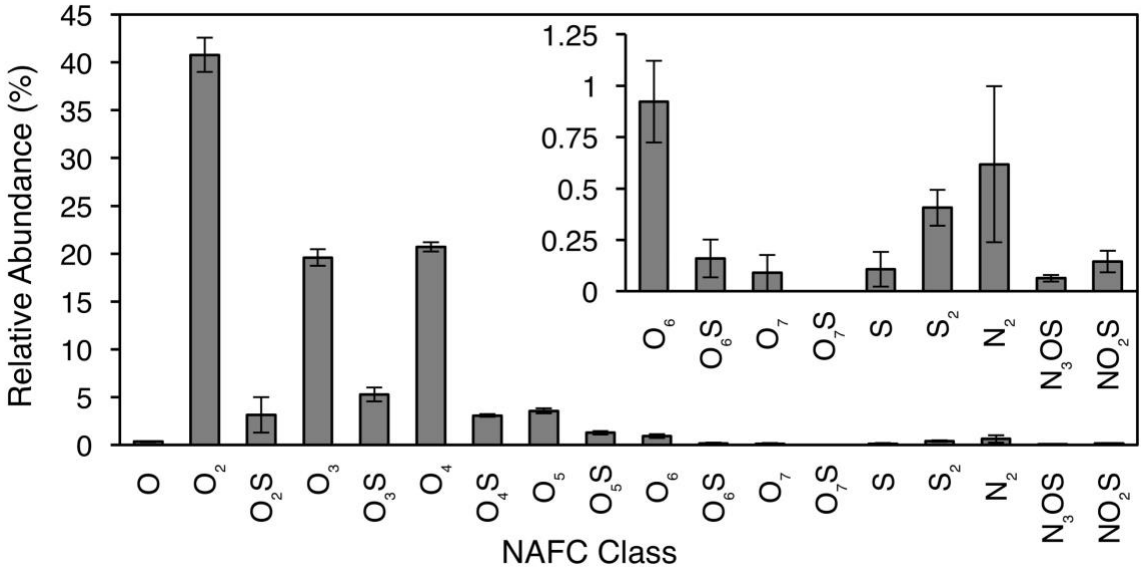
Relative Abundance (%)
45
40
35
30
25
20
15
10
5
0
1.25
1
0.75
0.5
0.25
0
O
O2
O2S
O3
O3S
O4
O4S
O5
O5S
O6
O6S
O7
O7S
S
S2
N2
N3OS
NO2S
NAFC Class

Figure 2.

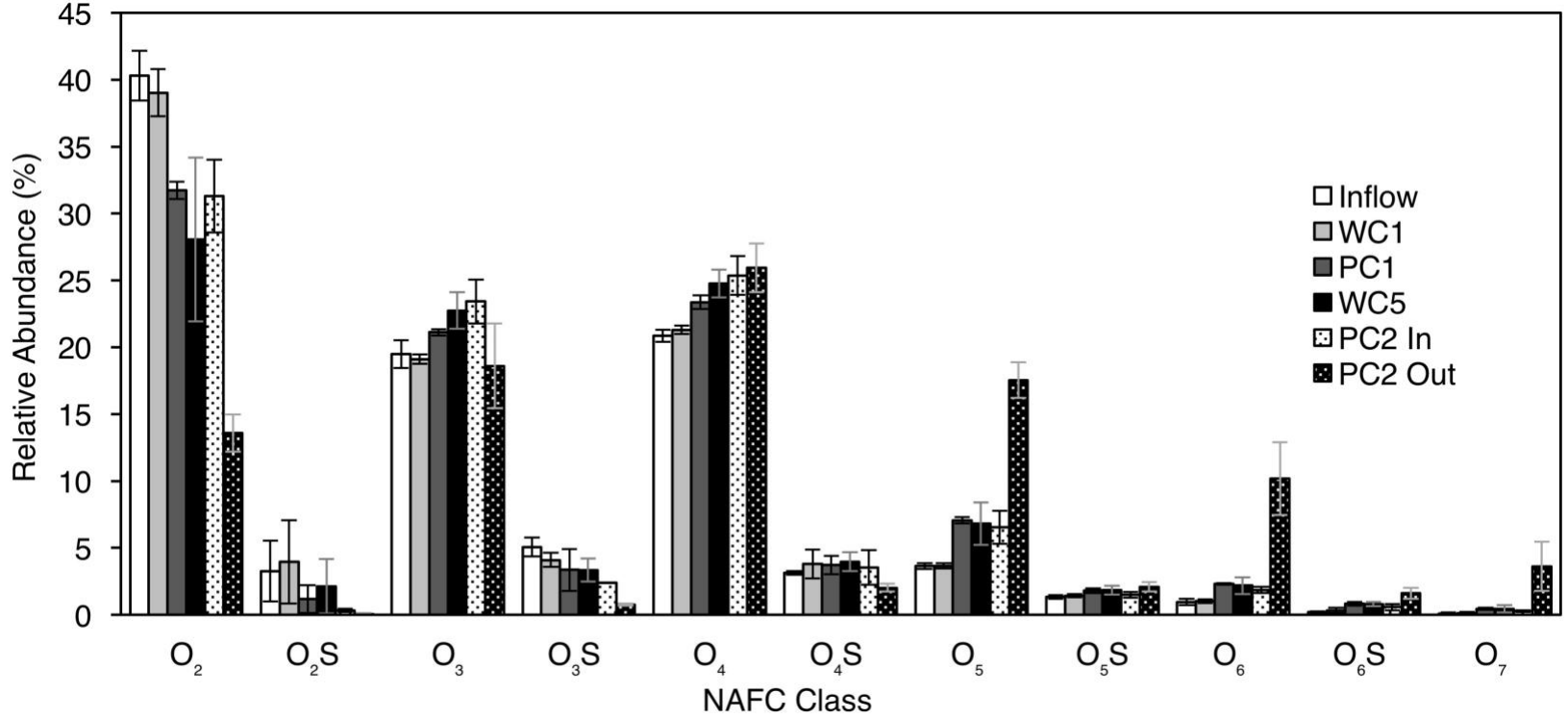
Relative Abundance (%)
45
40
35
30
25
20
15
10
5
0
Inflow
WC1
PC1
WC5
PC2 In
PC2 Out
O2
O2S
O3
O3S
O4
O4S
O5
O5S
O6
O6S
O7
NAFC Class

Figure 3.

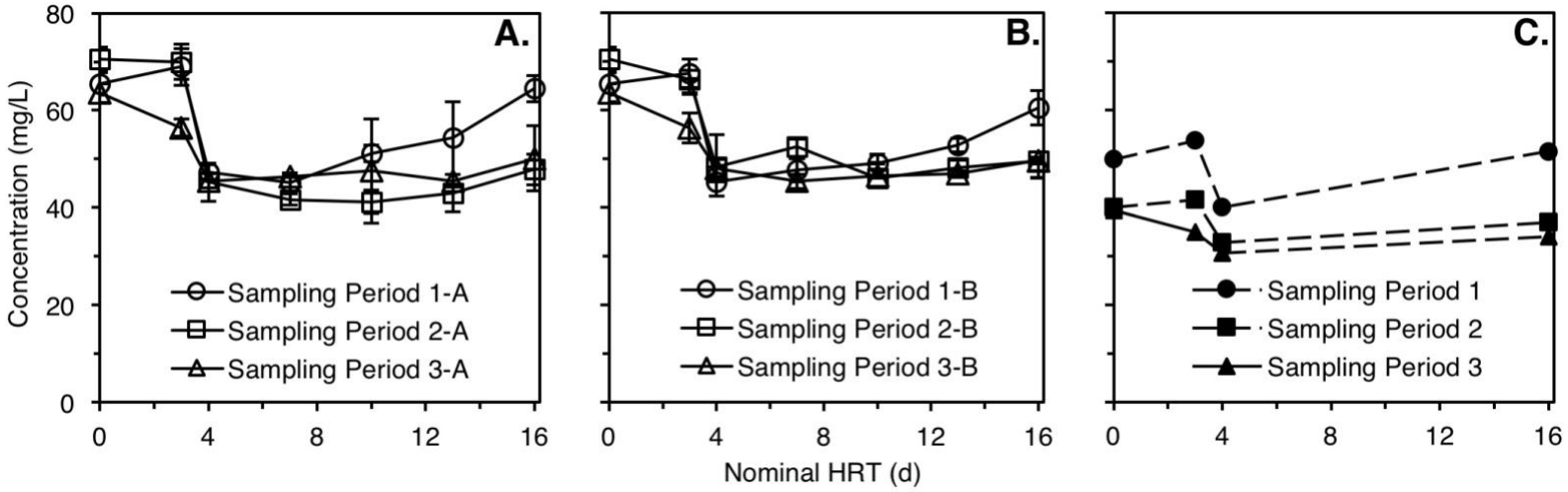
A.
B.
C.
Concentration (mg/L)
Nominal HRT (d)
Sampling Period 1-A
Sampling Period 2-A
Sampling Period 3-A
Sampling Period 1-B
Sampling Period 2-B
Sampling Period 3-B
Sampling Period 1
Sampling Period 2
Sampling Period 3
0
20
40
60
80
0
4
8
12
16

Figure 4.

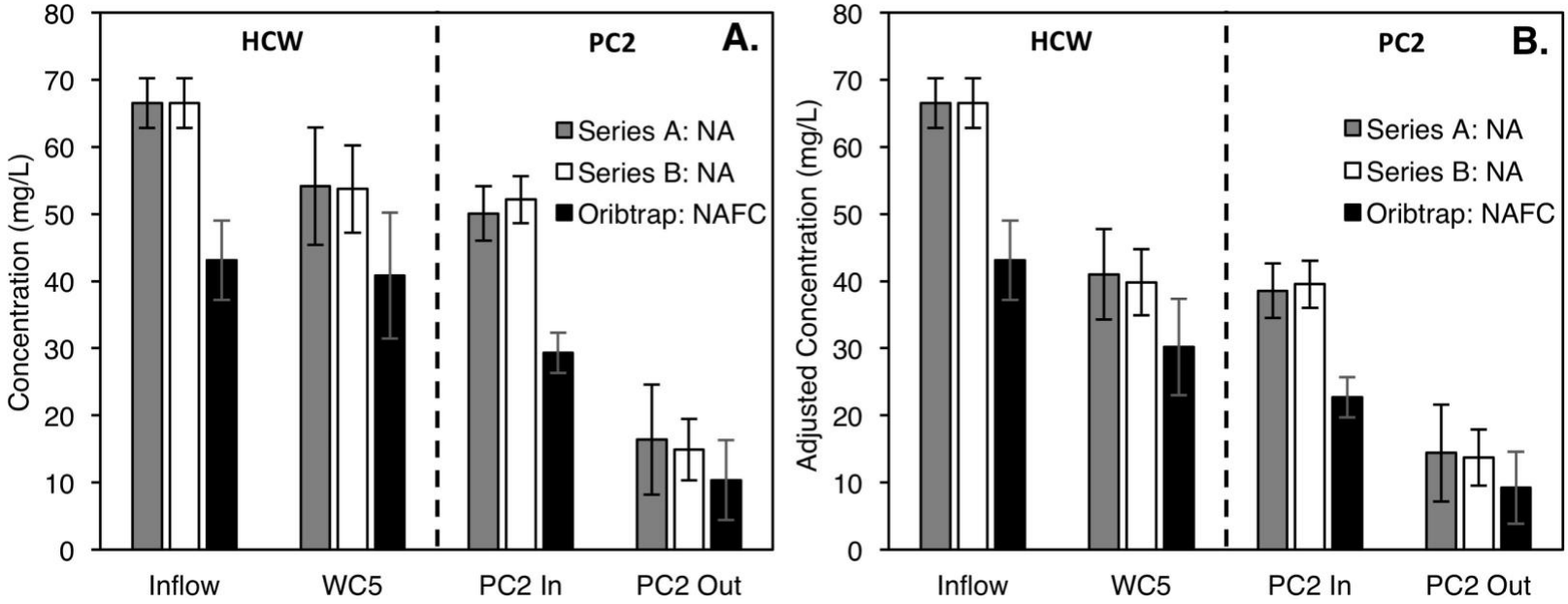
A.
B.
HCW
PC2
Concentration (mg/L)
Adjusted Concentration (mg/L)
Series A: NA
Series B: NA
Oribtrap: NAFC
Inflow
WC5
PC2 In
PC2 Out
0
10
20
30
40
50
60
70
80

Figure 5.

Table 1. Identification of constituents of concern (COC) in samples of oil sands process-affected water (OSPW) by comparison of water quality characteristics and concentrations of nutrients and major ions with lowest water quality criteria (WQC) from regulatory agencies including United States Environmental Protection Agency (USEPA, 2007), Canadian Council of Ministers of the Environment (CCME, 2011), and Alberta Environment and Parks (AEP, 2014).

Parameter (mg/L, unless noted)	Concentration in OSPW		Regulatory Agency	Water Quality Criteria	COC
	Mean (*n*=4)	(Min – Max)			Yes/No
Water quality characteristics and nutrients					
pH (S.U.)	8.76	(8.62 – 8.91)	USEPA	6.5-9.0	No
Conductivity (µS/cm)	1883	(1863 – 1929)	–	–	No
Alkalinity (mg/L as $CaCO_3$)	348	(304 – 368)	USEPA	20[a]	No
Hardness (mg/L as $CaCO_3$)	125	(116 – 132)	–	–	No
Total dissolved solids (TDS)	1386	(1026 – 1546)	–	–	No
Total suspended solids (TSS)	44	(6 – 113)	CCME	*	Yes
Total ammonia (N)	0.036	(<0.014 – 0.056)	CCME	0.17-1.5[b]	No
Total phosphorus (P)	0.069	(<0.020 – 0.174)	CCME	0.01-0.02[c]	No[d]
Major ions			–	–	
Bicarbonate (HCO_3^-)	382	(326 – 415)	–	–	No
Calcium (Ca^{2+})	18	(10 – 21)	CCME	1000	No
Carbonate (CO_3^{2-})	35	(<2 – 100)	–	–	No
Chloride (Cl^-)	256	(248 – 260)	CCME	120	Yes
Magnesium (Mg^{2+})	20	(19 – 21)	–	–	No
Potassium (K^+)	22	(21 – 23)	–	–	No
Sodium (Na^+)	390	(378 – 398)	–	–	No
Sulfate (SO_4^{2-})	90	(88 – 92)	AEP	309[e]	No

"–" Water quality criteria not available for characteristic or constituent

[a] Minimum threshold

[b] Temperature range from 5 to 20°C and pH range from 8.0 to 8.5 S.U.

[c] Trigger range for mesotrophic lakes and rivers

[d] Measured range considered beneficial to processes in constructed wetlands

[e] Hardness from 76 to 180 mg/L

* TSS cannot increase more than 25 mg/L above background level in receiving water body over a 24-h period

Table 2. Identification of constituents of concern (COC) in samples of oil sands process-affected water (OSPW) by comparison of concentrations of organics and acid soluble metal and metalloids with lowest water quality criteria (WQC) from regulatory agencies including United States Environmental Protection Agency (USEPA, 2007) and Canadian Council of Ministers of the Environment (CCME, 2011).

Parameter (mg/L)	Concentration in OSPW		Regulatory Agency	Water Quality Criteria	COC
	Mean (*n*=4)	(Min - Max)			Yes/No
Metals and metalloids					
Aluminum	0.058	(0.050 – 0.066)	USEPA	0.087	No
Arsenic	0.026	(0.022 – 0.029)	CCME	0.005	Yes
Barium	0.200	(0.175 – 0.220)	–	–	No
Boron	2.218	(2.114 – 2.425)	CCME	1.5	Yes
Cadmium	0.0002	(<0.0002 – <0.0002)	CCME	0.00038[a]	No
Cobalt	0.0023	(0.0005 – 0.0035)	–	–	No
Chromium	0.004	(<0.004 – <0.004)	CCME	0.0089	No
Copper	0.013	(0.010 – 0.016)	CCME	0.0024[a]	Yes
Iron	0.100	(0.018 – 0.218)	CCME	0.3[b]	No
Lead	0.012	(0.011 – 0.012)	USEPA	0.0025	Yes
Manganese	0.015	(<0.010 – 0.022)	CCME	0.2	No
Nickel	0.008	(0.006 – 0.009)	CCME	0.0096	No
Selenium	0.002	(<0.002 – <0.002)	USEPA	0.0031	No
Zinc	0.081	(0.010 – 0.208)	CCME	0.03	Yes
Organics					
Naphthenic acid fraction components (NAFCs)[c]	47.8	(39.4 – 57.8)	*	*	Yes
Naphthenic acids (NAs)[d]	71	(61 – 89)	*	*	Yes
Oil and grease (O&G)	16	(5 – 30)	**	**	Yes

"–" Water quality criteria not available for constituent

[a] Hardness: 100 mg/L as $CaCO_3$

[b] Dissolved fraction

[c] Measured by electrospray ionization Orbitrap mass spectrometry (ESI-Orbitrap MS)

[d] Measured by HPLC

* "No toxics in toxic amounts" (USEPA, 1991)

** No visible sheen, film, or discoloration (Health Canada, 2011)

Table 3. Inflow and outflow volumes, precipitation, ambient air temperature, and UV insolation during sampling periods in hybrid constructed wetland (HCW) and polishing photocatalytic reactor (PC2) Series A and B.

Sampling Period	Start Date	End Date	Inflow (L)		Outflow (L)		Cumul. Precip. (cm)[a]	Temperature[a]		UV Insolation		
			Series A	Series B	Series A	Series B		Min. (°C)	Max. (°C)	Mean Daily ($MJ \cdot m^{-2} \cdot d^{-1}$)[b]	Series A ($MJ \cdot m^{-2}$)[c]	Series B ($MJ \cdot m^{-2}$)[c]
Hybrid constructed wetland (HCW)												
1	10/14/16	10/31/16	240	241	146	147	0.00	14	27	0.690	0.682	0.698
2	11/9/16	11/26/17	258	250	179	168	0.18	6	20	0.461	0.315	0.311
3	12/9/16	12/20/17	245	246	247	244	4.10	0	11	0.341	0.545	0.484
Polishing photocatalytic reactors (PC2)												
1	12/1/16	12/15/16	104	107	88	95	NA[d]	4	12	0.999[e]	1.476	1.453
2	12/21/16	1/10/17	90	93	84	90	NA[d]	4	13	1.106[e]	2.084	1.883
3	1/12/17	1/28/17	107	107	93	98	NA[d]	9	19	1.342[e]	2.650	2.712

[a] Cumulative precipitation (cumul. precip.) and mean daily minimum and maximum temperature during each sampling period measured at local station: https://www.wunderground.com/history/airport/KCEU

[b] UV insolation accumulated during operation of photocatalytic reactors (i.e. when OSPW was pumped through uncovered photoreactors) divided by duration of pumping in days

[c] UV insolation measured during collection of samples from initial photocatalytic reactor (PC1) in HCW series and from outflow of final reactor units in PC2 series

[d] Not applicable (NA). Reactors were covered during precipitation events

[e] Photocatalytic reactors were only operated when exposed to direct sunlight and were covered during cloudy and inclement weather. Mean daily UV insolation in PC2 is thus equivalent to total UV insolation divided by photoperiod in days.

Table 4. Changes in concentrations of oil and grease (O&G) and total suspended solids (TSS) measured in hybrid constructed wetland (HCW) Series A and B.

Sampling Period	Inflow (mg/L)	Outflow (mg/L)		Percent Removal	
		Series A	Series B	Series A	Series B
Oil and grease (O&G)*,**					
1	5	<4	<4	20	20
2	30	<4	<4	87	87
3	11	<4	<4	64	64
Mean (±SD)	15 (±13)	<4 (±0)	<4 (±0)	57 (±34)	57 (±34)
Total suspended solids (TSS)**					
1	11	8	8	33	26
2	69	<4	<4	94	94
3	89	7	9	92	90
Mean (±SD)	56 (±40)	6 (±2)	7 (±3)	73 (±35)	70 (±38)

* Samples of O&G collected at outflow of initial wetland cells (WC1)

** Detection limit for O&G and TSS is 4 mg/L

Table 5. Changes in metal and metalloid concentration from inflow to outflow of hybrid constructed wetland (HCW) series during three sampling events. Adjusted concentrations are reported to assess changes in concentration independent of evaporation, transpiration, and precipitation (Section 2.4; Eqn. 3).

Sampling Period	Inflow (mg/L)	Concentration				Adjusted Concentration			
		Outflow (mg/L)		Percent Removal		Outflow (mg/L)		Percent Removal	
		Series A	Series B	Series A	Series B	Series A	Series B	Series A	Series B
Arsenic									
1	0.022	0.010	0.012	57	48	0.006	0.007	74	68
2	0.027	0.011	0.019	59	30	0.008	0.013	72	53
3	0.029	0.013	0.010	54	65	0.013	0.010	54	66
Mean (±SD)	0.026 (±0.004)	0.011 (±0.002)	0.013 (±0.005)	57 (±2)	48 (±17)	0.009 (±0.004)	0.010 (±0.003)	66 (±10.9)	62 (±7.9)
Boron									
1	2.31	3.39	3.24	-46.5	-40.1	2.06	1.98	10.9	14.5
2	2.25	2.93	2.91	-30.3	-29.5	2.03	1.96	9.59	13.0
3	2.43	2.35	2.30	3.05	5.28	2.37	2.28	2.26	6.05
Mean (±SD)	2.33 (±0.09)	2.89 (±0.52)	2.82 (±0.48)	-24.6 (±25.3)	-21.4 (±23.7)	2.15 (±0.19)	2.07 (±0.18)	7.58 (±4.65)	11.2 (±4.52)
Copper									
1	0.016	0.020	0.036	-25	-120	0.012	0.022	24	-37
2	0.016	0.016	0.021	3.1	-28	0.011	0.014	33	14
3	0.014	0.016	0.016	-11	-11	0.016	0.015	-12	-9.8
Mean (±SD)	0.015 (±0.001)	0.017 (±0.003)	0.024 (±0.011)	-11 (±14)	-53 (±59)	0.013 (±0.003)	0.017 (±0.004)	15 (±24)	-11 (±26)
Lead									
1	0.012	0.012	0.011	0.0	8.3	0.007	0.007	39	44
2	0.011	0.014	0.010	-27	17	0.010	0.007	12	44
3	0.011	0.011	0.012	0.0	-9.1	0.011	0.012	-0.8	-8.2
Mean (±SD)	0.011 (±0.001)	0.012 (±0.002)	0.011 (±0.001)	-9.1 (±16)	5.3 (±13)	0.009 (±0.002)	0.008 (±0.003)	17 (±20)	27 (±30)
Zinc									
1	0.208	0.089	0.061	57	71	0.054	0.037	74	82
2	0.107	0.055	0.050	49	53	0.038	0.034	64	69
3	0.071	0.042	0.044	41	39	0.042	0.043	40	39
Mean (±SD)	0.129 (±0.071)	0.062 (±0.024)	0.052 (±0.009)	49 (±8)	54 (±16)	0.045 (±0.008)	0.038 (±0.005)	60 (±17)	63 (±22)

Table 6. Percent survival and reproduction of *C. dubia* in static renewal, 7-day bioassays conducted according to Environment and Climate Change Canada protocols for single-concentration tests (ECCC, 2007). Samples were compared to laboratory controls to determine if survival and reproduction were impaired (α=0.05). Comprehensive toxicity data are presented in supplementary data (Table S5).

Treatment	Percent Survival		Reproduction	
	Series A	Series B	Series A	Series B
Sampling Period 1				
Inflow	70%		Impaired	
PC1	100%	100%	Impaired	Impaired
WC5	90%	75%	No effect	No effect
PC2 In	100%	95%	No effect	Impaired
PC2 Out	95%	95%	No effect	Impaired
Sampling Period 2				
Inflow	20%		No effect*	
PC1	100%	100%	No effect	No effect
WC5	100%	95%	No effect	No effect
PC2 In	100%	90%	No effect	No effect
PC2 Out	100%	100%	No effect	No effect
Sampling Period 3				
Inflow	90%		Impaired	
PC1	100%	95%	No effect	No effect
WC5	90%	90%	No effect	No effect
PC2 In	90%	80%	No effect	No effect
PC2 Out	80%	85%	No effect	No effect

*Only 2 out of 20 initial daphnids produced three broods, but reproduction was not inhibited in these two replicates

CHAPTER IV

CONCLUSIONS

This thesis investigated the application of hybrid constructed wetland treatment systems (CWTSs) to mitigate risks associated with oil sands process-affected water (OSPW) by decreasing concentrations and altering compositions of constituents of concern (COCs) in a specific OSPW. Solar photocatalysis over settled TiO_2 was investigated as an advanced oxidation process to degrade naphthenic acids (NAs) in OSPW and decrease toxicity to sentinel aquatic organisms. Following this proof of concept experiment, flow-through TiO_2 fixed-film photocatalytic reactors were implemented into a hybrid pilot-scale CWTS. The major objectives of this thesis were to 1) measure rates and extents of NA degradation and responses of sentinel aquatic organisms in OSPW treated by solar photocatalysis over settled TiO_2, and 2) to measure the performance of a hybrid pilot-scale CWTS treating a specific OSPW.

Measure rates and extents of NA degradation and responses of sentinel aquatic organisms in OSPW treated by solar photocatalysis over settled-TiO_2

A first-order investigation of film-based photocatalysis was conducted by assembling photocatalytic batch reactors consisting of thin films (~0.5 mm) of TiO_2 settled in OSPW and comparing changes in NA concentration and toxicity between photocatalytic, photolytic, and dark control reactors. Rates and extents of NA mass and concentration removal were calculated with respect to photoperiod and cumulative solar UV radiation (UV insolation). Specific objectives were to: 1) measure absorption and attenuation of UV radiation in a specific OSPW, 2) measure rates and extents of NA degradation with respect to UV insolation in settled TiO_2 photocatalytic reactors treating

the OSPW, and 3) compare survival and reproduction of *Ceriodaphnia dubia* and survival and biomass of *Pimephales promelas* exposed to OSPW before and after treatment.

UV light absorption and attenuation experiments determined that TiO_2 film-based solar photocatalysis is driven primarily by UV-A radiation and that suspended solids and residual hydrocarbon sheens increased attenuation of solar UV radiation in OSPW. UV radiation transmitted through OSPW activated settled layers of TiO_2 and decreased NA mass by 86% at an exponential with UV insolation and photoperiod half-lives of 1.1±0.2 $MJ \cdot m^{-2}$ and 10.2±0.8 h, respectively. Decreases in NA concentration were also modeled using first-order rate kinetics, and rates were slowed by evaporation, yielding UV insolation and photoperiod half-lives of 2.1±0.2 $MJ \cdot m^{-2}$ and 19±2 h. Adverse effects were not observed in survival and biomass of juvenile *P. promelas* after exposure to OSPW. Survival and reproduction of *C. dubia* were impaired in untreated OSPW, and no adverse effects were observed in any of the treatments (i.e. photocatalysis, photolysis, dark control). Daphnids exposed to OSPW treated by photocatalysis had significantly greater reproduction than *C. dubia* in the photolysis and dark control treatments. These data provide a proof-of-concept for film-based photocatalysis of OSPW and highlight the need for further bench-scale experimentation with flow-through fixed-film reactors to increase NA removal rates and efficiencies. This study is a first step in development of film-based photocatalysis for treatment of OSPW and the integration of this technology into hybrid systems capable of mitigating risks associated with this mixture.

Measure performance of a hybrid pilot-scale CWTS treating a specific OSPW

A hybrid pilot-scale CWTS for remediation of OSPW was assembled using information from UV attenuation, bench-scale photocatalysis, and previous pilot-scale constructed wetland experiments. Performance of the hybrid CWTS was measured in terms of changes in toxicity and constituent concentration and composition over three sampling periods. Specific objectives were to: 1) Characterize a specific OSPW treated by a hybrid pilot-scale CWTS for identification of COCs, 2) assemble and operate a hybrid pilot-scale constructed wetland for treatment of the OSPW, 3) analyze changes in concentration and class distribution of naphthenic acid fraction compounds (NAFCs) using ultrahigh resolution mass spectrometry (UHRMS) in Dr. John Headley's laboratory at the Environment and Climate Change Canada National Hydrology Research Center, and 4) measure changes in concentration of COCs and survival and reproduction of *Ceriodaphnia dubia.* Characterization of the OSPW indicated that NAFCs, As, B, Cl^-, Cu, Pb, Zn, total suspended solids (TSS), and oil and grease (O&G) were COCs, exceeding numeric or narrative water quality criteria (WQC). Fixed-film photocatalytic reactors were implemented in series with wetland cells, designed to promote aerobic degradation, in two hybrid constructed wetland (HCW) treatment trains. Initial wetland cells decreased concentrations of O&G and TSS and decreased attenuation of UV radiation in OSPW, prior to treatment in initial fixed-film photocatalytic reactors. To degrade residual NAFCs, outflows from HCW series were collected and treated by polishing photocatalytic reactors (PC2). The hybrid CWTS decreased NAFC concentrations by 75.9%, and changed class distributions from regimes dominated by

acutely toxic O_2 NAFCs (O_2=40.3%, $\sum O_{3–9}$=45.0%) to sparingly toxic poly-oxygenated classes ($O_{3–9}$; O_2=13.6%, $\sum O_{3–9}$=77.0%). The influence of weather conditions on performance was demonstrated by up to 53% increases in Cl^- concentrations caused by evapotranspiration during the first sampling period and inhibition of NAFC aerobic degradation by near-freezing temperatures in the third sampling period. In sampling periods 2 and 3, toxicity to *C. dubia* was eliminated in all samples collected from the hybrid CWTS. Reproduction of *C. dubia* was impaired in 4 of 8 samples collected during sampling period 1, likely due to increased Cl^- concentrations. Concentrations of As, B, Cu, Pb, and Zn in outflows of the HCW and PC2 exceeded protective WQC, but were below lowest observable effect concentrations (LOECs) for *C. dubia* reproduction and survival. This study demonstrates that hybrid CWTSs, implementing fixed-film photocatalysis, are capable of altering composition and decreasing concentrations of NAFCs and toxicity associated with this fraction. Currently, there is a dearth of literature concerning the use of constructed wetlands for treatment of OSPW and a scarcity of studies reporting performance data with biogeochemical conditions. This study, which reports changes in distribution of NAFC classes measured contemporaneously with biogeochemical conditions in a hybrid pilot-scale CWTS, is a pertinent contribution to the growing body of literature supporting the application of constructed wetlands for remediation of OSPW. Performance data, biogeochemical conditions, and design-criteria presented in this hybrid pilot-scale CWTS experiment will inform further development of this technology.

APPENDICES

APPENDIX A

Chapter II: Supporting Information

Figure S1. UV irradiance ($W \cdot m^{-2}$; solid line) measured while photocatalytic and photolytic reactors were exposed to direct sunlight (photoperiod=32 h). Irradiance was integrated with respect to photoperiod to calculate UV insolation ($MJ \cdot m^{-2}$; dashed line). Reactors were covered from 6:00 PM until 9:00 AM. Irradiance was not measured when reactors were covered.

Figure S2. Extraterrestrial and terrestrial solar spectra (Gueymard, 2003 and ASTM, 2012, respectively) for UV-A, UV-B, and UV-C radiation. Atmospheric transmittance of UV light is the quotient of terrestrial and extraterrestrial spectral irradiance. These data illustrate that the majority of UV irradiance reaching the earth's surface is from UV-A wavelengths.

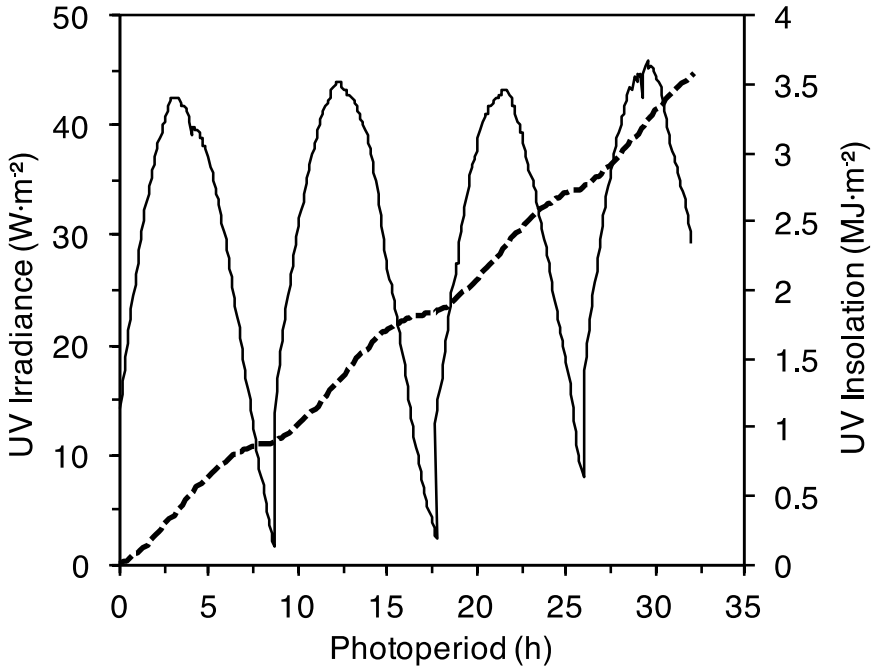

Figure S1.

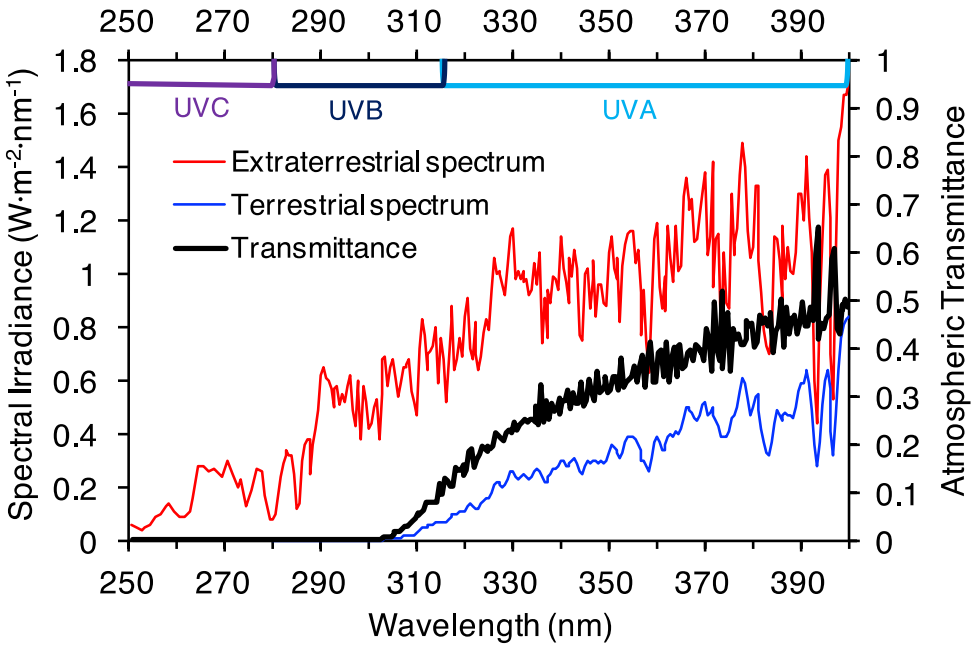

Figure S2.

Table S1. Methods for measurement of water quality characteristics, UV irradiance, and concentrations of metals, major ions, and naphthenic acid. Unless noted otherwise, methods were adapted from American Public Health Association (APHA) standard methods (APHA, 2012).

Parameter	Method	Method Detection Limit (MDL)
pH	Electrometric method 4500-H^+ B: Orion Star model A221 with Triode® electrode	0.01 SU
Temperature	Laboratory method 2550 B: Orion Star Model A221	0.1 °C
Dissolved oxygen	Membrane electrode method 4500-O G: HQ30d meter with LDO101 probe	0.1 mg/L
Conductivity	Laboratory method 2510 B: Orion Star Model A221 with 013010MD conductivity cell	1 μS/cm
Alkalinity	Titration Method 2320 B	2 mg/L as $CaCO_3$
Hardness	EDTA Titrimetric Method 2340 C	2 mg/L as $CaCO_3$
TSS	Total Suspended Solids Dried at 103-105°C: Method 2540 D	4 mg/L
TDS	Total Dissolved Solids Dried at 180°C Method 2540 C	20 mg/L
BOD_5	5-Day Biological Oxygen Demand Test Method 5210 B	1 mg/L
COD	Colorimetric Method Chemical oxygen demand 5220 D	4 mg/L
UV Irradiance	Direct Instrumentation: Apogee Instruments SU-100 UV Sensor and HOBO UX120-006M Analog Data Logger	0.188 $W \cdot m^{-2}$
Naphthenic Acids (NAs)	Derivatization and HPLC based on Yen et al. (2004)	6 mg/L
Oil and grease (O&G)	USEPA Method 1664 A (Environmental Express StepSaver Modification; USEPA, 1999)	4 mg/L
Metals and Metalloids (mg/L)	Inductively Coupled Plasma-Atomic Emissions Spectrometry (ICP-AES) EPA Method 200.7 (USEPA, 2001)	
	Aluminum (Al)	0.045 mg/L
	Boron (B)	0.01 mg/L
	Calcium (Ca^{2+})	0.002 mg/L
	Chloride (Cl^-)	0.03 mg/L
	Copper (Cu)	0.01 mg/L
	Iron (Fe)	0.036 mg/L
	Magnesium (Mg^{2+})	0.01 mg/L
	Manganese (Mn)	0.01 mg/L
	Potassium (K^+)	0.1 mg/L
	Phosphorus (P)	0.02 mg/L
	Sodium (Na^+)	0.03 mg/L
	Zinc (Zn)	0.01 mg/L

Table S2. Mean temperature, pH, dissolved oxygen (DO), and conductivity measured in photocatalytic, photolytic, and dark control reactors during the photocatalysis experiment.

Parameter (±SD)	Photocatalysis	Photolysis	Dark
Temperature (°C)	13.4 (±3.3)	13.0 (±3.6)	14.7 (±1.6)
pH (S.U.)	8.25 (±0.12)	8.79 (±0.12)	8.66 (±0.22)
DO (mg/L)	9.40 (±1.48)	10.62 (±0.67)	9.87 (±0.96)
Conductivity (µS/cm)	2,638 (±584)	2,589 (±568)	2,047 (±104)

Table S3. Water quality characteristics in exposures of untreated OSPW and from photocatalytic, photolytic, and dark control reactors used in bioassays. Reported values are means and standard deviations (*n*=3).

Parameter	OSPW	Photocatalysis	Photolysis	Dark
Temperature (°C)	22.8 (±0.3)	22.2 (±0.9)	24.4 (±4.7)	21.9 (±0.7)
pH (S.U.)	8.83 (±0.01)	8.41 (±0.14)	8.68 (±0.04)	8.47 (±0.12)
Dissolved O_2 (mg/L)	8.71 (±0.35)	8.38 (±0.37)	8.70 (±0.81)	8.35 (±0.53)
Conductivity (µS/cm)	1,965 (±6)	1,987 (±48)	1,940 (±63)	2,234 (±16)
Alkalinity (mg/L $CaCO_3$)	422 (±8)	368 (±11)	366 (±8)	445 (±9)
Hardness (mg/L $CaCO_3$)	165 (±8)	152 (±1)	142 (±1)	211 (±4)
Total Dissolved Solids (mg/L)	1,334 (±29)	1,327 (±29)	1,384 (±25)	1,509 (±56)
Total Suspended Solids (mg/L)	6 (±2)	4 (±1)	8 (±3)	4 (±2)

Table S4. Concentrations of organics and acid soluble elements in exposures of untreated OSPW and from photocatalytic, photolytic, and dark control reactors used in bioassays. Reported values are means and standard deviations (*n*=3).

Parameter (mg/L)	OSPW	Photocatalysis	Photolysis	Dark
Organics				
Naphthenic Acids	89 (±8)	18 (±5)	79 (±9)	97 (±8)
Oil and Grease	<4	–	–	–
Metals/Metalloids				
Boron	2.31 (±0.05)	2.14 (±0.01)	2.20 (±0.04)	2.62 (±0.04)
Copper	0.024 (±0.002)	< 0.01	0.019 (±0.002)	< 0.01
Iron	0.086 (±0.010)	0.057 (±0.002)	0.074 (±0.028)	0.073 (±0.037)
Manganese	< 0.01	< 0.01	< 0.01	< 0.01
Zinc	0.191 (±0.004)	< 0.01	0.070 (±0.002)	< 0.01
Major Ions				
Bicarbonate	409	372	372	427
Calcium	20.19 (±0.66)	24.23 (±0.45)	27.36 (±0.49)	21.85 (±0.35)
Carbonate	<2	<2	<2	<2
Chloride	246.79 (±4.13)	241.85 (±3.47)	243.01 (±3.67)	282.05 (±4.70)
Magnesium	20.16 (±0.48)	19.99 (±0.20)	20.54 (±0.47)	22.60 (±0.36)
Potassium	20.55 (±0.29)	21.15 (±0.14)	22.05 (±0.43)	23.88 (±0.48)
Phosphate	0.03	< 0.02	< 0.02	< 0.02
Sodium	380.37 (±6.32)	361.42 (±1.40)	368.51 (±5.84)	423.70 (±2.96)
Sulfate	87.66 (±2.26)	87.13 (±1.24)	87.98 (±2.26)	101.35 (±1.60)

"–" Oil and grease (O&G) not measured in photocatalytic, photolytic, and dark control reactors because concentrations were below detection in untreated OSPW.

Table S5. Survival and reproduction of *C. dubia* exposed to untreated OSPW, laboratory controls (Control 1 and 2), and photocatalysis, photolysis, and dark control treatments. Statistical comparisons were made between Control 1 and OSPW and between Control 2 and the treatments.

Name	Survival (%)	*p*-value	Mean Reproduction (±SD)	*p*-value
Control 1	95	–	28 (±6)	–
OSPW	55	0.004	14 (±7)	<0.001
Control 2	95	–	20 (±4)	–
Photocatalysis	100	1.000	23 (±6)	0.178
Photolysis	90	0.563	17 (±6)	0.336
Dark	90	0.563	17 (±4)	0.251

"–" *p*-values not calculated for controls because comparisons were made between controls and OSPW and the treatments

Table S6. Survival and biomass of *P. promelas* exposed to untreated OSPW, laboratory controls (Control 1 and 2) and photocatalysis, photolysis, and dark control treatments. Statistical comparisons were made between Control 1 and OSPW and between Control 2 and treatments.

Name	Survival (%)	*p*-value	Mean biomass of surviving fish (µg; ±SD)	*p*-value
Control 1	91	–	501 (±57)	–
OSPW	88	0.502	472 (±32)	0.321
Control 2	94	–	460 (±45)	–
Photocatalysis	97	0.869	494 (±39)	0.856
Photolysis	87	0.305	432 (±77)	0.967
Dark	100	1.0	409 (±28)	0.459

"–" *p*-values not calculated for controls because comparisons were made between controls and OSPW and the treatments

APPENDIX B

Chapter III: Supporting Information

Figure S1. Mean hydrosoil oxidation reduction potential (ORP) in wetland cells of hybrid constructed wetland Series A and B. ORP measured at probes inserted 15 cm deep in hydrosoil. Error bars represent one standard deviation (n=5).

Figure S2. Mean green shoot density in wetland cells of hybrid constructed wetland Series A and B. Daily mean water temperature at sediment-water interface in wetland cell B3. Error bars represent one standard deviation (*n*=5).

Figure S3. A) Mean concentrations of arsenic measured in hybrid constructed wetland (HCW) Series A and B during three sampling periods. B) Mean zinc concentrations measured in HCW Series A and B. Dotted lines represent water quality guidelines for As and Zn (0.005 and 0.03 mg/L, respectively; CCME, 2011). Error bars represent one standard deviation.

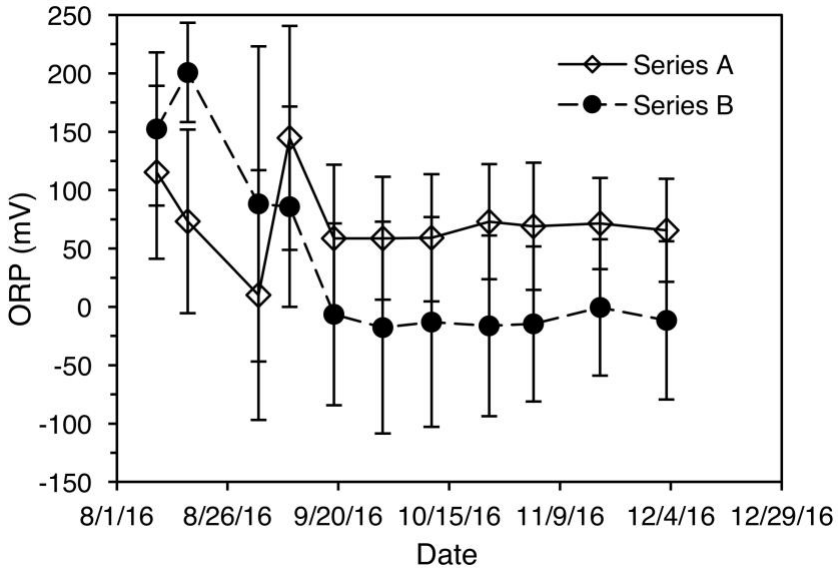

Figure S1.

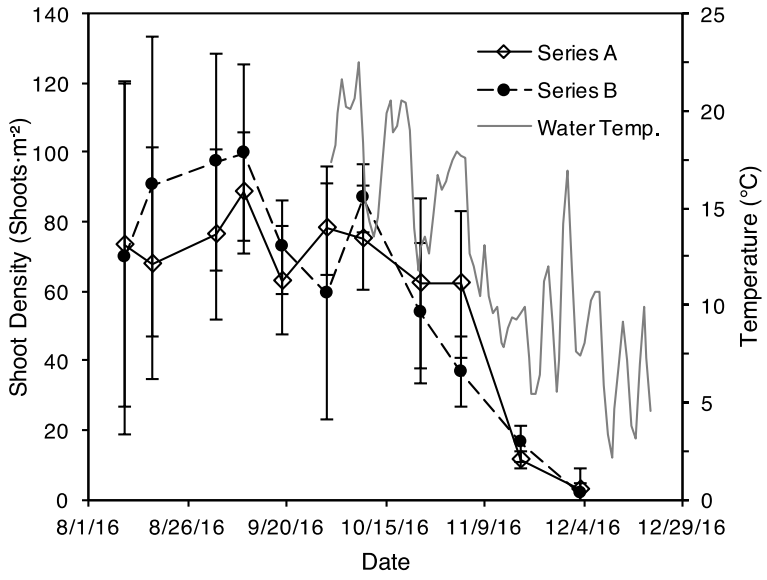

Figure S2.

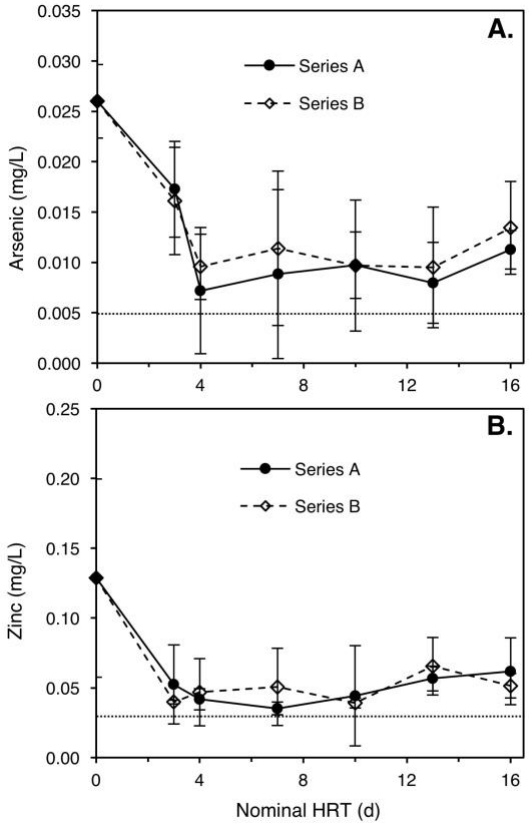
A.
Series A
Series B
Arsenic (mg/L)
0.035
0.030
0.025
0.020
0.015
0.010
0.005
0.000
0
4
8
12
16
B.
Series A
Series B
Zinc (mg/L)
0.25
0.20
0.15
0.10
0.05
0.00
0
4
8
12
16
Nominal HRT (d)

Figure S3.

Table S1. Hydrosoil oxidation-reduction potential (ORP), dissolved oxygen (DO), pH, and conductivity (Cond.) measured in wetland cells (WC1-5) and photocatalytic reactors (A/BPC1) of hybrid constructed wetland (HCW) Series A and B. All data were collected during three sampling periods and are reported as means with minimum and maximum values (n = 4 for DO, pH, Cond.; n = 5 for ORP).

Sample	Hydrosoil ORP. (mV)[a]	Dissolved Oxygen (mg/L)[b]	pH (S.U.)[b]	Conductivity (µS/cm)[b]
Hybrid Constructed Wetland (HCW) Series A				
A1	124 (121 – 129)	4.03 (1.75 – 7.68)	7.77 (7.52 – 8.06)	1,962 (1,773 – 2,113)
APC1	--	8.76 (6.64 – 11.09)	8.65 (8.20 – 8.88)	1,993 (1,683 – 2,239)
A2	104 (97 – 124)	2.13 (1.73 – 2.84)	7.53 (7.36 – 7.68)	2,329 (2,174 – 2,569)
A3	57 (35 – 70)	4.03 (1.75 – 7.68)	7.60 (7.53 – 7.68)	2,331 (1,850 – 2,713)
A4	13 (1 – 35)	3.49 (2.16 – 6.03)	7.79 (7.57 – 7.93)	2,480 (1,693 – 2,923)
A5	32 (27 – 41)	4.17 (1.77 – 8.21)	7.64 (7.29 – 7.96)	2,738 (2,110 – 3,190)
Hybrid Constructed Wetland (HCW) Series B				
B1	-13 (-26 – -4)	3.26 (2.31 – 4.27)	7.68 (7.50 – 7.89)	1,951 (1,807 – 2,010)
BPC1	--	9.17 (7.33 – 11.98)	8.56 (7.92 – 8.96)	1,962 (1,545 – 2,256)
B2	-77 (-93 – -37)	3.26 (2.31 – 4.27)	7.70 (7.61 – 7.83)	2,159 (1,896 – 2,382)
B3	-43 (-58 – -22)	3.86 (1.48 – 7.64)	7.79 (7.38 – 8.42)	2,363 (1,920 – 2,688)
B4	99 (94 – 103)	4.23 (2.21 – 8.25)	7.62 (7.41 – 7.77)	2,571 (1,802 – 3,000)
B5	-75 (-94 – -32)	2.74 (1.56 – 4.39)	7.68 (7.43 – 7.95)	2,650 (2,186 – 3,010)

[a] Measured at a depth of 15 cm in hydrosoil of wetland cells

[b] Measured in water column of wetland cells at 10 cm below water surface and in photocatalytic reactors

Table S2. Mean relative abundance of NAFC classes in hybrid pilot-scale CWTS measured over three sampling periods by ESI-Orbitrap MS. Samples were collected from untreated OSPW influent (inflow), outflows from initial wetland cells (WC1), initial photocatalytic reactors (PC1), and final wetland cells (WC5), and polishing photocatalytic reactor (PC2) inflow and outflow. Orbitrap-MS of composite samples from replicate Series A and B (Figure 1) was conducted in Dr. John Headley's laboratory at the Environment and Climate Change Canada National Hydrology Research Center. NAFC classes with relative abundance <1% at all positions in the hybrid pilot-scale CWTS were not included in this table.

Sample	Heteroatom Class Relative Abundance (%)				
	O_2	O_3	O_4	O_5	O_6
Sampling Period 1					
Inflow	39.4	18.8	20.6	3.8	1.1
WC1	38.0	18.8	21.0	3.7	1.1
PC1	31.9	20.9	23.0	7.1	2.4
WC5	24.6	24.0	25.4	7.2	2.3
PC2 In	28.2	24.8	26.9	7.8	2.1
PC2 Out	14.6	22.0	27.9	16.0	7.1
Sampling Period 2					
Inflow	39.1	19.0	20.6	3.8	1.1
WC1	38.0	19.5	21.4	3.9	1.1
PC1	31.0	21.4	23.2	7.3	2.4
WC5	24.4	23.0	25.4	8.2	2.8
PC2 In	32.4	23.9	25.1	6.4	1.8
PC2 Out	14.2	18.0	25.7	18.1	11.2
Sampling Period 3					
Inflow	42.4	20.7	21.4	3.4	0.7
WC1	41.1	19.0	21.6	3.4	0.9
PC1	32.3	21.1	23.9	6.8	2.2
WC5	35.1	21.3	23.6	5.1	1.5
PC2 In	33.4	21.6	24.1	5.4	1.6
PC2 Out	12.0	15.8	24.3	18.5	12.2
Mean (±SD)					
Inflow	40.3 (±1.8)	19.5 (±1.0)	20.9 (±0.5)	3.6 (±0.2)	1.0 (±0.2)
WC1	39.0 (±1.8)	19.1 (±0.4)	21.3 (±0.3)	3.7 (±0.2)	1.0 (±0.1)
PC1	31.7 (±0.7)	21.1 (±0.2)	23.4 (±0.5)	7.1 (±0.2)	2.3 (±0.1)
WC5	28.1 (±6.1)	22.8 (±1.4)	24.8 (±1.0)	6.8 (±1.6)	2.2 (±0.6)
PC2 In	31.3 (±2.7)	23.4 (±1.6)	25.4 (±1.4)	6.5 (±1.2)	1.9 (±0.2)
PC2 Out	13.6 (±1.4)	18.6 (±3.2)	26.0 (±1.8)	17.5 (±1.3)	10.2 (±2.7)

Table S3. General water quality characteristics and chloride concentrations measured in samples collected from hybrid constructed wetland (HCW) and polishing photocatalysis (PC2) Series A and B. All data were collected during three sampling periods and are reported as mean and range (n = 3).

Sample	Temperature (°C)	pH (S.U.)	Conductivity (µS/cm)[b]	Dissolved Oxygen (mg/L)	Alkalinity (mg/L $CaCO_3$)	Hardness (mg/L $CaCO_3$)	Chloride (mg/L)
Inflow	21.1 (19.9–23.0)	8.96 (8.81–9.08)	1,889 (1,866–1,929)	8.81 (8.62–8.91)	363 (356–368)	128 (120–132)	255 (248–260)
Series A							
APC1	20.0 (16.2–23.0)	9.46 (7.75–11.65)	2,049 (1,918–2,190)	8.40 (8.27–8.55)	388 (372–404)	131 (120–144)	273 (261–287)
A5	19.9 (13.8–23.0)	10.34 (8.68–11.30)	2,543 (2,004–3,040)	8.46 (8.24–8.62)	464 (396–516)	140 (124–164)	356 (277–430)
PC2 In	17.4 (17.3–17.5)	8.59 (7.56–9.20)	2,120 (1,728–2,650)	7.93 (7.66–8.09)	363 (292–404)	132 (116–156)	291 (240–362)
PC2 Out	19.0 (17.8–20.1)	6.59 (4.88–8.29)	2,524 (1,988–3,060)	8.21 (7.91–8.50)	438 (380–496)	148 (120–176)	353 (283–439)
Series B							
APC1	20.5 (17.3–23.0)	8.91 (8.15–10.24)	2,057 (1,917–2,190)	8.31 (8.13–8.43)	404 (364–440)	136 (124–160)	276 (262–292)
A5	19.9 (13.8–23.0)	10.28 (8.73–11.48)	2,543 (1,984–2,955)	8.44 (8.06–8.71)	453 (360–520)	151 (120–168)	357 (274–416)
PC2 In	17.0 (16.6–17.5)	8.62 (7.35–9.45)	2,075 (1,648–2,570)	7.92 (7.81–8.11)	387 (340–460)	120 (108–132)	294 (235–368)
PC2 Out	18.9 (17.5–20.3)	6.64 (4.76–8.52)	2,221 (1,533–2,908)	7.85 (7.36–8.33)	392 (300–484)	130 (96–164)	313 (218–414)

Table S4. Comparison of mean element concentrations measured in outflows of hybrid constructed wetland (HCW) and polishing photocatalysis (PC2) Series A and B (n=3 sampling periods; α=0.05).

Element	WC5 Mean		PC2 Out Mean		p-value	
	Series A	Series B	Series A	Series B	Series A	Series B
As	0.011 (±0.002)	0.013 (±0.005)	0.008 (±0.001)	0.007 (±0.006)	0.072	0.24
B	2.889 (±0.52)	2.816 (±0.48)	2.891 (±0.634)	2.751 (±0.857)	0.996	0.916
Cu	0.017 (±0.003)	0.024 (±0.011)	0.014 (±0.006)	0.017 (±0.005)	0.41	0.37
Pb	0.012 (±0.002)	0.011 (±0.001)	0.012 (±0.001)	0.013 (±0.003)	0.57	0.40
Zn	0.062 (±0.024)	0.052 (±0.009)	0.034 (±0.020)	0.049 (±0.012)	0.20	0.77

Table S5. Percent survival and reproduction of *C. dubia* in static renewal, 7-day bioassays conducted according to Environment and Climate Change Canada protocols for single-concentration tests (ECCC, 2011). Exposures from untreated OSPW and the hybrid CWTS are listed directly below the laboratory controls to which they were compared (α=0.05).

Treatment/ Control	Survival				Reproduction			
	Percent Survival		*p-value*		Neonates/ surviving adult		*p-value*	
	Series A	Series B	Series A	Series B	Series A	Series B	Series A	Series B
Sampling Period 1								
Control 1	95%		–	–	28 (±6)		–	–
Inflow	70%		0.046		21 (±3)		0.001	
PC1	100%	100%	1	1	19 (±5)	24 (±5)	<0.001	0.042
Control 2	100%		–	–	20 (±5)		–	–
WC5	90%	75%	0.244	0.024	19 (±4)	22 (±3)	0.506	0.219
Control 3	95%		–	–	23 (±6)		–	–
PC2 In	100%	95%	1.00	0.756	14 (±5)	21 (±4)	<0.001	0.979
Control 4	100%		–	–	25 (±4)		–	–
PC2 Out	95%	95%	0.500	0.500	22 (±4)	17 (±6)	0.144	<0.001
Sampling Period 2								
Control 5	100%		–	–	20 (±5)		–	–
Inflow	20%		<0.001		27 (±4)*		0.087	
Control 6	100%		–	–	26 (±7)		–	–
PC1	100%	100%	1.00	1.00	24 (±4)	23 (±5)	0.635	0.254
WC5	100%	95%	1.00	0.500	22 (±4)	23 (±5)	0.180	0.133
Control 3	95%		–	–	23 (±6)		–	–
PC2 In	100%	90%	1.00	0.500	23 (±4)	25 (±4)	0.997	0.645
PC2 Out	100%	100%	1.00	1.00	25 (±5)	21 (±4)	0.547	0.639
Sampling Period 3								
Control 4	100%		–	–	25 (±4)		–	–
Inflow	90%		0.500		15 (±3)		<0.001	
PC1	100%	95%	1.00	0.756	26 (±4)	26 (±4)	0.8501	0.9406
Control 7	100%		–	–	21 (±5)		–	–
WC5	90%	90%	0.244	0.244	25 (±6)	25 (±5)	0.297	0.173
PC2 In	90%	80%	0.394	0.061	22 (±5)	25 (±5)	1.00	0.214
PC2 Out	80%	85%	0.053	0.115	24 (±4)	23 (±6)	0.538	0.891

"–" *p* value not calculated for controls

* Only 2 out of 20 daphnids produced three broods, but reproduction was not inhibited in these replicates

APPENDIX C

Standard Operating Procedures

METHOD FOR MEASURING GENERAL WATER QUALITY PARAMETERS: PH, DISSOLVED OXYGEN, CONDUCTIVITY, TEMPERATURE, ALKALINITY, AND HARDNESS

Daniel P. Gaspari; Jeff Schwindaman, Brenda M. Johnson, Laura E. Ober, John H. Rodgers, Jr.

1.0 OBJECTIVE

The purpose of this protocol is to measure various general water quality parameters. Parameters such as pH, dissolved oxygen (DO), conductivity, temperature, alkalinity, and hardness are fundamental water quality parameters and are necessary for all water chemistry related studies.

2.0 HEALTH AND SAFETY

Proper laboratory attire, including scrubs, lab coat, gloves and safety glasses must be worn at all times.

3.0 PERSONAL/TRAINING/RESPONSIBILITIES

Any graduate research assistant familiar with the equipment and laboratory techniques and trained in this and referenced SOPs may perform this procedure.

4.0 REQUIRED MATERIALS

4.1 Reagents

Reagent:	Test:
NANOpure® water	All tests
pH buffers (4,7, and 10)	pH, Alkalinity
0.02 N standard sulfuric acid solution (H_2SO_4)	Alkalinity
Eriochrome Black T indicator	Hardness
Standard EDTA titrant (0.01M, 0.02N)	Hardness
Buffer solution (Reference Standard Methods 2340C)	Hardness

4.2 Supplies

Supply:	Test:
Graduated cylinder	Alkalinity, Hardness
100-mL beakers	All tests
Magnetic stir bar	Alkalinity, Hardness
50-mL burette and stand	Alkalinity, Hardness

4.3 Equipment

Orion Star A221 equipped with a 9157BNMD Triode pH probe
Orion Star A221 equipped with a 013010MD conductivity cell
HQ30d meter with a LDO101 optical dissolved oxygen probe
Magnetic stir plate

5.0 PROCEDURE

5.1 pH

1. Calibrate the pH meter using standard pH buffers 4, 7, and 10.
2. Rinse probe with NANOpure® water to remove any prior contaminant.
3. Remove the small blue rubber stopper from the probe
4. Submerge the tip of the probe in the sample and gentle stir the sample with the probe.
5. When the pH reading has stabilized, record pH in S.U. to a tenth of a S.U.
6. Rinse probe with NANOpure® water between measurements and return to holder when finished.

5.2 Dissolved Oxygen (DO)/Temperature

1. Turn on the dissolved oxygen Meter.
2. Rinse probe with NANOpure® water to remove any prior contaminant.
3. Completely submerge the tip of the probe in the sample.
4. When the DO reading has stabilized, record DO in mg/L. Also record the temperature to a tenth of a degree (i.e. 20.1°C).
5. Rinse probe with NANOpure® water between measurements and return to holder when finished.

5.3 Conductivity

1. Calibrate the conductivity meter using 10 and 1,413 µS/cm standards
2. Rinse probe with NANOpure® water to remove any prior contaminant.
3. Submerge the probe in the sample and gently stir the sample with the probe.
4. When the conductivity reading has stabilized the conductivity will record in (mS/cm) and temperature in degrees Celsius.
5. Rinse probe with NANOpure® water and return to holder.
6. When finished turn off the meter

5.4 Alkalinity

1. Using a graduated cylinder, measure 50 mL of sample water and pour it into a 100-mL beaker with a magnetic stir-bar.

2. Place sample beaker on magnetic stir-plate. Turn on stir-plate to begin mixing sample.
3. Calibrate the pH meter. Place probe in the appropriate stand, with the tip completely submerged in the sample water. (Make sure the stir-bar does not hit the pH probe).
4. Record the initial level of titrant (0.02 N H_2SO_4) in the burette (fill burette as necessary).
5. Slowly drip titrant into the sample, allowing time for the pH meter to stabilize.
6. Titrate to pH 4.5.
7. Record the volume (mL) of titrant used to reach the pH endpoint (pH=4.5).
8. Calculate: Total Alkalinity (mg/L as $CaCO_3$) = col. Titrant (mL)x 20
9. Turn off stir-plate and discard sample.

5.5 Hardness

1. Using a graduated cylinder, measure 50 mL of sample water and pour it into a 100-mL beaker with a magnetic stir-bar. (Dilutions can be made to conserve EDTA titrant, be sure to calculate dilutions into the final equation.)
2. Add 2-5 mL of buffer solution (to give the sample a pH of 10.0-10.1).
3. Add 2-4 drops of Eriochrome Black T Indicator. Sample should turn pink.
4. Place sample beaker on magnetic stir-plate. Turn on plate to mix sample.
5. Record the level of titrant (EDTA) in the burette (fill burette as necessary).
6. Slowly drip titrant into the sample, allowing time for the color change to stabilize.
7. Titrate until pink turns to a blue-green color.
8. Record the volume of titrant (mL) used to reach the color change.
9. Calculate: Hardness (mg/L $CaCO_3$) = volume titrant (mL) x 20.
10. Turn off stir-plate and discard sample.

6.0 QUALITY CONTROL CHECKS AND ACCEPTANCE CRITERIA

All procedures are subject to review by the Quality Assurance Unit.

METHOD FOR MEASURING OXIDATION-REDUCTION POTENTIAL

Daniel P Gaspari, Sarah E. Sundberg, Derek Eggert, J. Chris Arrington, John H. Rodgers Jr.

1.0 OBJECTIVE

Oxidation and reduction (redox) reactions mediate the behavior of many chemical constituents in wastewaters. The reactivities and mobilities of important elements in biological systems, as well as those of a number of other metallic elements, depend strongly on redox conditions. Like pH, Eh (redox) represents an intensity factor; it does not characterize the capacity of the system for oxidation or reduction. Measurements are made by potentiometric determination of electron activity (or intensity) with an inert indicator electrode and a suitable reference electrode. Electrodes made of platinum are most commonly used for Eh measurements. This protocol describes the method used to measure redox in the hydrosoil of a constructed wetland treatment system.

2.0 HEALTH AND SAFETY

Proper laboratory attire, including scrubs, lab coat, gloves and safety glasses must be worn at all times.

3.0 PERSONNEL/TRAINING/RESPONSIBILITIES

Any graduate research assistant familiar with the equipment and laboratory techniques and trained in this and referenced SOPs may perform this procedure.

4.0 REQUIRED MATERIALS

4.1 Supplies

Potassium ferrocyanide $K_4Fe(CN)_6 \cdot 3H_2O$
Potassium ferricyanide, $K_3Fe(CN)_6$
Potassium chloride, KCl

4.2 Equipment

pH or millivolt meter
Reference electrode
Oxidation-reduction indicator electrode
Beakers
Magnetic Stirrer

5.0 PROCEDURE

Prepare ZoBell's standard redox solution by adding 1.408 g potassium ferrocyanide, 1.098 g potassium ferricyanide and, 7.455 g potassium chloride to 1,000 mL of NANOpure® water at 25°C. These measurements must be as accurate as possible to result in a reliable solution. When stored in dark plastic bottles in a refrigerator, this solution is stable for several months.

Follow the manufacturer's instructions for using the pH/millivolt meter and in preparing electrodes for use. Immerse the reference electrode connected to the millivolt meter and the redox indicator electrode (platinum tip end) in the gently stirred, standard solution in a beaker. Connect the millivolt meter to the end of the indicator electrode opposite the platinum tip. Allow several minutes for electrode equilibrium then record the reading to the nearest millivolt. If the reading is within +10 mV from the theoretical redox standard value at 25°C (+183 mV), record the reading. The indicator electrode is ready for placement in the hydrosoil. If the reading is not within +10 mV, the indicator electrode must be remade.

Place the indicator electrode's platinum tip into the sediment making certain it is not near the plant roots and at a depth of 10 cm in the hydrosoil. Secure the electrode with cable ties. Allow the electrode to equilibrate for 24 hours prior to taking any readings. When measuring the redox potential of the hydrosoil place the reference electrode in the same water column as the probe. Connect the millivolt reader to the end of the indicator electrode opposite the platinum tip. Record the redox potential in mV. Repeat a second time by placing the reference electrode in another location. Successive readings that vary less than +10 mV over 10 minutes are adequate for most purposes. Adjust the reading according to field corrections and electrode calibration corrections.

Example: The field measurement of a hydrosoil was -206 mV. When the electrode was initially calibrated in the laboratory, the redox reading was +193mV, which is +10mV different from the theoretical redox standard value of +183 mV. The field redox measurement must be corrected for this difference by subtracting 10 mV from -206 mV. This gives a redox measurement of -216 mV. The standard correction factor for field redox measurements for the millivolt reader is +240 mV. Therefore, this correction factor is added to the redox measurement of -216 mV to yield a final redox measurement of +24 mV.

$$Eh_{system} = Eh_{observed} - Eh_{reference\ observed} + Eh_{field\ correction}$$

$$Eh_{system} = -206mV + 183mV - 193mV + 240mV$$

6.0 QUALITY CONTROL CHECKS AND ACCEPTANCE CRITERIA

All procedures are subject to review by the Quality Assurance Unit.

7.0 REFERENCES

Faulkner, S.P., W.H. Patrick, Jr., R.P. Gambrell, 1989. Field techniques for measuring wetland soil parameters. *Soil Science Society of America Journal* 53, 883-890.

ZoBell, C. E., 1946. Studies on redox potential of marine sediments. *Bulletin of the American Association of Petroleum Geologists* 30, 477-513.

METHOD FOR DERIVATIZING NAPHTHENIC ACIDS FOR HPLC ANALYSIS

Sam Muller

1.0 OBJECTIVE

The objective of this standard operating procedure is to clearly outline the methods for derivatizing naphthenic acids in solution for HPLC analysis.

2.0 HEALTH AND SAFETY

Proper personal protective equipment will be worn for the entirety of this procedure. Reagents for derivatization should be prepared and handled within a fume hood.

3.0 PERSONNEL/TRAINING/RESPONSIBILITIES

Any graduate research assistant familiar with the equipment and laboratory techniques and trained in this SOP may perform this procedure.

4.0 REQUIRED AND RECOMMENDED MATERIALS

4.1 Supplies

1 M NaOH
3 M HCl
0.4 M HCl
Ethanol, HPLC grade
Methanol, HPLC grade
Nano-pure water
Pyridine
KOH salt, reagent grade
2-NPH
1-EDC-HCl
50 mL opaque vials with screw caps
2-mL amber glass HPLC vials with caps and septa

4.2 Equipment

Water bath
Thermometer
Magnetic stir plate
Magnetic stir bar
pH meter with needle tip
100 mL volumetric flask
30 mL beakers

30 mL medicine cups
100-1,000 µL volumetric pipette and tips
5-10 mL volumetric pipette and tips
Syringe and 0.22 µm syringe filter

5.0 PROCEDURE

5.1 Reagent Preparation

Prepare a 95% ethanol in water (v/v) solution in a 1-L volumetric flask. For the 2-NPH reagent, mix 15 mL of the 95% ethanol solution, 5 mL 0.4 M HCl, and 60 mg of 2-NPH in a beaker. Stir fifteen minutes on a stir plate and store in an opaque vial with screw top at 4° C in refrigerator. Prepare a 3% pyridine solution by adding 3 mL pyridine to a 100 mL volumetric flask and filling with 95% v/v ethanol in Nano-pure water. Add 10 mL 95% ethanol solution, 10 mL 3% pyridine solution, and 480 mg EDC-HCl to a beaker and place on stir plate for fifteen minutes. Store the solution in an opaque vial with screw top at 4° C. Prepare a 1 M KOH solution by dissolving 5.61 g KOH salt in 100 mL 80% v/v HPLC grade methanol solution in Nano-pure water. Dilute to 140 mM by adding 14 mL of the prepared 1 M KOH solution to a 100 mL volumetric flask. Fill to 100 mL using 80% (v/v) methanol in Nano-pure water.

5.2 Sample Preparation

Pour 5 mL of sample into a medicine cup. Add 1 M NaOH until pH reaches 12. Filter with a syringe and 0.22 µm syringe filter. Adjust pH of filtered sample to between 8 and 10 with 3 M HCl solution, measuring with needle tip pH meter.

5.3 Derivitization

Turn on water bath and set temperature to 60°C. Pipet 600 µL of pH-adjusted, filtered sample into a clean HPLC vial. Add 240 µL of 2-NPH reagent and 240 µL of 1-EDC-HCl solution to each vial. Tightly cap the vial and place samples in water bath for 20 minutes. Remove samples from water bath. Add 120 µL of 140 mM KOH in 80% (v/v) methanol/water to each vial. Recap vials and place in water bath for 15 minutes. Measure pH to ensure it does not exceed 7.5. pH should read between 5.5 and 6.5. Cool samples and take to HPLC.

6.0 REFERENCE

Yen, T.W., Marsh, W.P., MacKinnon, M.D., Fedorak, P.M., 2004. Measuring naphthenic acids concentrations in aqueous environmental samples by liquid chromatography. *Journal of Chromatography* 1033, 83-90.

METHOD FOR MEASURING TOTAL SUSPENDED AND TOTAL DISSOLVED SOLIDS

Sarah E. Sundberg, Derek Eggert, J. Chris Arrington, John H. Rodgers, Jr.

1.0 OBJECTIVE

Solids refer to matter suspended or dissolved in water or wastewater. Solids may affect water or effluent quality adversely in a number of ways. Solid analyses are important in the control of biological and physical wastewater treatment processes and for assessing compliance with regulatory agency wastewater effluent limitations. This method determines the concentration of the total suspended and total dissolved solids in a water sample.

2.0 HEALTH AND SAFETY

Proper laboratory attire, including scrubs, lab coat, gloves and safety glasses must be worn at all times.

3.0 PERSONNEL/TRAINING/RESPONSIBILITIES

Any graduate research assistant familiar with the equipment and laboratory techniques and trained in this and referenced SOPs may perform this procedure.

4.0 REQUIRED AND RECOMMENDED MATERIALS

4.1 Supplies

Millipore glass fiber filter disks, 47mm
Filtration apparatus with reservoir & coarse (40 to 60 m) fritted disk as filter support
Graduated cylinder
Desiccator
Aluminum weight dishes

4.2 Equipment

Drying oven, for operation at 105°C
Analytical balance, capable of weighing 0.00001g

5.0 PROCEDURE

For one sample, label two aluminum weight dishes TSS and TDS. Place a glass-fiber filter disk in the TSS aluminum dish with the wrinkled side up and obtain the weight (in grams). Obtain weight of the empty TDS dish as well. Place the filter disk on the filtration apparatus, apply vacuum, and wash the disk with approximately 20 mL distilled

water. Continue suction to remove all traces of water on the disk, turn the vacuum off, and discard water from the wash. Apply vacuum again, and pour 100 mL of sample through the filter. Remove filtering apparatus, and collect 10 mL in the TDS aluminum weight dish. Replace the funnel, rinse the graduated cylinder with distilled water, and continue vacuum suction to remove all traces of water on the disk. Carefully remove the disk and place in the TSS aluminum weight dish. Place the weight dishes in the oven at 105°C and dry for 24 hours.

Once dry, remove the dishes from the oven and place in a desiccator for approximately 20 minutes, or until the dishes are at room temperature. Obtain weights (in grams) of the dishes.

$$\text{TDS} = \frac{Weight_{post} - Weight_{pre}}{10\ \text{mL}} \times \frac{1000\ \text{mL}}{1\ \text{L}} \times \frac{1000\ \text{mg}}{1\ \text{g}}$$

$$\text{TSS} = \frac{Weight_{post} - Weight_{pre}}{100\ \text{mL}} \times \frac{1000\ \text{mL}}{1\ \text{L}} \times \frac{1000\ \text{mg}}{1\ \text{g}}$$

6.0 QUALITY CONTROL CHECKS AND ACCEPTANCE CRITERIA

All procedures are subject to review by the Quality Assurance Unit.

METHOD FOR MEASURING CHEMICAL OXYGEN DEMAND (COD)

Sarah E. Sundberg, Derek Eggert, J. Chris Arrington, John H. Rodgers, Jr.

1.0 OBJECTIVE

The chemical oxygen demand (COD) is defined as the amount of a specified oxidant that reacts with the sample under controlled conditions. The quantity of oxidant consumed is expressed in terms of its oxygen equivalence. Because of its unique chemical properties, the dichromate ion ($Cr_2O_7^{2-}$) is the specified oxidant in this method. When a sample is digested, the dichromate ion oxidizes COD material from the hexavalent (VI) state to the trivalent (III) state. Both of these chromium species are colored and absorb in the visible region of the spectrum. The chromic ion absorbs strongly in the 600 nm region. The measured absorbance of the digested sample is the COD of the water sample.

2.0 HEALTH AND SAFETY

Proper laboratory attire, including scrubs, lab coat, gloves and safety glasses must be worn at all times.

3.0 PERSONNEL/TRAINING/RESPONSIBILITIES

Any graduate research assistant familiar with the equipment and laboratory techniques and trained in this and referenced SOPs may perform this procedure.

4.0 REQUIRED AND RECOMMENDED MATERIALS

4.1 Reagents

Water, 18 M Ω cm
Potassium hydrogen phthalate

4.2 Supplies

HACH COD digestion vials, dichromate, 0-1,500 mg/L range
Cuvettes

4.3 Equipment

Spectrophotometer, for use at 600 nm
Dry bath incubator, for operation at 150°C

5.0 PROCEDURE

Prepare five calibration standards by mixing 750 mg potassium hydrogen phthalate in 500 mL of water. This solution is good for 6 weeks. Dilute standard to 187 mg/L, 93

mg/L, 46 mg/L, and 0 mg/L. Add 2 mL of standard solutions to labeled COD digestion vials, carefully mix contents, and place on a dry bath incubator at 150°C for 2 hours, then let sit for 24 hours. Measure the turbidity of the standards on the spectrophotometer at 600 nm. Plot the turbidity readings and concentrations to determine the equation of the calibration curve.

Acidify water samples with approximately 2 drops of concentrated sulfuric acid to drop the pH to less than 2 for storage. Dilute the water sample to achieve less than 1,500 mg/L chlorides. Add 2 mL diluted sample to labeled COD digestion vials in duplicate. Carefully mix contents of the COD vials, and place on a dry bath incubator at 150°C for 2 hours, then let sit for 24 hours. Measure the turbidity of the standards on the spectrophotometer at 600 nm. Use the calibration equation of $y = mx + b$ to determine COD by substituting the spectrophotometer reading for y and solving for x, then multiplying by the dilution factor used.

6.0 QUALITY CONTROL CHECKS AND ACCEPTANCE CRITERIA

All procedures are subject to review by the Quality Assurance Unit.

METHOD FOR MEASURING BIOCHEMICAL OXYGEN DEMAND (BOD)

Sarah E. Sundberg, Derek Eggert, J. Chris Arrington, John H. Rodgers, Jr.

1.0 OBJECTIVE

The biochemical oxygen demand (BOD) is determined through the use of an empirical test in which standardized laboratory procedures are used to find the relative oxygen requirements of the wastewater. This method measures the molecular oxygen utilized during a specified incubation period for the biochemical degradation of organic material and the oxygen used to oxidize inorganic material such as sulfides and ferrous iron. It also may measure the amount of oxygen used to oxidize reduced forms of nitrogen unless their oxidation is prevented by an inhibitor.

2.0 HEALTH AND SAFETY

Proper laboratory attire, including scrubs, lab coat, gloves and safety glasses must be worn at all times.

3.0 PERSONNEL/TRAINING/RESPONSIBILITIES

Any graduate research assistant familiar with the equipment and laboratory techniques and trained in this and referenced SOPs may perform this procedure.

4.0 REQUIRED AND RECOMMENDED MATERIALS

4.1 Supplies

Incubation bottles, 300 mL foil-wrapped glass bottles having a ground-glass stopper and a flared mouth are preferred

4.2 Equipment

Dissolved Oxygen Meter

5.0 PROCEDURE

Fill an incubation bottle to overflowing with sample water at 20°C. Measure the dissolved oxygen (DO) in each bottle, insert stopper, and make an airtight seal. Incubate at 20°C in the dark. Measure the DO in each bottle once a day. If DO falls to about 2 mg/L, re-aerate for approximately 30 minutes to oxygenate the water. Measure the DO again. This concentration becomes the initial DO for the next measurement. Be sure to replace any sample lost by the cap and DO probe displacement by adding additional sample water. Calculate oxygen consumption during each time interval between

aerations. After a 5-day period, combine all measured oxygen consumptions to determine BOD_5 of the sample.

6.0 QUALITY CONTROL CHECKS AND ACCEPTANCE CRITERIA

All procedures are subject to review by the Quality Assurance Unit.

METHOD FOR MEASURING METAL CONCENTRATIONS USING INDUCTIVELY COUPLED PLASMA ATOMIC EMISSION SPECTROMETER (ICP-AES)

Daniel P. Gaspari, Maas Hendrikse, Michael J. Pardue, Jennifer Horner

1.0 OBJECTIVE

This method outlines the specific experimental details for analysis of select elements using the ICP-AES as it pertains to oil sands process water (OSPW). This protocol is intended for measuring acid soluble concentrations of metals and metalloids in aqueous samples and is adapted from standard methods (USEPA, 2001).

2.0 HEALTH AND SAFETY

Proper lab attire, including lab coat, gloves, and safety glasses must be worn at all times.

3.0 PERSONNEL/TRAINING/RESPONSIBILITIES

Any graduate research assistant familiar with the equipment and laboratory techniques and trained in this and referenced SOPs may perform this procedure.

4.0 REQUIRED AND RECOMMENDED MATERIALS

4.1 Supplies

Spectro Flame Modula ICP-AES (Spectro Analytical Instruments; Mahwah, NJ, USA), 500 mL acidified NANOpure® water for rinse, standards for the elements of interest.

4.2 Standards

Standards should not exceed a range of two orders of magnitude. Standards should be made in a matrix to resemble that of the samples. Acidified in same manner as samples (10% by volume with nitric acid). Standards should be made the day of sample analysis.

5.0 PROCEDURE

This procedure only includes the basic methods for sample collection, ICP-AES use and cleanup, and quality assurance controls. Instrumentation manual and EPA Method 200.7 (USEPA, 2001) should be reviewed.

5.1 Sample Collection and Preparation

Collect samples in clean 50 mL plastic centrifuge tubes, do not allow the tube to overfill when filling. Adjust sample pH to ≤ 2.0 with HNO_3 (approximately 1% by volume or 0.5 mL acid in 50 mL sample). Store sample in dark for storage up to 6 months at <3°C. Warm samples to room temperature before analysis.

5.2 ICP-AES Methods

The instrument manual for the ICP-AES contains procedures for calibration and analysis of samples, and an SOP, written by Brenda M Johnson, Derek A. Eggert, and Andrew McQueen (unpublished, 2007) containing step by step instructions for ICP-AES use. The USEPA (2001) recommends the following wavelengths and guidance for method detection limits.

Metal/Metalloid	Wavelength (nm)	Estimated Detection Limit (mg/L)[a]
Al	308.215	0.02
As	193.759	0.008
Ba	493.409	0.001
B	249.0678	0.003
Cd	226.502	0.001
Ca	315.887	0.01
Cr	205.552	0.004
Co	228.616	0.002
Fe	259.94	0.003
Pb	220.353	0.01
Mg	279.079	0.02
Mn	257.61	0.001
Ni	231.604	0.005
K	766.491	0.3
Se	196.09	0.02
Na	588.995	0.03
Zn	213.856	0.002

[a] Estimated detection limit for acid soluble (i.e. total recoverable) aqueous metals

5.3 Cleaning

After ICP-AES use the system lines should be flushed with acidified NANOpure® for 5-10 minutes. Prior to and at the conclusion of each use of the ICP-AES all lines and tubing should be checked for blocks and wear. Empty the waste container if necessary. The remainder of unused standards can be disposed of in appropriate waste containers and aqueous sample should be stored in centrifuge tubes in the refrigerator, in case further analysis is required.

5.4 Quality Assurance

Quality assurance and quality control measures for ICP-AES metal analyses should include standard recovery and standard addition every ten samples. Sample analyses can be considered acceptable if standard recoveries are within ±10% of the calibration concentration for individual metals. A middle standard should be used for standard additions and the percent recovery should be within 70-130%. A new calibration curve should be accepted every 20 samples and duplicate samples can be analyzed for additional assurance. These quality assurance and control measures should be considered as the minimum requirements of USEPA methods, additional quality measures should be performed for unknown or excessively cloudy (non-homogeneous) samples.

6.0 QUALITY CONTROL CHECKS AND ACCEPTANCE CRITERIA

All procedures are subject to review by the Quality Assurance Unit.

7.0 REFERENCES

United States Environmental Protection Agency (USEPA), 2001. Trace elements in water, solids, and biosolids by inductively coupled plasma-atomic emission spectrometry. 5th Revision. EPA Method 200.7. EPA-821-R-01-010. Office of Water, Washington, DC.

METHOD FOR MEASURING OIL AND GREASE (O&G)

Michael J. Pardue, Jennifer E. Horner

Adapted from the directions for the StepSaver apparatus manufactured by Environmental Express, www.envexp.com

1.0 OBJECTIVE

The following protocol provides a method for measuring the concentration of oil and grease (O&G) in a water sample. An apparatus manufactured by Environmental Express was used to measure O&G using a modification on EPA method 1664 Revision A. EPA Method 1664A is a performance based method, "The laboratory is permitted to modify the method to overcome interferences or lower the cost of measurements, provided that all performance criteria are met" (Section 1.7 of EPA 1664A). The procedure is a solid phase extraction for O&G (defined as any components extractable by n-hexane). The outlined procedure can yield false positive results because fatty acids in samples can be extracted as O&G. There is a secondary test using silica gel to further distinguish between n-hexane extractables and total petroleum hydrocarbons (TPH). This procedure can be competed with the StepSaver apparatus from Environmental Express but was not utilized in this research. The outlined procedure for O&G has four basic steps: rinse disk with elution solvent, condition disk with methanol, extract analytes from water sample, and elute analytes with elution solvent. Additional application notes on the StepSaver apparatus can be found at the manufacture's website www.envexp.com.

2.0 HEALTH AND SAFETY

Proper laboratory attire, including lab coat, gloves, and safety glasses must be worn at all times.

3.0 PERSONNEL/TRAINING/RESPONSIBILITIES

Any graduate research assistant familiar with the equipment and laboratory techniques and trained in this and referenced SOPs may perform this procedure.

4.0 REQUIRED AND RECOMMENDED MATERIALS

4.1 Reagents

n-hexane (85% purity or greater)
Methanol
Hydrochloric Acid
Hexadecane, stearic acid, and acetone
Deionized water

4.2 Apparatus and Supplies

47mm or 90mm StepSaver glass with filtration manifold, water trap, and vacuum source
Prefilter material such as Filter Aid 400, and/or appropriate sized glass fiber filters
Dried and weighed receiving flasks with 24/25 or 24/40 ground glass joint
5.5 g sodium sulfate drying cartridges
Stainless steel filter support screen
Teflon dispensing squirt bottles
Analytical balance
Desiccator
Water bath or other evaporative device capable of achieving at least 85°C

5.0 PROCEDURE

5.1 Sample Collection and Preparation

Collect 0.5 L samples in glass jars (EPA method recommends 1 L samples). Do not allow sample to touch any glassware or plastic besides the sample container because O&G will adhere to material and underestimate O&G sample concentration. Adjust sample pH to ≤ 2.0 with HCl (approximately 1% or 5 mL acid in 0.5 L sample). Cool sample in dark for storage up to 7 days.

5.2 O&G Extraction Methods

Extraction Disk Conditioning

Note: proper filter conditioning is essential for both adequate flow rate through the disk and good recovery
1. Place the stainless steel filter support screen in the top of the StepSaver head. The screen should be resting on the glass.
2. Place the Empore extraction disk into the filter gasket. The filter should be resting inside the gasket, mesh side down, white side up towards the 1 liter funnel. 3. Place the gasket and filter together onto the stainless steel screen, and center the funnel on the head. While holding the funnel with one hand, squeeze the clamp firmly into place.
4. Attach a flask to collect waste solvent to collection arm of StepSaver with keck clip.
5. For extremely dirty samples, place a scoop of Filter Aid 400 atop the disk. 90mm StepSavers have 4X the solids loading capacity of the 47mm StepSaver.
Note: Use of glass fiber pre-filters can result in low recoveries of the stearic acid fraction.
6. Turn the upper stopcock with the red handles so that flow will be toward the collection flask.
7. Position the valve on the manifold to the off/vent position. Wash the disk and walls of the funnel with 10-15 mL of n-hexane. Quickly turn the manifold valve to the on

(12 o'clock) position and then back to off/vent (9 o'clock/3 o'clock) position. This should draw a small amount of hexane through the disk. Allow the disk to soak for two minutes. Apply vacuum and pull remaining hexane through disk into collection flask. Allow disk to vacuum dry for one to two minutes, making sure all hexane is removed from the disk.
8. If the seal was leaking n-hexane repeat the n-hexane rinse steps above.
9. Position the valve on the manifold to the off/vent position.
10. Turn the StepSaver stopcock (upper stopcock) to the waste position. Add 10- 15 mL of methanol to the reservoir. If necessary, quickly turn manifold valve to on position and then quickly back to off/vent position, and back up to the off/off position (1 o'clock/ 6 o'clock) position. Allow the methanol to soak for one minute before adding sample.
Note: If the vacuum pressure is not fully vented from the StepSaver, the methanol will continue to flow through the disk even through the valve is in the off/off position. Also, a small amount of methanol may leak from the vent hole in the manifold if the stopcock is not moved up to the off/off position.
11. Add sample on top of methanol and immediately turn vacuum to 'on' position.
12. Set empty container on its edge so that the remaining water (1 to 3 mL) can collect, then add this remaining water to the reservoir before the extraction is complete.
13. After elution is complete, continue vacuum to air dry the filter for 5-20 minutes. The longer the better.
Note: While the filter is drying pre-weigh the collection flasks (5 decimal place accuracy).

Sample Elution

1. Position StepSaver stopcock (upper stopcock) to collection position.
2. Remove waste flask and properly dispose of collected solvents. Gently attach a 5.5 g sodium sulfate cartridge to the luer tip in the collection arm of the StepSaver. (When attaching and removing the cartridge be careful to pull straight up and down.) Attach collection flask that has been dried and weighed.
3. Add 10-15 mL of n-hexane to sample container, rinsing down the sides. Shake the hexane around the sample container, venting the cap occasionally. Pour the n- hexane from sample container into StepSaver funnel.
4. Carefully apply vacuum and release to pull a few drops of n-hexane through the disk. Allow the hexane to soak the filter for two minutes.
5. Carefully apply vacuum to slowly pull hexane through disk, through sodium sulfate drying cartridge and into the pre-weighed flask. It is important to pass the n-hexane through the drying cartridge slowly to allow adequate contact time for water absorption.
6. After all hexane has passed into the collection flask, turn the vacuum to off/vent position.
7. Rinse down the sides of the 1-liter funnel with 10-25 mL of n-hexane. Be sure to rinse with hexane until all O&G is removed from the sides of the glass funnel.

Note: Stearic acid sticks to glassware. Be sure to rinse the funnel walls with hexane until all Stearic acid crystals dissolve. Failure to thoroughly rinse Stearic acid from the glassware will result in low recoveries.
8. Remove pre-weighed collection flask, and evaporate n-hexane at a temperature of 80-85°C in a hot water bath. Do not boil or evaporate to absolute dryness. Sweep with a vacuum tube to evaporate via air flow the final drops of n-hexane and fumes. Desiccate to room temperature. Reweigh flask to obtain final weight.
Note: Hexadecane will volatilize if the n-hexane boils. Further, hexadecane begins to volatilize soon after the weighing flask becomes dry. Be sure to weigh the flask within an hour or two of placing it into the desiccator. Do not store weigh flask in desiccator overnight. Reducing volatilization of hexadecane will improve recoveries.

5.4 Cleaning

For O&G applications only the funnel needs to be cleaned with soap and water after use. The stopcock and the head of the StepSaver may be cleaned by rinsing with hexane.

6.0 O&G STANDARDS AND QUALITY ASSURANCE

A method blank flask was carried through the procedure for quality assurance and control. Blank mass was subtracted from or added to final mass measurements of sample flasks. The reported method detection limit for EPA method 1664: Revision A is 1.4 mg L^{-1} O&G. The method limit of detection for this specific procedure and for research purposes was set at three times the standard deviation of the blanks for a given set of samples.

Motor Oil Standards

Motor oil standards (i.e. known mass of motor oil in a known volume of water) are used in this procedure to demonstrate calibration verification as part of ongoing precision and recovery. If the standard recoveries are within the range specified (78-114%), the extraction, distillation, and weighing processes are in control. Percent recoveries for standards can be calculated using the following equation:

$$P = 100 \times \frac{A}{B}$$

where, P is the percent recovery, A is the measured concentration of the calibration standard, and B is the theoretical concentration of the calibration standard (i.e. mass of motor oil (mg)/volume of standard (L).

Sample Matrix Spiking

Analysis of a matrix spike is required to demonstrate recovery and to monitor matrix interferences. Matrix spikes were completed by collecting duplicate samples and spiking one with a known mass of motor oil. Matrix spikes should be conducted for each set of

20 samples or less (USEPA, 1999). Acceptable matrix spike recoveries are 78-114%, calculated using the following equation:

$$P = 100 \times \frac{A - B}{TE}$$

where, P is the percent recovery, A is the measure concentration of analyte after spiking, B is the measured background concentration of the sample, and TE is the true concentration of the spike.

If any part of the ongoing precision and recovery quality assurance and controls measures are out of control (i.e. standards or matrix spike recoveries out of range) the operator should trouble shoot the O&G procedure and make modifications as needed. Duplicate samples may need to be collected and analyzed until the methods are under control.

7.0 QUALITY CONTROL CHECKS AND ACCEPTANCE CRITERIA

All procedures are subject to review by the Quality Assurance Unit.

8.0 REFERENCES

United States Environmental Protection Agency (USEPA), 1999. Revision A: n-hexane extractable material (HEM; oil and grease) and silica gel treated n-hexane extractable material (SGTHEM; non-polar material) by extraction and gravimetry. EPA Method 1664. EPA-821-R-10-001. Office of Water, Washington, DC.

METHOD FOR DETERMINATION OF ACID-VOLATILE SULFIDES IN HYDROSOIL

Daniel P Gaspari, Kristen N. Jurinko

1.0 OBJECTIVE

Concentrations of AVS in the hydrosoil and detritus were measured by the modified diffusion method (Leonard et al., 1996). AVS is operationally defined by Leonard et al. (1996) as sediment sulfide that is liberated by treatment of the sediment with 1-N hydrochloric acid. AVS is a measure of reactive sulfide, which includes primarily free sulfides, amorphous iron monosulfide (FeS), and sulfides of other divalent metals (e.g. Cd, Cu, Ni, and Zn; Di Toro et al., 1992; Yu et al., 2001).

2.0 HEALTH AND SAFETY

Proper laboratory attire, including scrubs, lab coat, gloves, and safety glasses must be worn at all times.

3.0 PERSONNEL/TRAINING/RESPONSIBILITIES

Any graduate research assistant familiar with the equipment and laboratory techniques and trained in this and referenced SOPs may perform this procedure.

4.0 REQUIRED AND RECOMMENDED MATERIALS

5.1 Supplies

50-mL polypropylene centrifuge tubes
500-mL glass bottle (capped)
Deionized water

5.2 Equipment

Magnetic stir bar
Magnetic stir plate
Analytical balance capable of weighing ± 0.1 mg

5.3 Reagents

1-N trace metal grade (37%) HCl

Sulfide Antioxidant Buffer (SAOB):
2 M NaOH to convert H_2S into S^{2-}
0.1 M ascorbic acid to prevent oxidation of S^{2-}

0.1 M EDTA to complex metals that may have catalyzed the oxidation of S^{2-}

1.0 M Sulfide stock solution:
Prepare using freshly washed sodium sulfide crystals to remove oxidized sulfide products & store at 4°C
For calibration of the ion-selective electrode (ISE), prepare dilutions over the range 10^{-1} to 10^{-4} M in SAOB solution.

5.0 PROCEDURE

5.1 Making Standards

5.1.1 SAOB
To make 500 mL, add 100 mL of deionized water to a 500 mL glass bottle. Next, add 40 g NaOH pellets and stir until NaOH completely dissolves to form a white liquid. Add 14.612 g EDTA and 8.8 g ascorbic acid. Make to volume and cover to prevent oxidation. Store at 4°C. Use before solution turns dark brown.

5.1.2 Stock Standard
Set up vacuum filtration. Weigh and crush 2.4018 g NaS crystals with mortar and pestol under fume hood. Rinse crystals with deionized water and vacuum filter water. Quickly add NaS to 50 mL SAOB in a 100 mL volumetric flask and fill to volume with deionized water. Stir with magnetic rod until crystals are dissolved. Cover with Parafilm and store at 4°C.

5.1.3 Standards & Calibration Curve
The stock solution prepared above is the 10-1 M standard. To make 10-2 M, mix 25 mL SAOB with 5 mL stock solution and fill to volume with deionized water in a 50-mL volumetric flask. Repeat making serial dilutions for 10-3 and 10-4 standards.

Clean and fill both the inner and outer filling solution of the reference probe. Place both the sulfide probe and the reference probe in the standard poured into a small beaker. Wait until the ISE reaches equilibrium; record mV readings to make a calibration curve.

5.2 Sample Preparation & Acidification

Add 50 mL of 1-N de-aerated trace metal grade (37%) HCl and magnetic stir bar to 500 mL glass bottle. Add 30 mL SAOB to a 50-mL centrifuge tube cut to fit inside of the glass bottle.

Weigh and cap 5 g of wet hydrosoil in a 50-mL centrifuge tube in an anaerobic chamber. Quickly, place sample in bottom of the 500 mL glass bottle and cap. Stir for 60 minutes allowing it to be briskly stirred.

Pour SAOB into a small beaker for measurement of sulfide.

5.3 Measurement of Sulfide

Measure the sulfide generated and trapped in the SAOB using an ion-selective electrode. Rinse probes with deionized water between each measurement.

6.0 QUALITY CONTROL CHECKS

All procedures are subject to review by the Quality Assurance Unit.

7.0 REFERENCES

Di Toro, D.M., Mahony, J.D., Hansen, D.J., 1992. Acid volatile sulfide predicts the acute toxicity of cadmium and nickel in sediments. *Environmental Science & Technology*, 26, 96–101.

Leonard, E.N., Ankley, G.T., Hoke, R.A., 1996. Evaluation of metals in marine and freshwater surficial sediments from the environmental monitoring and assessment program relative to proposed sediment quality criteria for metals. *Environmental Toxicology*, 15, 2221-2232.

Yu, K., Tsai, L., Chen, S., Ho, S., 2001. Chemical binding of heavy metals in anoxic river sediments. *Water Resources Research*, 35(17), 4086-4094.